DSCIM-Coastal v1.0.1: An Open-Source Modeling Platform for Global Impacts of Sea Level Rise

Nicholas Depsky[1,3,*], Ian Bolliger[2,3,4,*], Daniel Allen[3], Jun Ho Choi[7], Michael Delgado[2], Michael Greenstone[5,7], Ali Hamidi[2,4], Trevor Houser[2], Robert E. Kopp[6], and Solomon Hsiang[3,5]

[1]Energy & Resources Group, University of California, Berkeley, California, USA
[2]The Rhodium Group, Oakland, California, USA
[3]Global Policy Lab, Goldman School of Public Policy, University of California, Berkeley, California, USA
[4]BlackRock, San Francisco, California, USA
[5]National Bureau of Economic Research
[6]Department of Earth & Planetary Sciences and Rutgers Institute of Earth, Ocean and Atmospheric Sciences, Rutgers University, New Brunswick, New Jersey, USA
[7]Energy Policy Institute, University of Chicago, Illinois, USA
[*]These authors contributed equally to this work.

Correspondence: Nicholas Depsky (njdepsky@berkeley.edu), Ian Bolliger (ian.bolliger@blackrock.com)

Abstract.

~~Global sea~~ Sea level rise (SLR) may impose substantial economic costs to coastal communities worldwide, but characterizing its global impact remains challenging because SLR costs depend heavily on natural characteristics and human investments at each location—including topography, the spatial distribution of assets, and local adaptation decisions. To date, several impact models have been developed to estimate the global costs of SLR~~, yet~~. Yet, the limited availability of open-source and modular platforms that easily ingest up-to-date socioeconomic and physical data sources ~~limits~~ restricts the ability of existing systems to ~~transparently~~ incorporate new insights transparently. In this paper, we present a modular, open-source platform designed to address this need, providing end-to-end transparency from global input data to a scalable least-cost optimization framework that estimates adaptation and net SLR costs for nearly 10,000 global coastline segments and administrative regions. Our approach accounts both for uncertainty in the magnitude of global ~~SLR~~ mean sea level (GMSL) rise and spatial variability in local relative sea level rise. Using this platform, we evaluate costs across ~~110~~ 230 possible socioeconomic and SLR trajectories in the 21st century. ~~We find annual global SLR costs of $180 billion to $200 billion in~~ According to the latest Intergovernmental Panel on Climate Change Assessment Report (AR6), GMSL is likely to rise during the 21st century by 0.40-0.69 meters if late-century warming reaches 2° C and by 0.58-0.91 m with 4° C of warming (Fox-Kemper et al., 2021). With no forward-looking adaptation, we estimate that annual costs of sea level rise associated with a 2° scenario will likely fall between $1.2 and $4.0 trillion (0.1 and 1.2% of GDP, respectively) by 2100~~assuming optimal adaptation , moderate emissions (RCP 4.5)~~, depending on socioeconomic and sea level rise trajectories. Cost-effective, proactive adaptation would provide substantial benefits, lowering these values to between $110 and $530 billion (0.02 and ~~middle-of-the-road (SSP 2) socioeconomic trajectories. Under the highest SLR scenariosmodeled, this value ranges from $400~~ 0.06%) under an optimal adaptation scenario. For the likely SLR trajectories associated with 4° C warming, these costs range from $3.1 to $6.9 trillion

(0.3% and 2.0%) with no forward-looking adaptation and $200 billion to $~~520 billion . We make this platform~~ 750 billion (0.04 to 0.09%) under optimal adaptation. IPCC notes that deeply uncertain physical processes like marine ice cliff instability could drive substantially higher global sea level rise, potentially approaching 2.0 m by 2100 in very high emission scenarios. Accordingly, we also model the impacts of 1.5 and 2.0 m GMSL rises by 2100; the associated annual cost estimates range from $11.2 to $30.6 trillion (1.2% and 7.6%) under no forward-looking adaptation and $420 billion to $1.5 trillion (0.08 to 0.20%) under optimal adaptation. Our modeling platform used to generate these estimates is publicly available in an effort to spur research collaboration and support decision-making, with segment-level physical and socioeconomic input characteristics provided at ~~, source code for this dataset at , the modeling framework at ,~~ https://doi.org/10.5281/zenodo.7693868 and model results at https://doi.org/10.5281/zenodo.7693869.

1 Introduction

Global mean sea level (GMSL) is projected to increase between 0.40-0.69 m for 2°C of warming and 0.58-0.91 m for 4°C of warming by 2100, though accelerated ice-sheet instability could result in substantially higher values (approaching 2 m) by end-of-century (Fox-Kemper et al., 2021). Coastal communities and ecosystems will experience a variety of impacts, including more frequent tidal flooding, higher extreme sea levels (ESLs)[1], erosion, wetland degradation, salinization of soils and water reservoirs, and loss of land area to permanent inundation (Oppenheimer et al., 2019; Nicholls et al., 2006). The magnitude of relative sea level rise (RSLR) and associated impacts will vary by locality, depending upon global greenhouse gas (GHG) emissions (Fox-Kemper et al., 2021), ice sheet instabilities (DeConto et al., 2021; Bamber et al., 2019; Fox-Kemper et al., 2021), local atmosphere-ocean dynamics (Fox-Kemper et al., 2021), economic growth along coastlines (O'Neill et al., 2017; Neumann et al., 2015; Armstrong et al., 2016), and adaptation actions (Hinkel et al., 2018; Diaz, 2016; Hinkel et al., 2014; Lincke and Hinkel, 2021).

Despite advances in our understanding of GMSL, the global costs of these changes remain poorly constrained. A key obstacle to quantifying these global impacts is their strong dependence on the details of local conditions, such as topography, the spatial distribution of populations and assets, and local adaptation decisions. A challenge for modelers is the dual objectives of fully accounting for these various factors at the local granularity necessary for accurate representation while also scaling these calculations globally. Improvements in computation and data availability now make achieving these two objectives feasible, but it has remained challenging for existing custom-built systems to be regularly updated to reflect new insights or improvements to global data sets describing local conditions.

This paper presents what is to our knowledge the first fully open-source coastal modeling platform that (i) integrates up-to-date local data on socioeconomic and physical conditions along coastlines globally, (ii) projects the physical, socioeconomic and ecological impacts of SLR along coastlines and (iii) directly models the costs and benefits of both retreat and protection as potential adaptation strategies. The platform is ~~fulled~~ fully coded in the open-source computer language Python (v3.9) and integrates recently released, satellite-augmented global data layers describing coastal elevations, local sea levels, and the distri-

[1]Terminology and acronyms for concepts related to sea level align with those recommended for contemporary use in Gregory et al. (2019).

bution of population and physical capital with widely used socioeconomic datasets. These data layers are projected onto 9,~~087~~ 568 unique coastal segments that span global coastlines. Each of these segments is then modeled as independently choosing across local, forward-looking adaptation strategies in an effort to minimize overall losses, following the framework developed in Diaz (2016). Using this platform, we evaluated net costs across ~~110~~ 230 possible socioeconomic and SLR trajectories in the 21st century to present here, though the tool is capable of accommodating tens to hundreds of thousands of future simulations in parallel if desired.

~~We find annual global SLR costs of $180 billion to $200 billion in~~ With no forward-looking adaptation, we estimate that annual global costs of sea level rise associated with 2° of warming (+0.40-0.69 m GMSL by 2100~~assuming optimal adaptation , moderate emissions (RCP 4.5))~~ will fall between $1.2 and $4.0 trillion (0.1% and 1.2% of GDP) by 2100, depending on socioeconomic and SLR trajectories. Locally cost-effective adaptation strategies could drastically lower these estimates to between $110 and $530 billion (0.02 and ~~middle-of-the-road (SSP 2) socioeconomic trajectories. Under the highest SLR scenarios modeled, this value ranges from $400~~ 0.06%). For the likely SLR trajectories associated with 4° C warming, these costs range from $3.1 to $6.9 trillion (0.3% and 2.0%) with no forward-looking adaptation and $200 billion to $~~520 billion~~ 750 billion (0.04 to 0.09%) under optimal adaptation. Under a very high emissions scenario with SLR projections that include the influence of deeply uncertain physical processes like marine ice cliff instability, end-of-century GMSL rise reaches +1.5-2.0 and the associated annual cost estimates range from $11.2 to $30.6 trillion (1.2% and 7.6%) with no forward-looking adaptation and $420 billion to $1.5 trillion (0.08 to 0.20%) under optimal adaptation.

All code used to aggregate and combine input data, as well as to estimate SLR impacts, is publicly available. This encourages further development by the coastal impacts research community and modularizes the modeling process to facilitate seamless incorporation of future improvements to input datasets and additional model components.

1.1 The Basic Architecture of Global Coastal Impact Models

Global coastal models that estimate impacts of SLR and ESLs seek to quantify the exposure of some variable(s) of concern, such as human population, capital assets, and coastal ecosystems, to these physical hazards. They generally report the magnitude of exposure to these hazards as their final output, and convert this exposure into some outcome of interest, such as economic losses (Hinkel et al., 2014; Diaz, 2016; Lincke and Hinkel, 2018). These models usually contain spatially explicit representations of physical coastline characteristics (e.g. coast lengths, elevation and land surface areas), exposure variables, and physical hazard variables.

To estimate future impacts, global coastal models must assume or model trajectories of pertinent physical and socioeconomic values over time. Most climate change-oriented impacts models assess multiple trajectories of GMSL and many account for local RSLR and associated ESLs, which commonly correspond to different GHG emissions pathways (Hinkel et al., 2014; Diaz, 2016; Lincke and Hinkel, 2018, 2021). They may also contain different future trajectories of human population and capital asset growth, such as those represented in the Shared Socioeconomic Pathways (SSPs) database (Riahi et al., 2017; Hinkel et al., 2014; Lincke and Hinkel, 2018; Tiggeloven et al., 2020; Lincke and Hinkel, 2021).

The spatial and temporal resolution of model components can vary between studies and is sometimes limited by the resolution of available input datasets and/or by available computing resources. Additionally, many models also include some form of adaptive decision-making, such as allowing different coastal segments to construct protective coastal barriers (Hinkel et al., 2014; Diaz, 2016; Lincke and Hinkel, 2018; Tiggeloven et al., 2020; Lincke and Hinkel, 2021) or retreating inland (Diaz, 2016; Lincke and Hinkel, 2021), usually guided by some form of local cost-benefit analysis.

1.2 Closely Related Efforts and Platform Genealogy

Several past studies employed ~~high-resolution~~ global coastal impact models to estimate future damages from SLR and ESLs under various trajectories of global GHG emissions, socioeconomic scenarios, and adaptation pathways for thousands of sub-national coastline segments (Hinkel et al., 2014; Diaz, 2016; Lincke and Hinkel, 2018, 2021). Many of these studies used the Dynamic Interactive Vulnerability Assessment (DIVA) Coastal Database and modeling tool as their source of information for describing local coastlines. Originally developed by the Dynamic and Interactive Assessment of National, Regional and Global Vulnerability of Coastal Zones to Climate Change and Sea-Level Rise (DINAS-COAST) project (Vafeidis et al., 2008; Hinkel and Klein, 2009), the DIVA database partitions global coastlines into 12,148 segments and provides local physical attributes (e.g., inundation areas by elevation, extreme sea level heights, wetland areas, erosion characteristics) as well as socioeconomic characteristics (e.g. population densities, land use), allowing for ~~more~~ spatially disaggregated coastal impact analyses (Vafeidis et al., 2008; Hinkel and Klein, 2009). At the time of its initial release in 2008, DIVA represented a substantial improvement over previous global, coastal databases and impact studies, which were most commonly performed using data at much coarser spatial resolutions (Hoozemans et al., 1993; Yohe and Tol, 2002; Nicholls, 2004, 2002; Dronkers et al., 1990; Pardaens et al., 2011; Hinkel et al., 2013). Presently, however, the DINAS-COAST program is no longer funded, and the accessibility of the DIVA database has fluctuated. Recently, a landing page has been created for the DIVA model at http://diva.globalclimateforum.org, though as of early ~~2022~~ 2023 the corresponding dataset is only available via direct correspondence with its authors. The underlying code and input data used to construct the DIVA database is not publicly available, making it difficult to replicate prior studies' results and diagnose issues that have appeared in previous versions of the dataset (Sect. 2.5.1). In this work, we address these issues of accessibility and transparency by generating a publically-available global dataset of coastal socioeconomic metrics, updating all core data layers used to generate DIVA and releasing the data assimilation model used to aggregate these into the final data product. The full set of data updates are described in Sect. 2 below.

In a key early analysis, Hinkel et al. (2014) employed the DIVA database to model the combination of coastal flood damages and adaptation (specifically, protective levee construction) under twelve scenarios of future RSLR and socioeconomic projections for sub-national coastal zones. Sea level rise scenarios in this study were constructed from estimates of global thermal expansion and regional ocean dynamic sea level data corresponding to low-, medium-, and high-emissions Coupled Model Intercomparison Project Phase 5 (CMIP5) experiments (Taylor et al., 2012) (Representative Concentration Pathways 2.6, 4.5, and 8.5) in four Earth System Models (ESMs), combined with low, medium, and high land-ice scenarios. The study also evaluated two different digital elevation models (DEMs) for estimating population exposure in coastal floodplains to SLR and ESLs, the GLOBE DEM (GLO, 1999), which was the original DEM used in DIVA (Hinkel and Klein, 2009), and the more recent

Shuttle Radar Topography Mission (SRTM) DEM (Rodriguez et al., 2005). They found that their results were highly sensitive to the choice of DEM, which underscores the importance of updating global data layers used in coastal impact modeling as improved products are made available, which is one of the central aims of the work we present in this paper.

Expanding on the approach of Hinkel et al. (2014), Diaz (2016) developed the Coastal Impact and Adaptation Model (CIAM), a global modeling tool that estimated 21st century costs and adaptation strategies for each DIVA segment. One core innovation presented in CIAM was that it allowed for each segment to choose between dike construction, as in Hinkel et al. (2014), and managed or reactive retreat. However, an obstacle to widespread usage of CIAM was its development in the commercial General Algebraic Modeling System (GAMS) closed-source platform. We build on the work by Diaz (2016), using the underlying decision-making framework of CIAM; however, we adapt, re-code, and optimize CIAM in the open-source Python computing language.

The architecture of CIAM was designed to capture key aspects of local adaptive decision-making that will likely be used by coastal communities worldwide. The objective of CIAM was to develop an optimization framework that could be applied locally, but generalized globally. To limit the computational challenge of solving stochastic dynamic programs for thousands of independent coastline segments, Diaz (2016) simplified the set of possible adaptation choices to a set of discrete decisions that are calibrated to local conditions. CIAM differentiated between six types of costs (~~a.k. a. "impacts" or "~~i.e. "damages") due to RSLR and ESLs (Sect. 2.2): (a) the cost of permanent inundation of immobile capital or land, and ESL-related (b) damages to capital, (c) mortality, (d) expenditures on protection (i.e. infrastructure construction), (e) relocation costs, and (f) wetland loss. Possible protection actions include constructing levees at the 10, 100, 1000, and 10000-year ESL heights at each segment, and possible retreat actions include proactively vacating all land area under local mean sea level ~~(MSL)~~ or within the 10, 100, 1000, or 10000-year ESL floodplain. Simulations in CIAM are implemented using ~~discreet~~ discrete time-steps, termed "adaptation planning periods" (40-50 years), during which each segment updates their retreat or protection height based on the maximum RSLR projected to occur within the period. CIAM also allows for modelers to select a "no planned adaptation" option that constrains retreat to to be reactive, rather than forward-looking, such that the population and capital assets only choose to relocate inland once they are permanently inundated by rising sea levels. Diaz (2016) considered a single socioeconomic growth trajectory based on the 2012 United Nations World Population Prospects (UN DESA, 2012), Penn World Table version 7.0 (Heston et al., 2011) and the 2011 IMF World Economic Outlook (IMF, 2011) projections and uses DIVA's older GLOBE DEM. The SLR trajectories used by Diaz (2016) were the 5th, 50th, and 95th percentiles of probabilistic RSLR projections from Kopp et al. (2014) for RCPs 2.6, 4.5, and 8.5, as well as a no-SLR baseline.

Here, we build on the approach of Diaz (2016), adapting and optimizing the decision-framework of CIAM to an entirely new set of global data inputs (i.e. replacing DIVA) and an open-source computer language. Given continued advancement in sea level rise modeling efforts and the improvement of global data inputs (e.g. coastal DEMs), it is essential that coastal impacts modeling platforms are able to integrate these updates. Additionally, we believe that these platforms should be developed in an open-source, transparent, and reproducible framework that will allow for increased collaboration and more rapid iteration amongst coastal impacts researchers, as has been done for modeling communities across numerous scientific disciplines (von Krogh and von Hippel, 2006). The platform we develop addresses these objectives by integrating the latest available physical,

climate, and socioeconomic input data for an expanded suite of future SLR and economic growth trajectories in an updated and open-source version of the CIAM framework that, in addition to improved accessibility and transparency, results in greater resolution and substantially improved computational efficiency.

1.3 This Study: The Data-driven Spatial Climate Impact Model - Coastal Impacts~~Architecture~~

This modeling platform was developed as the sea level rise impacts module of the Data-driven Spatial Climate Impact Model (**DSCIM**) architecture ~~(Rode et al., 2021)~~(Rode et al., 2021; Carleton et al., 2022), and is thus named **DSCIM-Coastal**. It is partitioned into two distinct components (see Fig. 1), each made available as open-source products: (i) the collection, harmonization, and aggregation of updated physical and socioeconomic input datasets by coastal segment, which is named the Sea Level Impacts Input Dataset by Elevation, Region, and Scenario, or **SLIIDERS**, and (ii) the modeling platform itself, called **pyCIAM** (short for "Python-based CIAM"). Both components have been developed in accordance with FAIR Guiding Principles for scientific data management (Wilkinson et al., 2016) that are intended to improve the Findability, Accessibility, Interoperability, and Reuse of scientific data.[2]

The SLIIDERS data set is conceptually similar to DIVA in that it contains a suite of variables defined across a collection of coastal segments designed for coastal impact modeling efforts. However, while DIVA is not publicly accessible, SLIIDERS and all of its components are available with open access licenses, thereby supporting transparency and replicability of coastal damage analyses for research communities around the globe.[3] In addition, the partition of global coastlines that defines separate coastal segments as units of analysis has been revamped in order to achieve greater balance in geographic coverage and reduce redundant computations.

~~SLIIDERS is broken into two major elements, **SLIIDERS-ECON** and **SLIIDERS-SLR**. SLIIDERS-ECON~~ SLIIDERS also contains updated topographic, geographic, and socioeconomic input datasets, including refined coastal DEMs ~~, SLR projections,~~ and socioeconomic growth trajectories. ~~In SLIIDERS-SLR, we pair each coastal segment with the nearest projection of probabilistic RSLR from the LocalizeSL framework (Kopp et al., 2014, 2017) for 11 combinations of emissions scenario and ice sheet dynamics, resulting in a companion oceanographic dataset.~~

pyCIAM is an open-source, computationally efficient and functional modeling platform for segment-level adaptation decision making that incorporates the following improvements to the original implementation of CIAM (Diaz, 2016): (i) updates to (and expansion of) all ~~input data (~~topographic, geographic ~~, socioeconomic~~ and socioeconomic input data using SLIIDERS,

[2] These data and modeling components abide by the FAIR criterion as specified by The Future of Research Communications and e-Scholarship (FORCE11). Specifically, they are i) Findable via unique and persistent identifiers, with these identifiers specified in component metadata and indexed in a searchable resource (Zenodo, Github); ii) Accessible in that they are retrievable via these identifiers and are open, free and universally implementable; iii) Interpretable through the use of a formal, accessible, shared and broadly applicable language/vocabulary (manuscript and metadata in standard English and code in Python) and the inclusion of appropriate references to other data where necessary (e.g. input data sources); and iv) Reusable by specifying accurate and relevant attributes, applying an accessible data usage license and complying with coastal modeling community standards of language and data/code provision (Force11.org).

[3] One of the input data sources used in generating SLIIDERS, CoastalDEM (Kulp and Strauss, 2019), is not freely available at the resolution employed in this study but is available for research use at a lower resolution.

and updated oceanographic inputs using a large suite of 23 SLR projections, ~~and oceanographic) using SLIIDERS,~~ (ii) improvements to model representation of different variables, such as population and capital asset distribution and storm damage calculations, (iii) availability as an open-source, self-contained Python package and input database, making the workflow easily accessible and modifiable for other researchers, and (iv) improved computational efficiency and scalability, enabling the application of CIAM to large, probabilistic ensembles of ~~sea-level~~ sea level change.

The pyCIAM model is configured to utilize the SLIIDERS ~~input data~~inputs and SLR projections presented here, but can easily be run using a modified set of inputs or SLR pathways, provided the data structure ~~matches that of SLIIDERS~~is consistent with this configuration. Similarly, the SLIIDERS product can be used independently from pyCIAM as inputs for other coastal analysis or as contextual information on coastal zones. ~~SLIIDERS consists of the model-ready inputs used in pyCIAM, as well as a collection of Python notebooks used for their construction from parent, raw data products. The pyCIAM package contains the model code itself, as well as a number of diagnostic and results visualization functions~~It can also be recreated using alternate input sources as desired, as the scripts to generate the product are provided with it.

The following sections describe how SLIIDERS and pyCIAM ~~were~~ are constructed, show example results of model outputs and diagnostics from ~~2000-2100~~ 2005-2100 and compare to the results of Diaz (2016), and discuss current limitations to the model and input datasets, outlining planned improvements and future research priorities.

~~**DSCIM-Coastal Impacts Modeling Hierarchy** 0.5ex**DSCIM** - Multi-sectoral Data-driven Spatial Climate Impact Model described in (Rode et al., 2021) **DSCIM-Coastal** - Open-source platform for computing global coastal impacts, presented in this paper **SLIIDERS** - Coastal segment datasets **SLIIDERS-ECON** - Physical coastal characteristics and socioeconomic growth projections **SLIIDERS-SLR** - Local relative sea level rise projections **pyCIAM** - Global decision-modeling and projection system using *SLIIDERS* to model coastal impacts, based on CIAM (Diaz, 2016) and implemented in Python (v3.9) 0.5ex2ex~~

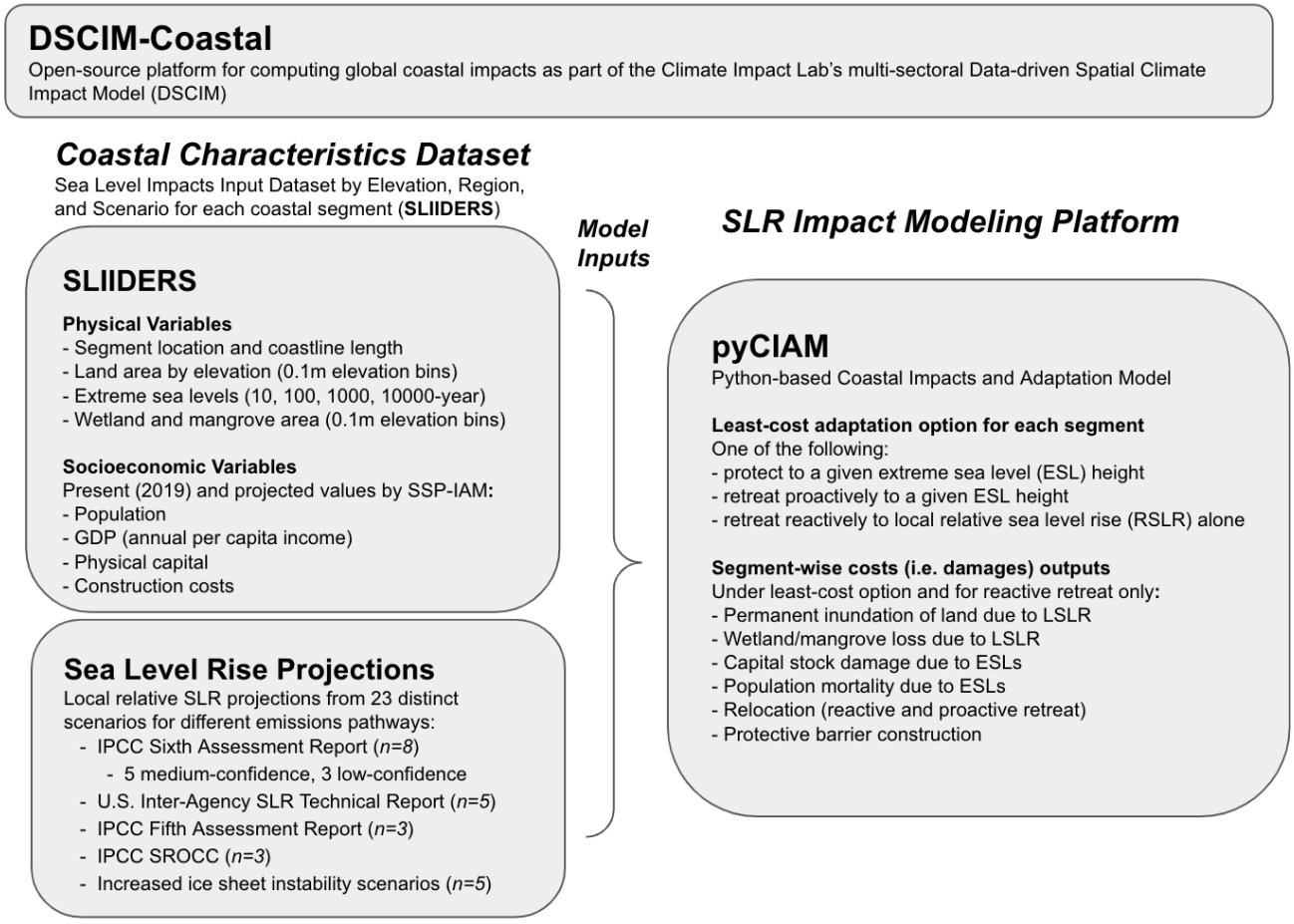

Figure 1. ~~The major elements comprising~~ Components of the Coastal portion of the Data-driven Spatial Climate Impact Model (DSCIM-Coastal)

2 Methods and Data

We constructed the Python Coastal Impacts and Adaptation Model (pyCIAM) by adapting the original code and structure of the Coastal Impacts and Adaptation Model (CIAM) (Diaz, 2016), obtained from http://github.com/delavane/CIAM in June 2020, with changes subsequently made in three phases:

1. Porting the model from GAMS to a standalone Python module (creating *pyCIAM*)
2. Updating all model inputs with the *SLIIDERS* data and SLR projections, constituting newer, improved physical and socioeconomic datasets
3. Implementing changes to the model functionality itself for the purposes of:
   - Computational efficiency

- Updating assumptions where new data provided previously unavailable insights
- Aligning model implementation with the model description in Diaz (2016)
- Reducing noise in numerical approximation algorithms

2.1 Model Structure

The aspects of CIAM as presented in (Diaz, 2016) that are maintained in pyCIAM include the segment-based structure of the model and the adaptation actions that each segment is permitted to take throughout the modeling period, comprised of the following options:

- *Reactive Retreat*: When a portion of land falls below MSL, all people and mobile capital are relocated to an unaffected~~area, ~~, inland region away from the coast that is not in danger of future impacts from SLR or ESLs, and immobile capital is abandoned.
- *Protection*: Construction of a generic levee to protect the entire coastline segment. Available choices for protection height include the 10, 100, 1000, and 10,000-year return values of ESL. This height changes linearly with RSLR.
- *Proactive Retreat*: All people and mobile capital below a certain retreat height are assumed to be relocated to a safe~~elevation, ~~, inland region, and immobile capital below that height is abandoned. The options for that retreat height level are discretized to the same values available for protection, with the addition of a "low retreat" option representing the maximum MSL projected during a "planning period" (10 years).

Note that, as described in Diaz (2016), each coastal segment may only choose one adaptation option, e.g. *retreat-1000*, for the entire model duration. While the height of the retreat level changes over time as the 1000-year ESL return value changes due to RSLR, the segment cannot, for example, choose retreat-100 for the first 40 years and then protect-10000.

The model is discretized into time steps (10 years in the original CIAM, annual in pyCIAM), during which all time evolving parameters are held constant. In addition, the segments use a configurable set of "planning periods" ~~, ~~(40-50 years each period in CIAM, 10 years each in pyCIAM), which each correspond to a set of one or more timesteps. For each planning period, a single height is chosen for retreat or protection (assuming the segment does not select "reactive retreat") that represents the maximum height projected for the chosen ESL return value during the planning period.

2.2 Cost Calculation

~~Costs estimated by pyCIAM are categorized in the same manner as described in (Diaz, 2016).~~ Following Diaz (2016), pyCIAM separately tracks inundation costs, retreat costs, protection costs, cost of wetlands loss, and extreme sea level damage and mortality. These categories of costs are all used in cost minimization, and each is detailed below.

2.2.1 Inundation Costs

~~The~~ This category reflects the value of land and immobile capital lost to inundation. In Diaz (2016), immobile capital was allowed to fully depreciate if the strategy chosen is proactive retreat, such that capital-related losses due to inundation are

always 0. This was based on a theoretical argument that for a planned retreat, a rational social planner would cease the creation of new physical capital far enough in advance that all remaining capital would have fully depreciated by the time the retreat occurs (Yohe et al., 1995). However, this assumption has been critiqued in subsequent work (Lincke and Hinkel, 2021) due to its lack of empirical grounding. Furthermore, it ignores the welfare loss associated with not replacing depreciating assets in the years leading up to retreat. These new capital investments would have been made in the absence of SLR, and thus the lack of investment should be counted when assessing total SLR impacts. Therefore, pyCIAM alters CIAM's assumption of full depreciation, instead modeling immobile capital to experience no excess depreciation beyond the background rate implicitly included in the capital growth model used to generate SSP-aligned capital projections. This results in the full estimated value of capital being lost when abandoned or inundated, in line with the assumptions of Lincke and Hinkel (2021).

2.2.2 Retreat Costs

~~The~~ This category reflects the costs of relocating population and mobile capital and of demolishing immobile capital. Following Diaz (2016), capital relocation costs are valued at 10% of total value, and immobile capital demolition costs are valued at 5%. In Diaz (2016), the intangible relocation cost is valued at one year of per capita income, which varies by country and over time~~and was an admittedly arbitrary assumption. We use a value of five~~ . As described in the Diaz (2016) Supplemental Information, this was an arbitrary value chosen because it lay between the value used in the integrated assessment model FUND (3, Tol (1996)) and a number derived from personal communication with Robert Mendelsohn (0.5). We update this value to 8.0 times local income, ~~for reasons described~~ based on analysis described below in Sect. 2.3.

2.2.3 Protection Costs

~~The~~ This category reflects the construction and maintenance costs of building a protective levee, along with the value of lost land. As in Diaz (2016), maintenance costs are assumed to be 2% of ~~baseline costs~~the initial construction cost, and the value of lost land is calculated as the local land value (which varies over countries and years) times the length and width of the barrier, assuming a ~~60°~~ 60° slope.

2.2.4 Wetlands Loss

~~The~~ This category reflects the value of wetlands lost to either SLR or protection. As in Diaz (2016), wetlands are assumed to be able to partially absorb SLR up to 1 cm year^{-1}, with the degree of loss increasing quadratically with the rate of SLR. Above the critical threshold of 1 cm year^{-1}, all inundated wetlands are lost. In addition, all wetland area below a protective barrier is also assumed to be lost. More details on the calculation of wetland loss can be found in Equation 8 of the Diaz (2016) supplemental information.

2.2.5 Extreme Sea Level Capital Damage

~~The~~ This category reflects the value of capital loss occurring due to ESL events, using a depth-damage relationship that takes the shape $\frac{d}{1+d}$. The probability density function of ESL values at each segment location is represented as a Gumbel distribution, derived from Muis et al. (2016) in Diaz (2016) and from Muis et al. (2020) in pyCIAM. The product of this PDF and the estimated capital loss conditional on each ESL height in the distribution is integrated to obtain the annual expectation of ESL-driven capital loss per elevation slice, and these costs are summed over elevation to obtain the annual damages per segment (see Diaz (2016), Supplementary Material Section 2.1, Eqs 9-12). For computational efficiency, this set of discrete products, integrations, and sums is performed on a variety of example inputs prior to executing the actual CIAM model. In Diaz (2016), functions are fit to these outputs to relate ESL height to loss for different adaptation options, with unique coefficients for each segment~~:~~.

$$D_{r,s,t} = (1-\rho_{s,t})C_{s,t}\left(\frac{\sigma_{0,r,s}}{1+\sigma_{A,r,s}exp(\sigma_{B,r,s}H_{r,s,t})}\right) \quad (1)$$

$$D_{p,s,t} = (1-\rho_{s,t})C_{s,t}\left(\frac{\sigma_{0,p,s}+\sigma_{1,p,s}S_{s,t}}{1+\sigma_{A,p,s}exp(\sigma_{B,p,s}H_{p,s,t})}\right), \quad (2)$$

where

$D_{r/p,s,t}$	is the ESL-driven expected capital loss conditional on retreat or protection to height r or p, respectively, for segment s in time step t,
$\rho_{s,t}$	is a country-level resilience factor (defined in Diaz, 2016),
$C_{s,t}$	is the capital density (in \$ per km^2),
$H_{r/p,s,t}$	is the difference between the retreat or protection height and local mean sea level,
$S_{s,t}$	is the local mean sea level, and
σ	are the fitted coefficients.

~~This~~

However, this has two notable issues. First, this fixed functional form may not fully represent heterogeneous relationships between adaptation height, MSL, and damage across segments, due to differing elevational distributions of capital at each segment. Second, ~~only the protection equation contains a MSL term. This means that for retreat, ESL damages are modeled as constant relative to MSL,~~ in Diaz (2016) the damages conditional on a ~~fixed~~ given retreat standard (e.g. 1-in-10 year ESL height) ~~. This cannot be true unless capital is homogenously distributed over elevation. This assumption is at odds with reality and with the rest of the Diaz (2016) CIAM model , which assumes that the elevational~~ are a function only of the difference between MSL and the retreat standard, not of the absolute MSL height. This approximation would be accurate if the same amount of capital exists at all elevations, independent of the area of land available at those elevations; however, elsewhere in the original CIAM model it is assumed that the elevation distribution of capital follows that of land area.

In pyCIAM, we ~~correct~~ address these issues by employing a multi-dimensional lookup table instead of these two functions. For each segment, we find the lowest and highest values of ~~H and~~ MSL (S) and of the difference between retreat/protection height and MSL (H) across all SLR scenarios we wish to simulate, all adaptation choices, and all timesteps. We then choose 100 equally spaced values between these bounds for each of the two variables. For both of the adaptation categories (retreat and

protection), we now have 10,000 scenarios reflecting different combinations of H and S. We normalize capital stock so that it sums to one, yielding fractional capital stock in each elevation slice. The current implementation assumes that these ratios remain fixed over time~~, though allowing for~~. However, should one wish to model within-country ~~population redistribution~~ migration due to considerations such as SSP-consistent coastal urbanization and migration flows (e.g. ~~Jones and O'Neill (2016))could~~ Jones and O'Neill (2016); Merkens et al. (2016)), such changes can be accommodated by ~~further indexing this lookup table by year~~updating the appropriate variables in the SLIIDERS input dataset. For each of the 20,000 scenarios, we calculate damages ~~under a $\rho = 0$ assumption~~ using a discrete double integral over ESL height and elevation slice. ~~This yields damages for 10,000 unique combinations of H and S, for both retreat and protection options.~~ In the pyCIAM model, the equations for damage are thus:

$$D_{r,s,t} = (1-\rho_{s,t})K_{s,t}\gamma(H_{r,s,t}, S_{s,t})$$
$$D_{p,s,t} = (1-\rho_{s,t})K_{s,t}\gamma(H_{p,s,t}, S_{s,t}),$$

$$D_{r/p,s,t} = (1-\rho_{s,t})K_{s,t}\gamma(H_{r/p,s,t}, S_{s,t}) \quad (3)$$

where

$D_{r/p,s,t}$ is the ESL-driven expected capital loss conditional on retreat or protection to height r or p, respectively, for segment s in time step t,

$\rho_{s,t}$ is a country-level resilience factor (defined in Diaz, 2016),

$K_{s,t}$ is the total value of capital stock in segment s at time t~~and~~ ,

$H_{r/p,s,t}$ is the difference between the retreat or protection height and local mean sea level,

$S_{s,t}$ is the local mean sea level, and

γ is the bilinear interpolation function across H and S, using the previously defined lookup table.

2.2.6 Extreme Sea Level Mortality

~~The~~ This category reflects the expectation of annual ~~VSL-valued~~ costs of mortality occurring due to ESL events~~. Diaz (2016) estimates this by assuming~~ , where death equivalents are valued using a Value of a Statistical Life (VSL) framework, as employed in Diaz (2016), which assumes 1% mortality for all populations exposed to a given ESL, based on Jonkman and Vrijling (2008). This is modeled similarly to the ESL-driven capital loss, except that the 1% mortality assumption is used in place of ~~of~~ the depth-damage function. In the implementation of Diaz (2016), both the mortality assumption ~~*and*~~ and the depth-damage function ~~were used together. This is at odds with the description of the approach in the associated paper, and is thus corrected in~~ appear to have been used in conjunction, although the text of the Diaz (2016) paper states that the depth-damage

function should only be used in the estimation of capital stock damage, not mortality. We therefore corrected this discrepancy in our implementation of ESL-driven mortality estimates in pyCIAM.

2.2.7 Least Cost Optimization

For each planning period, every segment considers each of the possible adaptation options and assesses costs at each annual time step within the period. ~~Like~~ Following Diaz (2016), we maintain the assumption that these decision-making agents have perfect foresight of projected RSLR over this planning period; however, we reduce these periods from 40-50 years to 10 years (Sect. 2.7.2). The maximum heights of projected RSLR at each segment during a given planning period in turn influence the heights at which protect or retreat adaptation options are employed. ~~Reactive retreatwould match~~ For segments that adapt via reactive retreat, the height of retreat exactly matches this projected RSLR~~and~~ , while segments employing 10, 100, 1000, 10000-year retreat or protect actions ~~would~~ consider the heights of these ESLs atop ~~the changing~~ this projected RSLR baseline for that planning period. Once adaptation costs are calculated for all adaptation periods, we follow (Diaz, 2016) and calculate the NPV across the entire model duration for each adaptation option, and each segment chooses the least cost option.[4]

2.3 Estimating Non-market Costs of Relocation

~~Diaz (2016) portrays the costs associated with "optimal adaptation" and "reactive retreat only" scenarios as bounds on future costs . This is justified by the observation that coastal adaptation at present does not appear to be economically rational, such that populations do not relocate or protect themselves when it seems optimal to do so (McNamara et al., 2015; Armstrong et al., 2016; Haer et al . This observation could be explained by uncaptured non-market costs of relocation associated with, for example,~~ In pyCIAM we introduce a calibration of non-market retreat costs based on observed patterns of settlement. Non-market retreat costs are those costs that are not directly visible to the market, but which nonetheless are incurred by individuals if they chose to relocate. For example, the non-pecuniary emotional ~~consequences~~cost associated with moving or the loss of social networks due to moving would both be non-market retreat costs. Accounting for these impacts would indicate that the total welfare impact of forced relocation is greater than simply the market costs associated with ~~simply~~ abandoning immobile capital. The existence of non-market relocation costs are thought to explain the observation that some patterns of coastal adaptation currently would not appear to be economically rational based on market costs alone (McNamara et al., 2015; Armstrong et al., 2016; Haer et al., 2017; Bakkens . Using only market costs, least-cost optimization would indicate that many real-world populations should relocate or protect themselves, thus there must exist unobserved non-market costs that keep those populations in their current locations. We leverage this observation to estimate the approximate magnitude of non-market relocation costs that would be necessary to explain current global settlement patterns.

Though CIAM ~~partially represents~~ does include some non-market costs associated with moving, equivalent to one year of GDP, the model does not re-create observed patterns of settlement when it is initialized and run under an optimal adaptation scenario. Instead, it results in an excess of instantaneous relocation ~~, suggesting that these~~ in the first period of the model run. This indicates that the non-market costs ~~may not be fully represented~~specified are likely too small, because they are

[4] In contrast to Diaz (2016), we include initial adaptation costs from the first planning period in this NPV calculation (Sect. 2.7.3).

insufficient to hold populations to their observed present locations before any SLR occurs in the model. Specifically, when the optimal adaptation scenario is run under the baseline parameterization in Diaz (2016) and with the assumption of no climate-driven sea level rise, we observe that $1.26T of capital and 33M people instantly relocate. Adjusting for population and capital growth over the century, this instant relocation represents 41% and 44% of the *cumulative* relocation realized by the end of the century under the median SLR scenario for RCP 4.5. This ~~large amount of instantaneous relocation clearly~~ instantaneous relocation conflicts with the ~~observed~~ distribution of people and capital observed in the world today and suggests that there ~~may be~~ are larger costs of relocation than are ~~realized in the~~ accounted for in the original parameterization of CIAM used in Diaz (2016).

~~Diaz (2016) assumed these~~ The original parameterization of CIAM in Diaz (2016) assumed that non-market costs are equal in value to consumption of one year of local GDP per capita, based on this value falling between two alternative estimates: 0.5 years (obtained from the author's personal communication with Robert Mendelsohn) and 3.0 years, the value assumed in the FUND Integrated Assessment Model (Tol, 1996). Notably, the more recent evolution of FUND – the GIVE model (Rennert et al., 2022) – relies directly on CIAM for estimating costs of SLR and thus now assumes costs equivalent to one year of local GDP per capita. In a similar modeling framework to CIAM, Lincke and Hinkel (2021) used the FUND value directly and further provided a literature review that finds empirical and theoretical estimates of total relocation costs varying between 2.3 and 9.5 years of average local income per capita. These ~~empirical~~ findings suggest that the factor of one used in Diaz (2016) may underestimate relocation costs.

To address this, we adopt an approach to calibrate these unobserved non-market costs of relocation against real world behavior. Our calibration approximates a "revealed preference" approach, in which the behavior of agents is thought to reveal information about their preferences and values that is not otherwise visible (other elements of DSCIM adopt related methods to estimate the undocumented costs of adaptation decisions in other sectors, e.g. see ~~Carleton et al. (2020)~~Carleton et al. (2022)). Intuitively, this strategy relies on the insight that if individuals found the benefits of moving to be larger than the combined market and non-market costs, they would relocate. We cannot observe the non-market costs, but we can estimate the benefits and the market costs. If we observe that individuals have not relocated but CIAM computes that the benefits outweigh the market costs even before considering SLR, then we can estimate a lower bound on the implied non-market costs (equal to the benefits minus the market costs) that must be present in order to prevent them from relocating and rationalize their observed behavior.

Our ability to ~~constrain~~ recover non-market costs using a revealed preference approach is constrained by our ability to accurately model benefits and market costs of relocation. There are inherent limitations in a global model (e.g. input data inaccuracies, preference heterogeneity) such that, at a segment-level, there will likely be some segments where benefits and/or market relocation costs are not measured exactly. Thus, we choose a relocation cost parameter by taking the exposure-weighted median value of segment-specific estimates of non-market costs.

To do this, we identify the total population and physical capital that would instantaneously relocate when the model is initialized in the absence of non-market relocation costs, assuming median estimates of RSLR in a no-climate change scenario (i.e., no change in GMSL, and RSLR associated only with land subsidence). For this simulation, we choose middle-of-the-road

socioeconomic projections characterized by SSP2 and the International Institute for Applied Systems Analysis (IIASA) GDP growth model (Crespo Cuaresma, 2017). We then steadily increase the relocation cost parameter until 50% of ~~that~~ this population and capital no longer instantaneously relocates under the optimal adaptation scenario. This median approach balances the desire to capture the non-market costs causing observed non-relocation with the recognition that data and parameter limitations associated with a global model will inevitably cause some ~~seemingly irrational~~ discrepancy between modeled and observed behavior. Because this median occurs at different values for population and physical capital, we average the two values (~~3.0 and 7.0~~ 6.7 and 10.9 years of local income, respectively) to obtain the ~~5.0~~ 8.0 factor used in pyCIAM. Fig. 2 illustrates this calculation.

We note that this approach is facilitated by the ~~data fidelity~~ resolution of the input data represented in SLIIDERS~~and resolution provided by pyCIAM~~. The DIVA inputs used in Diaz (2016) ~~assumed homogeneous~~ assume that population and capital density ~~within each segment. This could introduce substantial noise in~~ are homogeneously distributed throughout each segment, and are non-varying by elevation. This both distorts the elevation distribution of the observed present-day state of these two variables and ~~would prohibit~~ prohibits the analysis described above. By leveraging global gridded datasets of population, capital, and elevation, SLIIDERS and pyCIAM capture heterogeneous density and better represent the true present-day elevation distribution of population and capital within each segment (Sects. 2.6.1, 2.6.3, and 2.5.3).

After updating the non-market relocation cost parameter, we additionally follow the approach of Lincke and Hinkel (2021) and do not distinguish between the non-market costs of reactive and proactive retreat. Diaz (2016) assigns five times higher costs to reactive retreat, though there is no empirical basis reported for this additional cost. Thus, we assume that both proactive and reactive retreat in pyCIAM incur losses equivalent to ~~five~~ 8.0 years of income, rather than one and five years, respectively, in Diaz (2016).

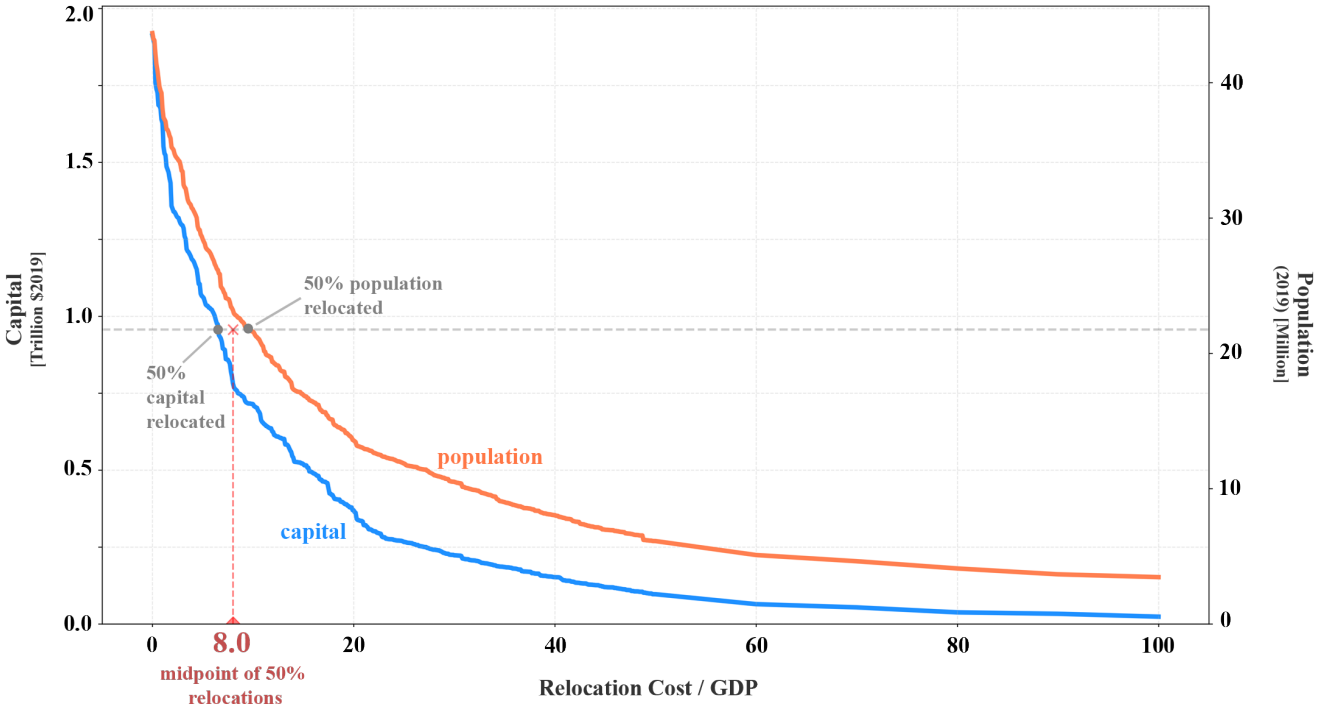

Figure 2. ~~Estimation of~~ Calibrating the non-market relocation cost parameter ~~through~~ based on the revealed preference of current populations. Curves show the magnitude of the population (~~blue~~orange) and physical capital (~~green~~blue) that is instantaneously relocated in the optimal adaptation scenario of pyCIAM, assuming SSP2-IIASA socioeconomic projections and median no-climate change RSLR, as a function of this parameter. The parameter is normalized by local GDP per capita. We identify the parameter values for which 50% of the population and capital instantaneously relocated under an assumption of zero non-market costs ~~is~~ are no longer relocated, and average these two values to estimate the relocation parameter used in pyCIAM.

2.4 Porting CIAM from GAMS to Python

CIAM was constructed in the closed-source General Algebraic Modeling System (GAMS) language. However, the model does not require the dynamic programming capabilities offered by GAMS. Therefore, porting the model to Python, a commonly used, open-source programming language, offers greater flexibility, access, and efficiency without loss of functionality. Before adding additional resolution to the model, pyCIAM computed a global run of a single SLR trajectory in 15-20 seconds, compared to 6-8 hours for CIAM. To ensure that this first stage of changes did not introduce changes to model functionality, we ensured that this version of pyCIAM replicated the results from the CIAM (in GAMS) model obtained from its source repository before updating model inputs. This replication was largely confirmed, with only very minor deviations between the computed results and those reported in (Diaz, 2016). The observed deviations were also reflected in the outputs of the unaltered CIAM model we obtained, suggesting that the configuration of the publicly available CIAM model was likely slightly altered from that used in Diaz (2016) (Table 1).

~~Billion USD ($2010)~~	Diaz 2016 (~~paper results~~GAMS, reported in original paper)	CIAM (GAMS, computed in this study)	pyCIAM (Python, computed in this study)
Global NPV (2010-2100)	1700	1692.2	1692.2
U.S. NPV (2010-2100)	419	419.7	419.7
Australia NPV (2010-2100)	208	208.6	208.6
Brazil NPV (2010-2100)	98	97.5	97.5
China NPV (2010-2100)	87	87.0	87.0
Wetland Loss in 2100	80	79.3	79.3
Global Costs in 2100 (optimal adaptation)	270	282.1	282.1
Global Costs in 2100 (no adaptation)	2200	2251.5	2251.5
Calculation runtime	-	6-8 hours	15-20 seconds

Table 1. Comparison of select model ~~results~~ estimated costs (in $2010B USD) as reported in Diaz (2016) with those calculated from the original CIAM code in GAMS obtained from its online source repository and those calculated by pyCIAM after porting CIAM to Python and before any additional changes. Values reflect median relative sea level rise projections from Kopp et al. (2014) under a high emissions scenario (RCP 8.5). Estimates also reflect total coastal costs. In other words, costs from a baseline "no climate change" scenario, including only background local relative sea level changes unrelated to changing global sea level, have not been subtracted. Model runs were conducted on an Apple MacBook Pro laptop with a 2.8 GHz Quad-Core Intel Core i7 processor and 16GB of RAM.

2.5 Physical Model Inputs in SLIIDERS

2.5.1 Coastal Segments

To improve the traceability of data inputs and the efficiency of model optimization, we replaced the irregular DIVA coastal segments with segments based on the points at which ESLs are estimated in the Coastal Dataset for the Evaluation of Climate Impacts (CoDEC)~~,~~. This represents a roughly uniform, 50-km spacing of global coastline points (Muis et al., 2020). We made a number of slight alterations to the original CoDEC point set and ~~use~~ used these points as midpoints of 50-km coastline segments (Sect. A). The alterations ensured that (a) the coastline segments were nested by country boundaries, as the DIVA segments are, and (b) any extra points corresponding to offshore buoy gauges (used for validation in CoDEC) were removed. We also thinned European CoDEC points, originally provided at an extra fine 10km spacing, to 50km in order to have globally

uniform spacing. ~~We also manually added 15~~ In addition, we manually added 19 segments for small island states or small slivers of national coastlines not represented in the original CoDEC point set (e.g. Anguilla, Tokelau, Jordan's small coastline, etc.). The final subset of CoDEC coastal points utilized in pyCIAM totaled 9,~~087.~~ 568. Natural Earth coastlines were used to make the point-to-segment conversion (1:~~50m resolution for the majority of segments and 1:~~10m ~~for small island segments unresolved at coarser resolutions~~resolution[5]). The coastline lengths of each segment, used to calculate the potential costs of building protective barriers, were derived from this final set of segments (Sect. A1).

The decision to replace the coastal segments was motivated by several reasons. First, in the version of DIVA (v1.5.5) used in Diaz (2016), we found that many of the coastal segment lengths in high latitude regions were substantially overestimated, likely due to a geographic projection error. This error ~~looked~~ appeared to be corrected in versions of DIVA used in subsequent studies; however, we nevertheless wished to avoid dependence of pyCIAM on DIVA, with uncertainty surrounding its ongoing development support and dataset availability. Second, we found that DIVA contains a substantial over-representation of small, mostly unpopulated land masses in island regions within its set of 12,148 segments. For example, DIVA contains 1,316 individual segments for French Polynesia, constituting 10.8% of all global segments ~~despite~~ but representing less than 0.004% of global population. This created substantial computational inefficiencies, as all segments require roughly equivalent computation.

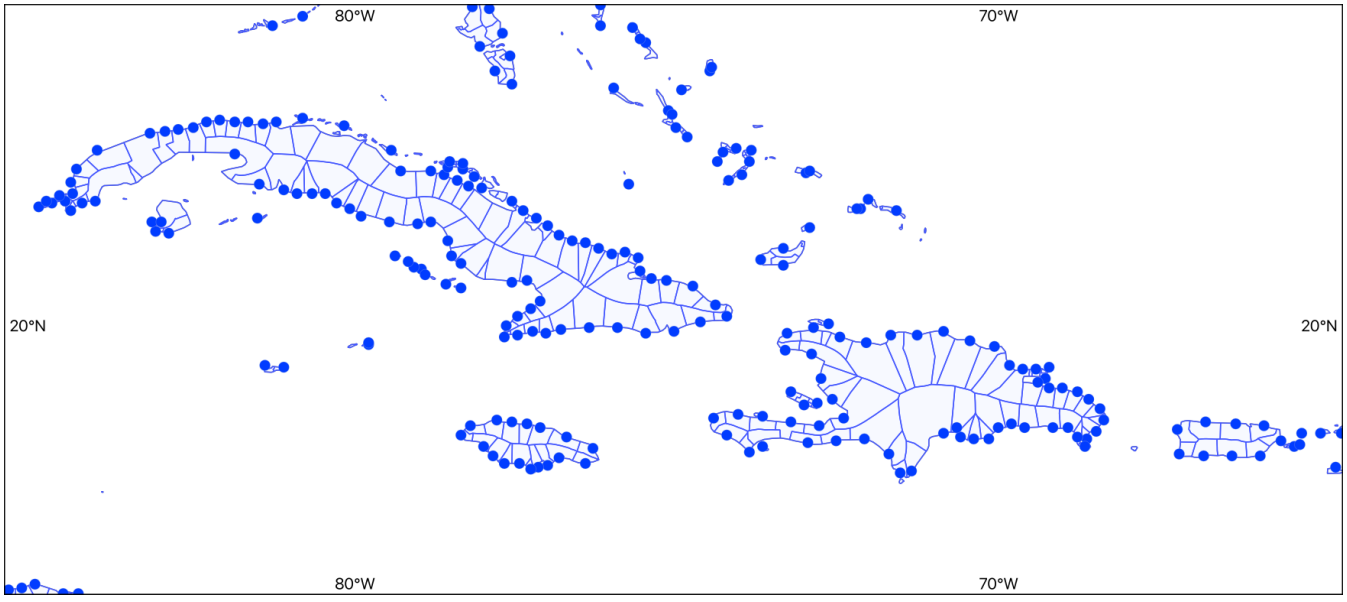

Figure 3. Example pyCIAM coastal ~~segment~~ segments (areas) and their centroids (points) ~~and areas~~ for a ~~subregion of~~ region within the Caribbean.

[5]The '1:10m' label indicates the scale of the physical vector layers, which can also be thought of as the maximum length of coastline across which simplification of complex coastlines into straight line segments can occur. 1:10m coastlines are the most granular product provided by Natural Earth.

2.5.2 Extreme Sea Levels

We obtained ESL distributions from CoDEC v1 (https://doi.org/10.5281/zenodo.3660927), which uses the third generation Global Tide and Surge Model (GTSM) combined with the ERA5 reanalysis to create a reanalysis product of historical sea levels (Muis et al., 2020). The CoDEC data provide the location and scale parameters of a Gumbel extreme value distribution fit to modeled ESLs at each coastline point, which we used to obtain the return periods required by CIAM (1, 10, 100, 1000, 10000-year). In validation analysis that compares CoDEC to observed tide gauge values, CoDEC values slightly underestimate annual ESL maxima by an average of 0.04m across all observed tide gauge stations, with 1-in-10 year mean ESL heights underestimated by 0.10m. Certain areas exhibit greater model bias, with 25% of tide gauge stations included in the validation showing absolute biases greater than 0.2m and 0.3m for annual and decadal maxima, respectively. In regions with a large tidal range and/or frequent tropical cyclones, biases are generally larger. See Muis et al. (2020) for a full discussion of CoDEC model validity.

2.5.3 Elevation

The use of accurate elevation data is crucial to appropriately representing sea level rise impacts (Kulp and Strauss, 2019). We ~~make three updates to the~~ have implemented an updated elevation model used to define the ~~the~~ population and physical capital exposed to SLR in pyCIAM ~~:~~ in the following manner.

1. We utilize the CoastalDEM ~~v1~~v2.1 dataset ~~(Kulp and Strauss, 2018)~~ (Kulp and Strauss, 2021) to define elevations at 1 arc-second resolution (roughly 30m). The v2.1 release of CoastalDEM represents further improvements to the initially-released product (v1.1) (Kulp and Strauss, 2018), though both datasets represent substantial accuracy improvements to prior DEMs, such as the widely used SRTM DEM. In addition to higher resolution elevation estimates compared to the 30-arc-second GLOBE DEM used in Diaz (2016), CoastalDEM significantly reduces bias found in ~~previous DEMs~~SRTM, as presented in a comparative analysis based on CoastalDEM's initial release (v1.1) (Kulp and Strauss, 2019). Compared to ~~the widely used SRTMDEM, CoastalDEM~~ SRTM, CoastalDEM v1.1 suggests that roughly three times the amount of present day population resides below projected high tide levels under low emissions sea level rise scenarios by 2100 globally (Kulp and Strauss, 2019). It should be noted that the high-resolution version of CoastalDEM v2.1 is the only input used in this study that is not publicly available. It is obtained via license with Climate Central, the developers of the DEM, though lower-resolution versions of the dataset are freely available for academic use. For the small number of regions that we model where CoastalDEM does not exist (e.g. above and below 60N and 60S, respectively), we derive elevations from the SRTM15+ v2~~.3~~ .5 dataset (Tozer et al., 2019).
2. We pair this DEM with ~~our~~ 30 arc-second population ~~(LandScan 2019 (Rose et al., 2020)~~estimates (LandScan 2021, Sims et al. (2022)) and capital stock (LitPop (Eberenz et al., 2020)) rasters, which allows for independent calculations of the distribution of land area, capital, and population with respect to elevation. ~~This differs from the approach used in Diaz (2016)~~We also rescale LitPop at the country-level to match more recently available data from Penn World Table 10.0 (Feenstra et al., 2015) and other sources (see Section 2.6.3). This approach differs from that of Diaz (2016), where

population and capital stock densities were defined at the segment level and assumed to be homogeneously distributed within a segment.

3. We discretize the distributions of population and capital to 0.1m elevation slices, rather than 1.0m.
4. We mask all pixels that are not hydraulically connected to the ocean at 20 meters of SLR from analysis. This screens out most inland low-elevation areas not exposed to SLR. 20 meters is the highest elevation bin that we consider, reflecting the upper end of the ESLs that we consider combined with the upper end of local RSLR.

2.5.4 Wetlands and Mangroves

For wetland areas, pyCIAM utilizes the European Space Agency's GLOBCOVER v2.3 global land cover dataset from 2009, offered at a 300m resolution (obtained in May 2021 from http://due.esrin.esa.int/page_globcover.php) (European Space Agency and UCLouvain, 2010). Three different land cover classifications from this layer, as defined in (Hu et al., 2017), were coded as "wetlands":

1. Closed to open ($> 15\%$) broadleaved forest regularly flooded (semi-permanently or temporarily) - Fresh or brackish water
2. Closed ($> 40\%$) broadleaved forest or shrubland permanently flooded - Saline or brackish water
3. Closed to open ($>15\%$) grassland or woody vegetation on regularly flooded or waterlogged soil - Fresh, brackish or saline water

Mangrove extents were updated using values from UNEP's Global Mangrove Watch 2016 dataset (Bunting et al., 2018) (obtained from https://data.unep-wcmc.org/datasets/45 in May 2021). The final wetland area used in pyCIAM consists of the spatial union of these two datasets.

2.5.5 Sea Level Rise

We ~~use the LocalizeSL framework (Kopp et al., 2014, 2017) () to "localize" probabilistic estimates of global SLR under a variety of assumptions of future global SLR and of the physical dynamics driving global ice sheet loss, similar to the approach taken in Sweet et al. (2017). Accounting for~~ integrate local SLR projections from 23 different future scenarios drawn from six different global and regional sea level change research efforts conducted in recent years. These are detailed in Table 2. We model and present results for the median projections for each of these ~~different assumptions better captures structural uncertainty in how a given amount of global SLR will result in a particular spatial pattern of local SLR .~~

~~The computational improvements included in pyCIAM enable the application of the model to large probabilistic ensembles of SLR scenarios. Specifically, we apply the model~~ 23 future SLR scenarios in this paper, although we also ran pyCIAM using the 17th and 83rd percentile SLR runs for all 23 scenarios. The broad range of scenarios covered in our analysis (from 0.25 to ~~110,000 Monte Carlo draws~~ 2m of GMSL rise in 2100) cover the plausible set of SLR trajectories; however, it can also be useful to assess the variation in impacts across different quantiles within a single scenario to assess uncertainty in impacts conditional on one emissions scenario. Such within-scenario assessment is outside of the scope of this manuscript but is an appropriate use of pyCIAM. To address this, results for the 17th and 83rd percentile of each SLR scenario are

available in the model output dataset available on Zenodo (Section 5). We also note that pyCIAM is also configurable to run a probabilistic large ensemble of SLR trajectories ~~generated from LocalizeSL. These draws correspond to 10,000 draws each from 11 input scenarios : RCP 2.6, 4.5, and 8.5 projections from Kopp et al. (2014), as used in Diaz (2016), these same RCPs paired with different models of Antarctic ice sheet loss from DeConto et al. (2021) and Oppenheimer et al. (2019), and two non-RCP scenarios using Structured Expert Judgment to quantify the magnitude of contributions from global ice sheet loss to global SLR under a world in which global mean surface temperature stabilizes in 2100 at either~~ on a multi-core computing platform, an approach used in recent research efforts using pyCIAM (Climate Impact Lab (CIL), 2022).

Our modeled future SLR pathways include the seven principal projections underlying the future sea level change trajectories detailed in the Intergovernmental Panel on Climate Change's (IPCC) Sixth Assessment Report (AR6) (Fox-Kemper et al., 2021) . The data for these projections were generated using the Framework for Assessing Changes To Sea Level (FACTS, Kopp et al. (2023)) and were obtained from the report's public data repository (https://doi.org/10.5281/zenodo.6382554) (Garner et al., 2022). These seven trajectories represent different combinations of future emissions and underlying physical processes that influence sea levels. These scenarios are partitioned into two groups: *low confidence* (n=2~~°C or~~) and *medium confidence* (n=5~~°C above pre-industrial temperatures~~), which refer to the relative level of confidence of the underlying physical processes reflected in each future scenario. *Medium confidence* projections are considered to be of higher likelihood but do not incorporate deeply uncertain physical processes, such as marine ice cliff instability, that could have large impacts on future sea levels, particularly in higher emission scenarios. These processes are represented in the *low confidence* AR6 projections and project higher end-of-century GMSL values compared to their *medium confidence* counterparts (Table 2).

It should be noted that each of the AR6 emissions scenarios were originally constructed using Integrated Assessment Models (IAMs) driven by a single socioeconomic trajectory (i.e. a single SSP). However, when assessing economic impacts of climate change it is often useful to separate future changes in welfare caused by non-climate-related socioeconomic trends from climate impacts. This is done by holding baseline growth rates fixed across emissions scenarios. For this reason, we assess damages from each of the AR6 emissions scenarios under each of the 5 SSPs, even though some emissions trajectories may be more or less plausible under different SSPs.

We also incorporate the five main SLR scenarios represented in the U.S. interagency Sea Level Rise Technical Report (2022), led by the National Oceanic and Atmospheric Administration (NOAA) (Sweet et al., 2022) and derived from the FACTS-based projections in Garner et al. (2022). The SLR pathways in this report were organized by their projected GMSL value in 2100~~, respectively (Bamber et al., 2019).~~ , rather than by global emissions trajectories. As such, they are grouped into five bins, based on different plausible GMSL values in 2100: Low (0.3m), Intermediate-Low (0.5m), Intermediate (1.0m), Intermediate-High (1.5m) and High (2.0m)[6]. These data were obtained from the report's public data repository (https://doi.org/10.5281/zenodo.6382554).

~~Each of these 11 scenarioscorresponds to particular assumptions about future emissions and the contributionsof ice sheets to SLR~~The remaining 11 SLR projections are derived from the LocalizeSL framework (Kopp et al., 2014, 2017) (https://

[6]These GMSL values are expressed relative to GMSL in 2000, while pyCIAM expresses GMSL relative to 2005, making its end-of-century values associated with these scenarios in pyCIAM approximately 2cm lower (Table 2) than those specified in (Sweet et al., 2022).

doi.org/10.5281/zenodo.6029807). LocalizeSL was used in the IPCC AR5 report (Church et al., 2013) and in subsequent publications (e.g. Kopp et al. (2017), Sweet et al. (2017), Rasmussen et al. (2018), Bamber et al. (2019), DeConto et al. (2021) , Tebaldi et al. (2021)) prior to the introduction of FACTS. Similar to the AR6 SLR projections derived from FACTS, these based on LocalizeSL reflect a distribution across emissions scenarios, as well as across the component models used to represent the various contributing factors to SLR. These differences in component models refer to alternate assumptions and process representations regarding all contributors to sea level rise, with particularly influential differences in assumptions relating to ice sheet contributions. ~~At the high end of these projections, contributions from poorly constrained ice sheet instability could drive total GMSL rise approaching 2 m (Bamber et al., 2019; DeConto et al., 2021; Fox-Kemper et al., 2021)~~

Overall, these 23 scenarios cover a likely range of plausible SLR trajectories in the 21st century and allow us to estimate the marginal welfare costs of additional SLR across this full range (Fig. 4). Scenarios based on emissions trajectories may be most relevant for users interested in evaluating the benefits of emissions mitigation while those based on GMSL levels may be most relevant for local planners seeking to design adaptation strategies.

~~Each of the 10, 000 draws within each scenario corresponds to an equally likely realization of global and local SLR trajectories, conditional on those assumptions. For the~~ Notably, each of these scenarios contains a Monte Carlo sampling of a distribution of local SLR projections. However, because the 23 scenarios we reflect in this analysis cover a broad range of outcomes, for the purposes of this paper, we present results ~~from each of these different SLR scenarios that correspond to the median draw~~ only for the median SLR projection at each coastal segment. In other words, the ~~results for each SLR scenario reflect the impacts experienced by each segment~~ presented results reflect impacts in a world in which ~~the emissions and ice sheet dynamics of that scenario play out, and each region of the world experiences the~~ all regions experience the median projected RSLR for that scenario. Given the computational improvements in pyCIAM and its scalable design, it is suited for execution on a full Monte Carlo distribution. Climate Impact Lab (CIL) (2022), for example, applies CIAM to a 110,000-sample ensemble, using 10,000 draws from each of the 11 LocalizeSL-based SLR projections.

In addition ~~, similar to~~ to projections of climate change-induced SLR, and in alignment with Diaz (2016), we run a "no climate change" counterfactual scenario in which all SLR components are set to 0 except for a spatially heterogeneous and empirically estimated background rate of change parameter that includes drivers assumed to be unaffected by climate change (e.g. glacial isostatic adjustment, tectonics, sediment compaction, and other processes contributing to vertical land motion). This is a probabilistic parameter in the LocalizeSL ~~framework~~ and FACTS frameworks that is held fixed across ~~the 11 scenarios . Within each scenario draws from the "no climate change" scenario are matched to those from the 11 "climate change" scenarios such that each group of 12 draws experiences the same~~ all scenarios from a given modeling framework. The impacts estimated under these scenarios are subtracted from those in the climate change-driven scenarios to isolate the contributions of climate change to global 21st century coastal economic impacts (see Fig. 4).

To estimate local sea level extremes, we linearly combine the fixed ESL distributions from CoDEC with an annually interpolated version of the decadal SLR projections from each of these 23 scenarios. This allows us to maintain a globally consistent representation of extremes at reasonably fine resolution. Limitations of this "local bathtub" approach are described in Section 3.3.

ID	SLR Scenario	Model Used	GMSL in 2100 [m] (median)
NCC	No Climate Change*	CIAM, pyCIAM	0.00
AR6-Med	IPCC AR6 *Medium Confidence* (2021): SSP1-1.9, SSP1-2.6, SSP2-4.5, SSP3-7.0, SSP5-8.5	pyCIAM	0.38, 0.44, 0.56, 0.68, 0.77
AR6-Low	IPCC AR6 *Low Confidence* (2021): SSP1-2.6, SSP5-8.5	pyCIAM	0.45, 0.88
Sweet	US Interagency SLR Technical Report (2022): Low, Int-Low, Int, Int-High, High	pyCIAM	0.28, 0.48, 0.98, 1.48, 1.98
K14	Kopp et al. (2014): RCP 2.6, RCP 4.5, RCP 8.5	CIAM, pyCIAM	0.48, 0.58, 0.78
SR	IPCC-SROCC (2019): RCP 2.6, RCP 4.5, RCP 8.5	pyCIAM	0.49, 0.60, 0.88
B19	Bamber et al. (2019): Low (2° C), High (5° C)	pyCIAM	0.68, 1.10
D21	DeConto et al. (2021): RCP 2.6, RCP 4.5, RCP 8.5	pyCIAM	0.52, 0.62, 1.10

*Includes local background rates of relative sea level rise at each segment due to non-climatic ~~rates of RSLR.~~ background processes. Because of model differences, the FACTS-based projections (AR6 and Sweet) will use slightly different no-climate-change scenarios than those based on LocalizeSL.

Table 2. GMSL rise between 2005 and 2100 for each median SLR scenario used in the pyCIAM and Diaz (2016) models, representing the x-axis positions of costs by scenario displayed in Fig. 4.

Values for median GMSL rise throughout the 21st century are detailed in Table 2 below. For reference, an equivalent table for the 17th and 83rd percentile SLR projections for each scenario is provided as Supplemental Table C1.

2.6 Socioeconomic Variables

2.6.1 Population

In SLIIDERS, we use information from LandScan ~~2019 (Rose et al., 2020)~~ 2021 (Sims et al., 2022) to represent the present-day spatial distribution of population~~, scaled such that the aggregated country level population estimates match the 2019 estimates contained within the Penn World Table (PWT) v10.0 (Feenstra et al., 2015). In pyCIAM, we~~ . We then maintain this within-country distribution and scale the country totals to match the SSPs (Riahi et al., 2017), exponentially interpolated between ~~bi-decadal~~ 5-year projections to annual values. Because the SSPs begin in 2010 and pyCIAM ~~, like Diaz (2016), begins in 2000~~begins in 2005, we must scale populations back to ~~2000.~~ 2005. To do so, we use observed country-level growth rates from ~~2000~~ 2005 to 2010 ~~and apply these to SSP2 to estimate an initial population that is used for all SSPsin 2000.~~ to backcast from the 2010 SSP projections, which are constant across all SSPs. Observed rates are drawn ~~from PWT~~primarily from the Penn World Table (PWT) 10.0 dataset (Feenstra et al., 2015), with missing countries filled ~~by the 2019~~ through a variety of sources including the 2022 UN World Population Prospects ~~(UN DESA, 2019).~~ (United Nations, Department of Economic and Social Affairs, Popu , multiple iterations of the CIA World Factbook (Agency, 2021), World Bank World Development Indicators (WDI, Bank (2021)), and local government statistics for some small island states. To project population forward For countries and territories not covered by the SSP data, we use global average population growth rates applied to 2010 estimates.

2.6.2 GDP

pyCIAM combines SSP-consistent, country-level GDP projections ~~(from IIASA~~ from two growth models - one from IIASA (Crespo Cuaresma, 2017) and one from the Organisation for Economic Co-operation and Development (OECD, Dellink et al. (2017)) OECD) and ~~OECD) and~~ population projections ~~(from IIASA) to create projected~~ from IIASA (Kc and Lutz, 2017) to create country-level ~~income (i.e.,~~ GDP per capita ~~) values~~ projections. These data are available on the SSP Database (Riahi et al., 2017). SSP interpolation and extrapolation approaches match those used for population values. Observed values for 2005-2010 are again drawn from PWT 10.0 where available, with alternative sources including (Fariss et al., 2022), OECD Regional Statistics (for Economic Cooperation and Development, 2020), the 2021 International Monetary Foundation World Economic Outlook (IMF, 2021), and the WDI. Where and when country-level estimates are unavailable but estimates do exist for associated sovereign entities, we use a regression estimator described in Bertram (2004) to estimate per capita GDP for the territories. For the countries and territories not covered by IIASA and OECD projections, we take the global-average ~~income~~ per capita estimates in 2010 and interpolate/extrapolate using the global average yearly growth rates for missing years.

~~While we do not use historical GDP directly in the pyCIAM workflow, we utilize it in deriving the initial 2010 country level capital stock values; the methodology is described in Sect. A3. For this, we primarily derive historical national GDP levels between the years 1950 to 2020 from PWT 10.0. For countries and territories not covered by PWT 10.0, this data is augmented by multiple sources in a specified order of preference. These sources, in order, are the World Bank World Development Indicators (Bank, 2021), the 2021 IMF World Economic Outlook (IMF, 2021), the Maddison Project database (Bolt and van Zanden, 2020), OECD regional statistics (for Economic Cooperation and Development, 2020), the CIA World~~

Factbook (Agency, 2021), various national account information sources, and academic papers (Treadgold, 1998, *Pacific Economic Bulletin*; Treadgold, 1999, *Asia Pacific Viewpoint*). Any remaining missing historical values of income and GDP per capita were imputed using income growth rates (further detail in Sect. A3).

To create per capita income GDP estimates (ypc) for coastal segments in pyCIAM for each year (t), we use the same national-to-segment downscaling approach as Diaz (2016), which assumes that urban coastal areas tend to have higher incomes than national average incomes, as follows:

$$ypc_{t,\text{segment}} = ypc_{t,\text{country}} \max\left\{1, \left(\frac{\sigma_{t,\text{segment}}}{250}\right)^{0.05}\right\}$$

where σ represents population density , in people per square kilometer, at the segment level. The 250 value is a population density constant that signifies an assumed dividing threshold between urban and rural areas and the income elasticity value of 0.05 is based on a regression presented in Lagerlöf and Basher (2005). relates population density to income. See Equation 8 in the Diaz (2016) Supplemental Information for further details. In Diaz (2016) population density is assumed to be homogeneous within segment, and thus which implies that all elevation slices within a coastal segment are prescribed the same local income. In pyCIAM, each elevation slice within each region has a unique population density. Thus, we apply this downscaling approach separately to each elevation slice.

2.6.3 Physical Capital

In addition to assessing the exposure of human population to SLR-related hazards, pyCIAM also assesses the exposure of physical capital stock to these threats. Both the IIASA (Crespo Cuaresma, 2017) and OECD (Dellink et al., 2017) and OECD GDP growth models utilize projections of capital growthphysical capital; however, neither model has publicly released these projections. Therefore, to create future capital stock estimates, we extract the capital relevant growth equations for the OECD's Env-Growth model as described in Dellink et al. (2017). The capital growth trajectory in the IIASA model is exogenously specified, constant across SSP scenario, and yielded implausibly large capital stocks in later years. For instance, the IIASA model projects that Macau experiences a capital growth rate of 14% per annum from 2010 to 2100. This trajectory implies that Macau reaches $30.8 quadrillion in 2100 capital stock, which is 23 times that of the U.S. in 2100 ($1.3 quadrillion) and 200,000 times that of Macau in 2010 ($134 billion) (all values in constant 2019 PPP USD). Due to such implausible growth rates, we do not use the IIASA capital growth trajectory in pyCIAM.

We use country-level 2010 capital stock information from PWT 10.0 (Feenstra et al., 2015) capital stock estimates up through 2020 and then use 2020 estimates as the initial conditions for this growth model. For the countries not represented in PWT Like with population and GDP, historical estimates of capital come primarily from PWT 10.0(Feenstra et al., 2015), pyCIAM combines physical capital data from Global Assessment Report (GEG-15) (Bono and Chatenoux, 2014) and LitPop (Eberenz et al., 2020) (for the years 2005 and 2014, respectively) , historical GDP values, and methods from Higgins (1998) and Inklaar et al. (2019) to estimate 2010 capital stock . . Where these values are missing and outside of the special cases of Cuba and North Korea, SLIIDERS uses estimates of the ratios of non-financial wealth (NFW) to GDP derived from the 2022 Credit Suisse Global Wealth Databook (Credit Suisse Research Institute, 2022), combined with nominal GDP information

from United Nations System of National Accounts (UNSD, 2021). Following the approach taken in (Eberenz et al., 2020), we then multiply PPP GDP by these NFW-to-GDP ratios to acquire proxies of physical capital. For Cuba, we use the ratio of Cuban and the U.S. capital stock values from Berlemann and Wesselhöft (2017) and multiply this ratio with the U.S. capital stock values from PWT 10.0. For North Korea, we multiply the capital-to-GDP ratio in Pyo and Kim (2020) with PPP GDP.

Then, we apply the OECD capital stock equations with the estimated ~~2010~~ 2020 capital stock values and SSP-consistent GDP projections to obtain projections of capital stock for each SSP scenario and for each GDP growth model. To parameterize these equations, we use a value for the partial elasticity of GDP with respect to capital taken from Crespo Cuaresma (2017) (0.326), since this is not reported in Dellink et al. (2017). We also estimate country-specific initial conditions for the marginal product of capital using a modified Cobb-Douglas production function fit to the historical capital ~~and income~~ data. See Sect. A3 for further methodological detail.

pyCIAM uses the LitPop dataset (Eberenz et al., 2020) to represent within-country spatial distribution of physical capital stock at 30 arc-second resolution. LitPop combines population information from the Gridded Population of the World dataset (v4.1) (University, 2016) with nightlight intensity (Román et al., 2018) to downscale country-level estimates of total physical assets. In some countries, e.g. Libya and Syria, LitPop does not provide any downscaled estimates. In these locations, we use the downscaled estimates provided by the GEG-15 dataset (Bono and Chatenoux, 2014). For the small number of island countries that do not have capital distributions reflected in either dataset, we assume homogeneous capital stock.

In pyCIAM, the ratio of mobile to immobile capital is used to determine costs of inundation. Diaz (2016) used a fixed ratio of 10%. However, PWT 10.0 contains country-level information that can be used to estimate across-country heterogeneity in this ratio. PWT decomposes physical capital into four categories:

1. Residential and non-residential structures
2. Machinery and non-transport equipment
3. Transport equipment
4. Other assets

For SLIIDERS, we assume that the first category (residential and non-residential structures) represents immobile capital and the others represent mobile capital. We take the average mobile fraction from 2000-2019 and apply this at the country level. These country specific values vary from 1% (Haiti) to 52% (Equitorial Guinea) with 25th, 50th, and 75th percentiles of 14, 18, and 20%, respectively.

2.6.4 Construction Costs

We maintained the same reference unit cost of coastal protection utilized in CIAM but updated the national construction cost index scaling factors by using the ratio of construction cost indices from ICP 2017 (World Bank, 2020) instead of 2011. For countries not included in this dataset, we augment with the country-level construction cost indices used in Lincke and Hinkel (2021), averaged across the rural and urban distinction.

2.7 Other Features

2.7.1 Model Duration

Diaz (2016) runs from 2000-2200. However, the SSPs stop at 2100 and thus the ~~SLIIDERS-ECON~~ SLIIDERS dataset does as well. Because of this, and because the AR6 SLR scenarios begin in 2005, we limit pyCIAM to ~~2000-2100~~2005-2100. Using the 4% discount rate employed in Diaz (2016) and pyCIAM, the discount factors for 2100-2200 costs vary from 2% in 2100 to ~~0.04~~0.03% in 2200, so the exclusion of these additional years is unlikely to have a substantial effect on the optimal adaptation option selected by each segment.

2.7.2 Timesteps and Planning Periods

We increase temporal resolution from the decadal timesteps used in Diaz (2016) to annual. In addition to the exponential interpolation of ~~bi-decadal SSP inputs ,~~ 5-year SSP inputs described above, decadal SLR projections are linearly interpolated to yield annual values. The 40-50 year planning periods used in Diaz (2016) yield substantial step-changes in realized costs at mid-century and end-of-century due to substantial simultaneous global adaptation actions. To generate a smoother time series of costs, we use decadal planning periods. A potential trade-off of using shorter planning periods is that this may overestimate the frequency with which governments and populations are able to update major adaptation actions. An unrealistically agile representation of large-scale adaptation actions may underestimate associated ~~costs~~net present cost because some adaptation costs can be postponed to future years with lower discount factors. Future work may empirically estimate the frequency at which adaptation approaches are updated and explore further options for incorporating planning periods that are not globally simultaneous and thus do not lead to substantial step-changes in global SLR costs at the start of each period.

2.7.3 Net Present Value Calculation

In ~~pyCIAM~~Diaz (2016), the NPV each segment uses to calculate an optimal adaptation approach is calculated from 2010-2200, excluding the initial planning period of 2000-2009. In this way, each segment is allowed a "free" initial relocation or protection action. For example, if a segment chooses to protect to the 1-in-10,000 year ~~ESL~~ sea level height, which is 3 meters in 2000, they do not consider the costs of building a corresponding seawall when calculating the NPV of this action. They only consider the marginal cost of extensions to this seawall to remain at the 1-in-10,000 year height as local sea levels increase. ~~This is not reflective of the full costs of relocation or protection. Thus, in pyCIAM, we include these initial costs in the NPV calculation, using the~~

The rationale for this initial "spin-up" period in Diaz (2016) was to allow each segment to choose an optimal adaptation approach without including costs for adaptation measures that may already exist but are not reflected in observed values due to the lack of high quality global input data describing population distribution and coastal protection measures. In other words, segments were allowed to choose their optimal adaptation approach based only on adaptation costs associated with *updating*

adaptation (e.g. through height increases of protection or additional managed retreat) but not based on the costs of initial implementation (e.g. the initial protection construction or managed retreat).

By using finer resolution population and capital stock estimates, SLIIDERS partially ameliorates this need by providing more accurate observed measures of coastal exposure. In addition, we argue that any existing adaptation measures would have to have been implemented at some point in history when they were presumably determined to be a cost-effective approach, even including the initial costs of implementation. This deviates from the assumption in Diaz (2016) that such initial adaptation does not incur costs, which we believe is likely to overestimate the state of present-day adaptation. Including the costs in this "spin-up" period when calculating NPV, along with calibrating the non-market costs of relocation (see Section 2.3), reduces the amount of instantaneous relocation observed under the optimal adaptation scenario.

For these reasons, in the configuration of pyCIAM presented here, each segment uses costs from the entire model duration of ~~2000-2100.~~ 2005-2100, inclusive of the initial adaptation costs, to calculate NPV and choose an optimal adaptation approach. This configuration is applied to costs from all scenarios, including those from the "no climate change" counterfactual scenario that are subtracted from the "with climate change" scenarios in order to isolate the climate change contributions to coastal welfare impacts.

~~In addition,~~ Because of this consistency in application, the choice of the initial NPV year is likely to have a minimal effect on the estimated climate change costs. However, it will substantially affect the "un-differenced", total costs associated with both the "with climate change" and "no climate change" in the initial adaptation period. This is reflected in substantially different NPV calculations between this paper and Diaz (2016) in this un-differenced context (see Fig. B1). pyCIAM provides users with a configurable parameter to determine whether initial adaptation costs should be accounted for in each segments NPV calculation or not.

In addition to modifying the starting year of the NPV calculation, we make one change to the application of a discount rate. Diaz (2016) applied the discount rate at the start of each decadal timestep to the full 10 years of costs incurred in that timestep. This approximation overestimates the discounted cost for all years after the first. We avoid this issue by using annual timesteps; however, when comparing NPV results to Diaz (2016) (Fig. 4), we apply annually varying discount rates to the Diaz (2016) outputs as well.

2.7.4 ~~Observed Present-Day Protection~~

~~In Diaz (2016), no observed protection standards were included. In pyCIAM, we use the National Levee Database (US Army Corps of Engi to define protected areas in the U.S. and we assume that all population and capital stock in the Netherlands is protected due to the country's massive "Delta Works" project. All population, capital, and land area within these areas are excluded from SLIIDERS-ECON and from the pyCIAM model. Future work will increase the spatial coverage and improve the representation of present-day protections.~~

2.7.4 Manual Correction Factors

In pyCIAM, the following manual correction factors in the original code underlying Diaz (2016) have been removed. These correction factors were originally used by Diaz (2016) in order to correct for certain limitations in data availability or quality that are no longer necessary after incorporating the data updates in SLIIDERS:

1. Doubling the price of construction on all "island" segments. The new construction cost index values utilized in pyCIAM should ~~theoretically capture~~ reflect any increased construction costs on island nations. Additionally, segments defined as "island" in CIAM were not entirely consistent, with some islands receiving the label and others not.
2. Halving the protection heights under the protection adaptation scenario corresponding to 10-year ESL heights. This was originally implemented to account for elevation profiles found in the GLOBE DEM that were deemed physically implausible (extremely high area totals from 0-1m), but is no longer required following the updated CoastalDEM elevation values.
3. Averaging of the inundated land area-by-elevation bins for the first two (0-1m, 1-2m) bins in order to smooth the elevation profile due to the high 0-1m area totals in the GLOBE DEM values. This adjustment, too, is no longer required following the updated CoastalDEM elevation values.

3 Results and Discussion

Upon implementing the changes described above, global costs estimated by pyCIAM diverge modestly from those in Diaz (2016). Additionally, we obtain estimates for a greater breadth of socioeconomic and ~~emissions scenarios, using multiple assumptions of ice sheet instabilities to~~ SLR trajectories that reflect deep uncertainty in these processes. Fig. 4 displays estimated global costs for the following global SLR-driven cost metrics reported in Diaz (2016): (i) ~~end-of-century annual costs of wetland loss~~global net present costs under an optimal adaptation scenario using a 4% discount rate, (ii) ~~,~~end-of-century annual total costs under ~~an optimal adaptation~~ that same scenario, (iii) end-of-century annual total costs under a "reactive retreat only" scenario, and (iv) ~~global net present costs using a 4% discount rate~~end-of-century annual costs of wetland loss under the optimal adaptation scenario. Global NPV and end-of-century costs for the highlighted scenarios in Fig. 4 and for a "middle of the road" socioeconomic growth scenario (SSP2/IIASA) are shown in Table 3.

Results are shown for the pyCIAM model both in its replicated CIAM configuration and after all the above changes were applied. Values are expressed such that each vertical group of points comprise the spread of results between the different socioeconomic projections for a given SLR scenario, with the position along the x-axis representing that scenario's median GMSL value in 2100. As described in Sect. 2.5.5, all of the pyCIAM results use a constructed "median" SLR trajectory where each location experiences the median RSLR across the probabilistic projected distribution. This matches the approach ~~in Diaz (2016), used to create the displayed CIAM results~~used in Diaz (2016).

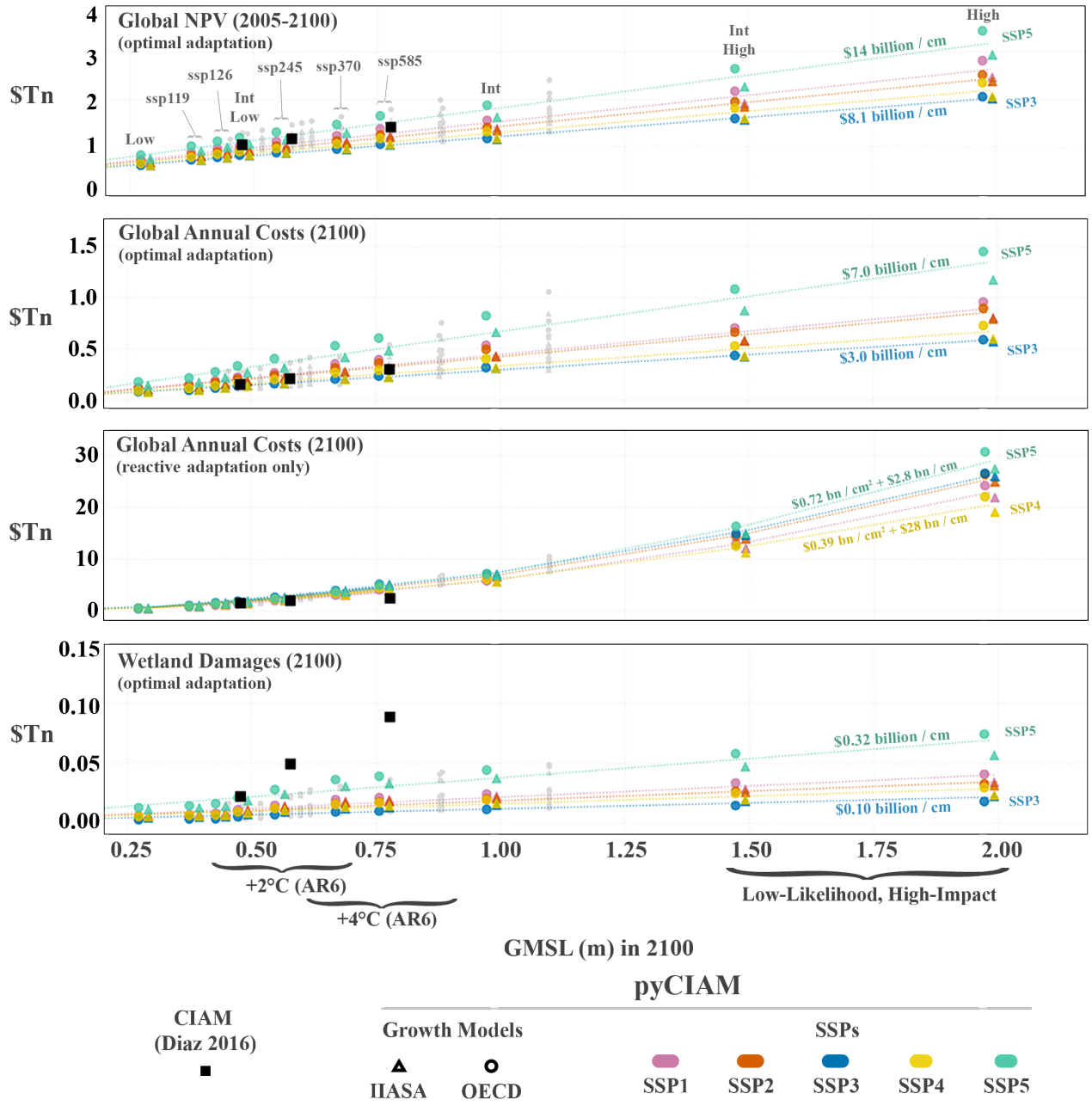

Figure 4. Comparison of global cost estimates under each SLR scenario. Values are costs from climate change induced SLR only, i.e. after differencing the costs under a "no climate change" scenario that reflects median projections of non-climatic RSLR rates and no GMSL rise. All costs are expressed in constant 2019 PPP USD. Each vertical group of points describes a single SLR scenario, with each point in the group representing a unique combination of SSP and economic growth model. For visual clarity, only *medium confidence* AR6 and Sweet et al. (2022) scenarios are indicated with colored markers and jittered slightly along the x-axis based on runs using the OECD (-1cm) or IIASA (+1cm) economic growth model. The remaining SLR scenarios are shown in grey without jitter. Dashed lines represent fitted relationships between the cost metric and 2100 GMSL across the full set of SLR scenarios. Relationships are estimated for each SSP scenario and are linear for all metrics except for global annual costs under a reactive adaptation scenario.

ID SLR Scenario	SLR Scenario GMSL [m] (2100)	Model Used NPV $Tn (bp) *Optimal*	2100 median GMSL NPV $Tn (bp) *Reactive*	Costs (2100) $Tn (bp) *Optimal*	Costs (2100) $Tn (bp) *Reactive*
[m0.5ex] Low (Sweet et al.)	0.28	0.66 (1)	1.21 (3)	0.09 (2)	0.56 (11)
NCC SSP1-1.9 (AR6-Med)	No Climate Change* 0.38	CIAM, pyCIAM 0.80 (2)	0.00 2.00 (4)	0.12 (2)	1.03 (20)
[0.5ex] K14 SSP1-2.6 (AR6-Med)	Kopp 0.44	0.86 (2)	2.41 (5)	0.15 (3)	1.47 (28) 0.5ex 0.5ex>
Int-Low (Sweet et al.2014 (RCP 2.6, RCP 4.5, RCP 8.5)	CIAM, pyCIAM 0.48	0.49, 0.59, 0.79 0.91 (2)	2.46 (5)	0.18 (3)	1.74 (33)
[0.5ex] SR SSP2-4.5 (AR6-Med)	IPCC-SROCC (RCP 2.6, RCP 4.5, RCP 8.50.56	0.98 (2)	pyCIAM 3.28 (7)	0.49, 0.61, 0.89 0.21 (4)	2.46 (47)
[0.5ex] B19 SSP3-7.0 (AR6-Med)	Bamber 0.68	1.08 (2)	4.15 (9)	0.27 (5)	3.66 (69) 0.5ex 0.5ex>
SSP5-8.5 (AR6-Med)	0.77	1.20 (3)	5.24 (11)	0.31 (6)	4.79 (91) 0.5ex 0.5ex>
Int (Sweet et al.2019 (Low, High)	pyCIAM 0.98	0.69, 1.11 1.34 (3)	6.19 (14)	0.42 (8)	6.64 (126)
D21 Int-High (Sweet et al.)	DeConto 1.48	1.84 (4)	13.62 (30)	0.58 (11)	13.93 (264) 0.5ex 0.5ex>
High (Sweet et al.2021 (RCP 2.6, RCP 4.5, RCP 8.5) [0.5ex]	pyCIAM 1.98	0.53, 0.63, 1.11 2.38 (5)	24.61 (54)	0.79 (15)	24.85 (471)

*Includes local background rates of relative sea level rise at each segment due to non-climatic background processes.

Table 3. GMSL rise between 2000 Global estimated NPV (2005-2100) and annual costs of climate-driven SLR in 2100, expressed in constant 2019 PPP USD, for each the *medium confidence* AR6 and Sweet et al. (2022) SLR scenario used in scenarios. Each metric is presented for

~~Estimated annual average costs in 2100 by "admin 1" region (equivalent to state-level in the U.S.). Results shown reflect optimal adaptation, using the IPCC - Special Report (SROCC - RCP 8.5) SLR scenario and SSP2/IIASA socioeconomic projections.~~

~~Estimated annual adaptation benefits in 2100 by "admin 1" region (equivalent to state-level in the U.S.). Results shown reflect the IPCC - Special Report (SROCC - RCP 8.5) SLR scenario and SSP2/IIASA socioeconomic projections.~~

~~Comparison of four global cost metrics for median model results under each SLR scenario, for CIAM (black) and pyCIAM (colored). Values represent costs from climate change induced SLR only, i.e. after differencing the time series of costs under a "no climate change" scenario with median non-climatic RSLR rates and no GMSL rise. All costs are expressed in constant 2019 PPP USD. Each vertical group of points represents a single SLR scenario (Table 2), with each point in the group representing a unique combination of SSP and growth model. n.b. The D21-RCP8.5 and B19-High SLR scenarios share the same projected GMSL in 2100 (1.11m) and were jittered by +/- 0.007m for plotting clarity.~~

3.1 Total SLR Costs

The global distribution of end-of-century average annual costs of climate-driven SLR under optimal adaptation, aggregated to ~~"admin 1"~~ first-level administrative regions (equivalent to state-level in the U.S.), is shown in Fig. 5, using the ~~SROCC-RCP8~~AR6 (*medium confidence*) SSP2-4.5 SLR scenario and SSP2-IIASA socioeconomic trajectory. Fig. 6 similarly demonstrates spatial heterogeneity in the ~~total benefits~~ annual cost savings realized through optimal adaptation, relative to ~~the "reactive retreat only"~~ costs in the reactive retreat scenario.

~~Generally, global estimates of the SLR-driven costs of climate change in pyCIAM are similar to those of Diaz (2016) (Fig. 4).~~

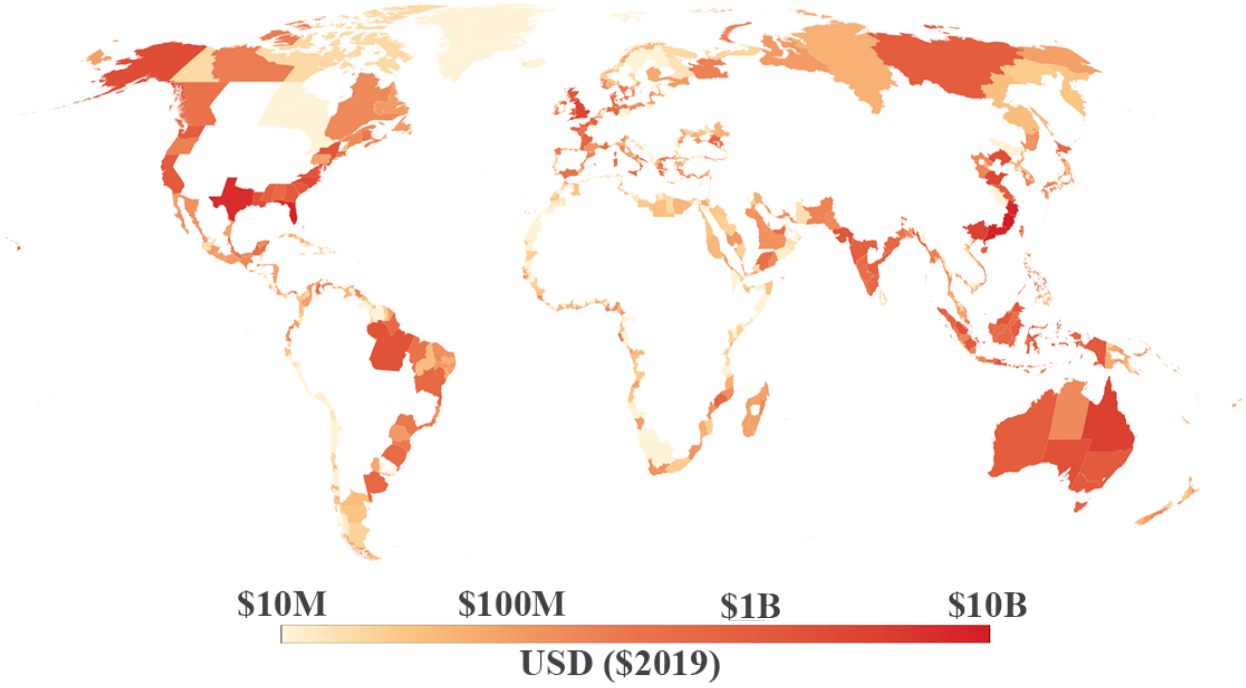

Figure 5. Example estimated annual average costs in 2100 by first-level administrative region (equivalent to state-level in the U.S.). Results shown reflect optimal adaptation, using the AR6 (*medium confidence*) SSP2-4.5 SLR scenario and SSP2, IIASA socioeconomic projections.

Median global NPV values from ~~2000-2100~~ 2005-2100 under optimal adaptation ranges from ~~$680~~ 00 billion to $~~2.1~~ 3.4 trillion in pyCIAM across its ~~110 SLR-SSP-IAM~~ 230 SLR-SSP-economic growth model scenarios, corresponding to end-of-century GMSL rise values between ~~0.49 and 1.11m.~~ 0.28 and 1.98m, relative to 2005 mean sea level (Fig. 4). Estimates of global NPV from Diaz (2016) range from $~~1.1 to $1.5~~ 1.0 to $1.4 trillion in the three SLR scenarios considered (end-of-century GMSL rise from ~~0.49 to 0.79~~0.48 to 0.78m, Table 2). Comparing the three SLR scenarios used in pyCIAM that match those employed in Diaz (2016) (K14 RCPs 2.6, 4.5, 8.5), pyCIAM's median global NPV values from ~~2000-2100 are generally slightly below~~ 2005-2100 are similar to those estimated by CIAM, with some socioeconomic projections yielding higher estimates and some yielding lower (Fig. 4, Table ~~??). However, when~~ C2).

When considering total damages~~under both the 11 "climate change" scenarios and the "no climate change" scenario~~, rather than the difference between them, pyCIAM estimates significantly higher global NPV (~~3-4x~~~5-6x) and moderately higher end-of-century costs ~~than~~ (~2x) compared to Diaz (2016) (Fig. B1). ~~This may be largely attributed to the fact that~~ There are several reasons for these differences. First, the decision to include initial adaptation costs in the NPV calculation and optimal adaptation selection for each segment contributes to the substantially higher NPV values seen in pyCIAM (see Section 2.7.3). Second, we use a calibrated value for non-market relocation costs almost an order of magnitude larger than that used in Diaz (2016) (see Section 2.3). This drives more segments toward choosing protection and thus drives up global construction and maintenance

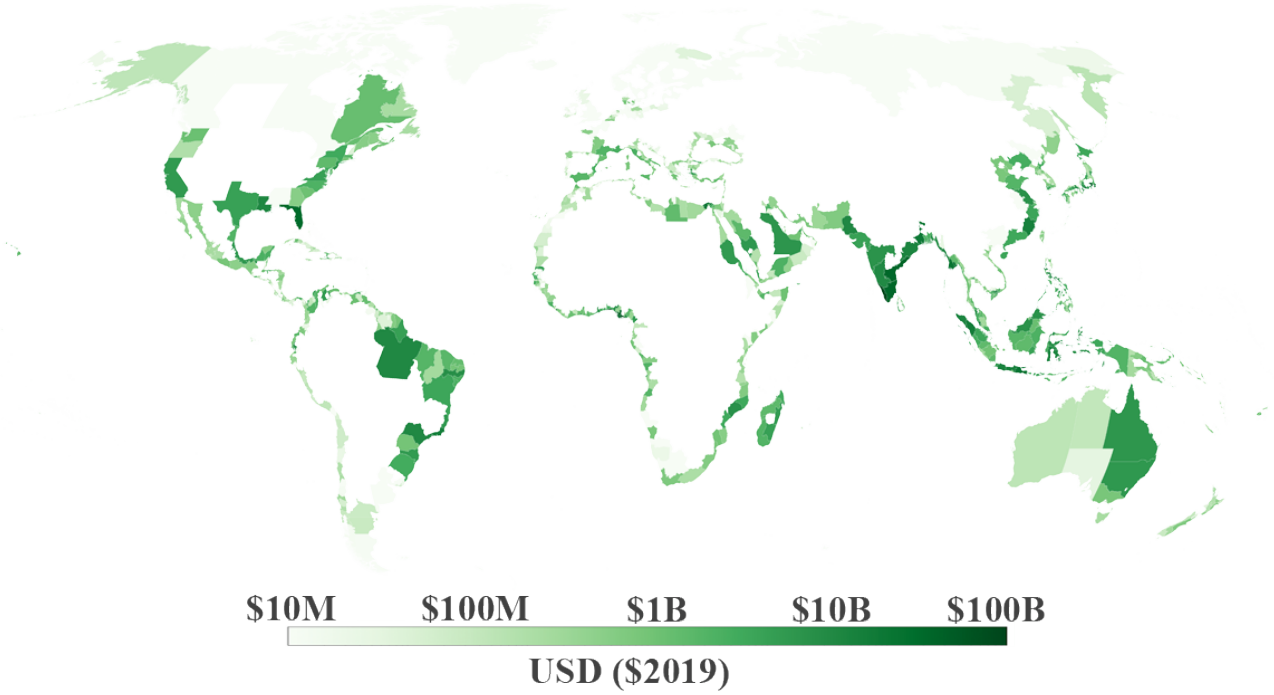

Figure 6. Example estimated annual adaptation benefits in 2100 by first-level administrative region (equivalent to state-level in the U.S.). Results shown reflect the AR6 (*medium confidence*) SSP2-4.5 SLR scenario and SSP2, IIASA socioeconomic projections.

costs in addition to relocation costs. Third, Diaz (2016) assumes that all abandoned capital has fully depreciated by the time of abandonment for proactive retreat scenarios, while pyCIAM avoids this assumption due to a lack of empirical evidence (Section 2.2.1). Fourth, in Diaz (2016), segments choosing reactive adaptation were assumed to retreat at least up to a height deemed optimal under current sea levels. This often led to retreat higher than mean sea level in order to minimize ESL-related damages; however, land abandonment and relocation costs were not assessed for this full retreat height. Instead, they were only assessed up to mean sea level, lowering estimated costs for these two cost types. Fifth, Diaz (2016) reduced the 10-year protection height by 50% for all segments as an ad hoc adjustment to account for an implausibly large land area contained in the 0-1m elevation slice, as reported by DIVA and derived from GLOBE DEM (Section 2.7.4. Sixth, projected capital stock and population in SLIIDERS across its SSP and growth model scenarios are significantly higher than those modeled in Diaz (2016). For example, the mid-century global capital stock located between 0 and 15 meters above sea level ranges from $~~210~~ 220 to $370 trillion (2019 USD) across the five SSPs and two growth models in SLIIDERS, compared to $97 trillion in Diaz (2016). Similarly, SLIIDERS' mid-century population ranges from ~~1.39 to 1.58 billion people~~ 1.19 to 1.35 billion people across the five SSPs (population is equivalent in each economic growth model), compared to 1.18 billion in Diaz (2016). The SSP-based ranges differ most from the Diaz (2016) trajectories around mid-century before beginning to converge toward end-of-century. ~~This behavior aligns with the observation that end-of-century annual costs are more similar across pyCIAM and Diaz (2016)~~

~~than total NPV~~Finally, higher modeled costs in pyCIAM may also be driven by updated topographic maps and other physical input datasets used for estimating exposure to SLR in pyCIAM.

Annual global costs due to climate-driven SLR in 2100 under optimal adaptation range from $~~85~~ 70 billion to $~~1.1~~ 1.5 trillion across all pyCIAM scenarios, and from $~~85~~ 100 billion to $~~590~~ 540 billion across the K14-pyCIAM scenarios that correspond to those used in Diaz (2016). The corresponding ~~Diaz (2016) values~~ values from Diaz (2016) range from $150 billion to $290 billion~~. Under "reactive retreat only"~~, with the smaller range being largely driven by Diaz (2016) considering only one socioeconomic growth scenario. Under a reactive retreat scenario, pyCIAM values ~~generally exceed~~ are generally similar to those of Diaz (2016) for ~~all~~ low and medium-SLR scenarios and higher for high-end SLR scenarios (Fig. 4~~, Table ??~~).

~~**NPV (2000-2100) $Trillion** pyCIAM (~~Considering the AR6 (~~*min) pyCIAM (max)CIAM (min)CIAM (max)0.5exOptimal Adaptation 0.680 2.08 1.14 1.49 0.5exReactive Adaptation Only 2.66 11.9 6.07 8.41 0.5ex2exRange of net present costs of climate-driven SLR from 2000 to 2100 in constant 2019 PPP USD across all 110 socioeconomic and SLR scenarios. Minimum and maximum NPV values are shown for the fully updated pyCIAM model, as well as CIAM as configured in Diaz (2016).~~ *low* and *medium-confidence*) warming scenarios and associated ranges of global SLR by 2100, we estimate that under 2°C of warming by 2100 (+0.40-0.69m GMSL), annual end-of-century costs will be between $110 billion and $530 billion (between 0.02 and 0.07% of global GDP), depending on SSP, economic growth model, and SLR magnitude and assuming optimal adaptation. For AR6's 4°C scenario (+0.58-0.91m GMSL), these costs range from $200 billion to $750 billion (0.04 to 0.09%). Also, for two low-likelihood, high-impact scenarios (Sweet-IntHigh, Sweet-High), which incorporate more uncertain physical processes like accelerated marine ice sheet and marine ice cliff instability, and correspond to GMSL rises of 1.5-2.0m by 2100, global annual costs range from $420 billion to $1.5 trillion (0.08 to 0.20%) by end-of-century under the same set of assumptions.

~~**End of Century Annual Costs $Trillion** pyCIAM (*min*)pyCIAM (*max*)CIAM (*min*) CIAM (*max*) 0.5exOptimal Adaptation 0.0853 1.11 0.146 0.293 0.5exReactive Adaptation Only 1.57 12.0 1.58 2.50 0.5ex2exRange of end-of-century average annual costs of climate-driven SLR from 2000 to 2100 in constant 2019 PPP USD across all 110 socioeconomic and SLR scenarios (for pyCIAM, paired with SLIIDERS inputs) and across three SLR scenarios (for CIAM).~~ Upon projecting costs across this wide range of SLR scenarios, we find a strongly linear relationship for both NPV and annual end-of-century wetland and total damages with respect to end-of-century GMSL. Depending on socioeconomic projections, the marginal NPV costs associated with 1 cm of end-of-century GMSL range from $8 billion to $14 billion, the marginal annual end-of-century total costs range from $3 billion to $7 billion, and the marginal annual end-of-century wetland costs range from $110 million to $350 million. In a scenario with only reactive adaptation, annual end-of-century costs are not only much higher in absolute terms but also increase in a much sharper (quadratic) manner with respect to GMSL.

3.2 Adaptation Costs and Benefits

The ~~global~~ results of this analysis support the finding of Diaz (2016) that adaptive measures (through protection or retreat) can dramatically reduce the cost of sea level rise. For a GMSL rise of one meter by 2100 and a "middle-of-the-road" socioeconomic growth trajectory (SSP2/IIASA), optimal adaptation would reduce the NPV of coastal impacts by about $5 trillion, inclusive of

these adaptation costs. This represents ~0.9% of the net present value of GDP over that same time horizon. Similarly, it would reduce average annual costs at end-of-century, inclusive of adaptation costs, by ~$6 trillion (1.2% of end-of-century annual GDP) 3. This would require substantial global investment in protection ($770 billion NPV under the same scenario) and retreat ($310 billion NPV, including both market and non-market costs of relocation). Across all socioeconomic and SLR scenarios modeled, we find that optimal adaptation can lower the NPV of impacts by a factor of 1.6 to 12, relative to a reactive adaptation approach.

The global distribution of optimal adaptation strategies is displayed in Fig. 7 for the ~~SROCC-RCP8~~AR6 (*medium confidence*) SSP2-4.5 SLR ~~scenario~~ and SSP2~~/IIASA socioeconomic~~, IIASA scenario. Notably, the majority of segments that protect are located in Asia, where coastal population densities are generally high and construction costs, at least as parameterized by CIAM and pyCIAM, are relatively low. Scattered high-density areas across OECD countries in Europe and North America are protected as well. The fact that most protecting segments opt for the maximum level of protection (1-in-10,000-year ESL height) also suggests that, for segments where protection is optimal, the parameterized marginal costs of building higher protection are almost always lower than the benefits they provide, up to the point where the protection heights have provided safety from an exceedingly rare event. Future work should ~~further explore the empirical validity of the~~ develop approaches to empirically calibrate the construction cost functions used in Diaz (2016) and ported to pyCIAM, as these may control the spatial distribution of protection. Similar to the ~~dominance of maximum~~ pattern of maximizing protection, there is a common preference to retreat to the 1-in-10-year ESL height amongst segments that adopt retreat as their optimal strategy. This suggests that increasing the resolution of retreat options around this level may better reflect heterogeneity in optimal retreat height. Finally, segments for which reactive retreat is optimal are generally sparsely populated or unpopulated~~, as seen in the low percentages of global population residing in these segments (Fig. 8).~~.

Fig. 8 displays the proportion of global segment populations adopting different adaptation strategies (protection, proactive retreat, and reactive retreat), across the various socioeconomic and SLR scenarios for both pyCIAM/SLIIDERS and CIAM. In general, while CIAM indicates that roughly 50% of the world's population would be protected under optimal adaptation and 50% would be relocated, pyCIAM, paired with SLIIDERS inputs, finds these ratios to be closer to ~~75% and 25~~80% and 20%, respectively. This is ~~primarily~~ largely due to our increased relocation cost parameter (Sect. 2.3), which disincentivizes retreat relative to protection. In contrast to the influence of relocation cost on adaptation type, little ~~variance~~ variation is observed in these percentages across pyCIAM's different socioeconomic scenarios ~~. This high stability is seen~~ (Fig. 8). This stability is visible even within individual segments' adaptation choices and suggests that particular choices of adaptation strategy ~~at a local level may often~~ (protection versus retreat) and the return value to which the chosen adaptation strategy is enacted may be robust to a range of future socioeconomic and SLR trajectories for most coastal regions. Similar results are shown normalized by coastline length rather than population in Fig. B2.

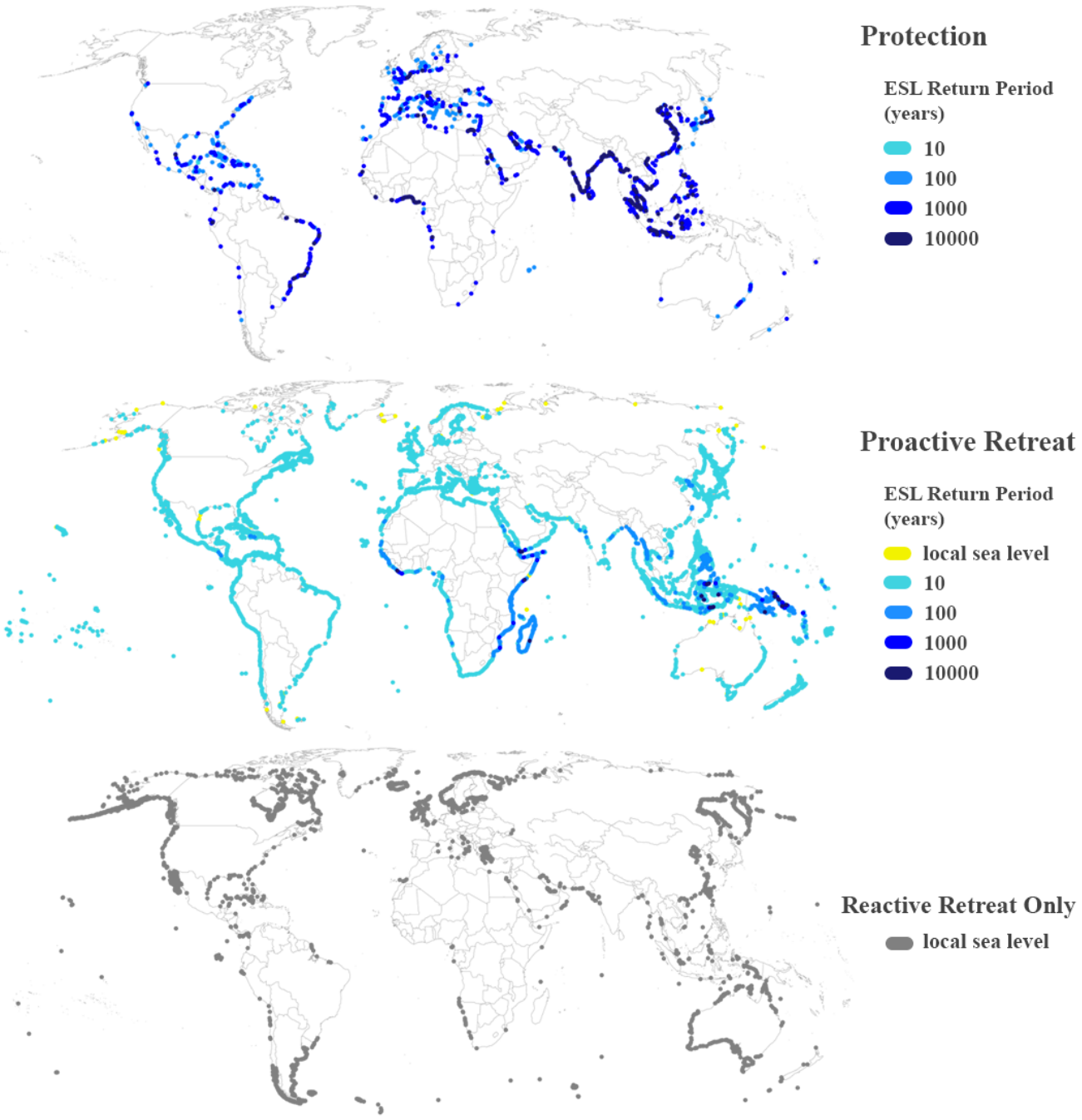

Figure 7. Adaptation strategies chosen by each segment in the "optimal" adaptation scenario. Each segment is represented by a marker at its centroid. Results reflect the IPCC – Special Report AR6 (SROCC – RCP 8.5*medium confidence*) SSP2-4.5 SLR scenario , and SSP2 and IIASA growth model socioeconomic growth projections. Return periods indicate the level of protection/retreat that is adopted by each segment.

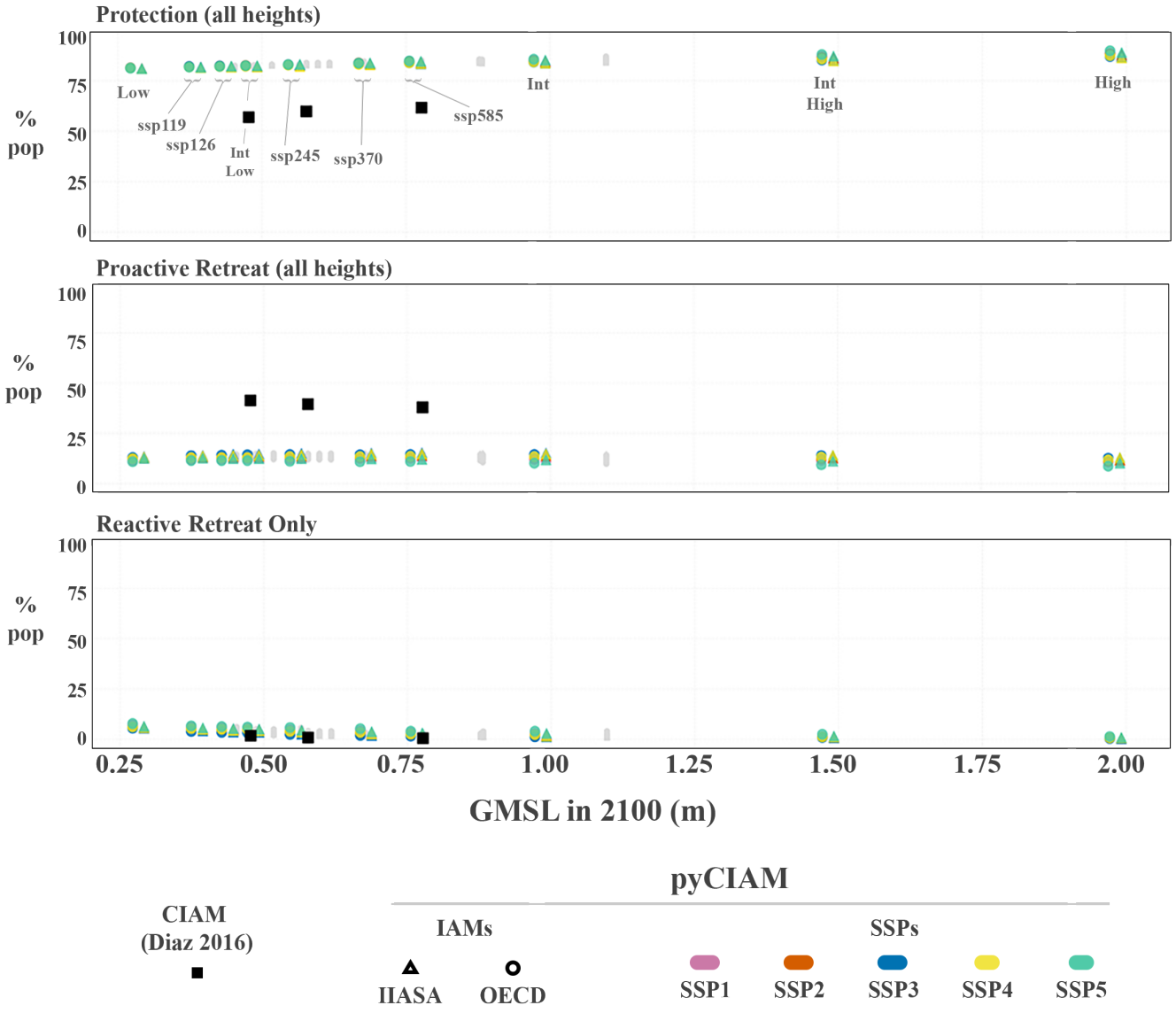

Figure 8. Comparison of optimal adaptation strategies adopted across all segments. Values represent percentages of global population residing at ~~that reside below at~~ elevations below 15 meters in segments adopting each respective adaptation strategy. Proactive retreat and protection values are aggregates of all possible heights for each. Solid black squares represent the results from Diaz (2016). For visual clarity, only *medium confidence* AR6 and ~~the~~ Sweet et al. (2022) scenarios are indicated with colored ~~circle and triangle~~ markers ~~represent pyCIAM/SLIIDERS results for all SLR~~ and jittered slightly along the x-axis based on runs using the OECD (~~differentiated by GMSL values~~ 1cm) ~~, SSP and~~ or IIASA (+1cm) economic growth model~~scenarios~~. ~~n.b.~~ The ~~D21-RCP8.5 and B19-High~~ remaining SLR scenarios ~~share the same projected GMSL~~ are shown in ~~2100 (1.11m) and were jittered by +/- 0.007m for plotting clarity~~grey without jitter.

3.3 Model Limitations and Planned Improvements

~~The benefits of adaptation presented here reflect the difference between costs in a scenario where only reactive SLR adaptation is allowed and one where all segments adapt optimally. However, "optimal" adaptation modeling in~~ pyCIAM is subject to some of the same limitations as its predecessor CIAM. First, adaptation is limited to the ten possible options introduced in Diaz (2016) — four protection heights, five proactive retreat heights and a reactive retreat action. Second, segments are only allowed one protection or retreat standard throughout the model duration. They cannot, for example, retreat to the 1-in-10 year ESL height for the first 20 years and then retreat to the 1-in-100 year height~~, rather an optimal retreat timing and height~~. Rather a single optimal standard is chosen given the full distribution of potential future outcomes. ~~Segments also cannot retreat to a certain height and then protect from there~~Similarly, segments cannot combine both retreat and protection. More flexible approaches may enable lower-cost outcomes (Kopp et al., 2019; Haasnoot et al., 2019), though computational constraints have limited the implementation of more dynamic adaptation approaches to models with local domains (Lickley et al., 2014). A preliminary approach to this problem, such as allowing for a one time, mid-century alteration of adaptation strategies, could be a simple scheme to allow for some level of dynamic adaptation strategies. Third, insurance, subsidies or other policies may discourage proactive retreat even when the NPV would be positive, and these interventions are not taken into account by segment agents in the model when determining the least cost adaptation path. Fourth, many cost functions and parameters in the model are based on limited empirical evidence, as little evidence at fine resolution and global scale is available to inform the magnitude and heterogeneity of these costs. ~~Fifth, existing~~

Existing coastal protections are not directly modeled ~~at a global scale, though this is addressed for some regions such as the U.S. and the Netherlands (Sect. **??**). Lastly, retreat~~ due to a lack of globally consistent data. Instead, existing protections are assigned in the model like those of any other year based on the least cost adaptation scenario for each segment. This means that protection costs in the initial year of the model will include the cost of constructing these existing structures, though these additional costs will be differenced out of our climate impact estimates because they will occur in both the "with climate change" and "no climate change" SLR trajectories.

Retreat or protection heights within each decadal planning period are chosen under perfect foresight of projected RSLR at that segment during the entire period, such that any maximum projected change in ESL return values due to RSLR is perfectly anticipated and incorporated into adaptation cost considerations and decisions. Notably, segments also chose their optimal adaptation strategy (e.g. protection to the 1-in-100 year ESL height) based on an NPV calculation that utilizes perfect foresight over the entire model duration. While this assumption cannot be correct in its extreme form, Fig. 8 suggests that these choices are very robust to uncertainty in future sea level and socioeconomic change.

~~Limiting possible protect and retreat heights to local 1, 10, 100, 1000, 10000-year ESL heights makes the range of adaptation heights dependent on the distribution of local ESL heights, which may artificially restrict options for modeled relocation or levee construction heights. Similarly, the model's current implementation does not allow for multiple adaptation strategies over the course of the modeling period. For example, a segment that chooses the 1-in-10 year protection height will continue to build higher protections as RSLR shifts the local ESL distribution, but it is not allowed to change to a greater protection standard (e.g. 1-in-100 year heights) or switch to retreat in the middle of the model duration. More flexible approaches may enable lower-cost outcomes (Kopp et al., 2019; Haasnoot et al., 2019), though computational constraints have limited the~~

implementation of more dynamic adaptation approaches to models with local domains (Lickley et al., 2014). A preliminary approach to this problem, such as allowing for a one time, mid-century alteration of adaptation strategies, could be a simple scheme to allow for some level of dynamic adaptation strategies.

pyCIAM also does not currently represent accommodation measures (e.g., infrastructure hardening and building elevation), which in some cases may be more cost-effective than either protection or retreat Oppenheimer et al. (2019); Kopp et al. (2019); Rasmussen et al. (2020). Accommodation encompasses a broad range of actions and is thus difficult to parameterize within the model. To our knowledge, accommodation is not represented in other coastal modeling platforms but could be the subject of future updates to pyCIAM. Additionally, the potential changing feasibility of both adaptation and accommodation measures in future decades, due to potential factors related or unrelated to climate change, like shifting supply chain and/or labor market dynamics, are not currently represented. These may prove to be relevant to society's capacity to effectively adapt in the future.

Our current estimation of the non-market costs of relocation detailed in Sect. 2.3 is intended to represent the fact that many coastal areas are observed to currently be under-adapted to present ESL hazards (Houser et al., 2015; McNamara and Keeler, 2013; McNamara et al., 2015; Armstrong et al., 2016; Haer et al., 2017; Hinkel et al., 2018; Suckall et al., 2018; Lorie et al., 2020). However, improved estimates of these non-market relocation costs could potentially be guided by more detailed empirical assessments of present-day under-adaptation to coastal hazards. Other forms of adaptation behavioral "inertia" preventing or delaying economically rational action may exist as well. For example, Mendelsohn et al. (2020) estimated the cost-benefit ratio of building seawalls to be at least 2:1 in East Haven, CT, Council (2017) estimates this ratio for elevating coastal homes up to 9:1 in some U.S. locations, and Bakkensen and Mendelsohn (2016) found that the U.S., in particular, may be up to 14x less adapted to tropical cyclone hazards than other OECD countries threats presently. Improved estimates of these non-market relocation costs could potentially be guided by more detailed empirical assessments of present-day under-adaptation to coastal hazards. While some of this under-adaptation is rationalized by our non-market costs of relocation, other factors such including challenges of permitting and funding costly infrastructure projects, subsidized insurance (Craig, 2019) or limited risk information may play a role as well. We are aware of efforts to further understand adaptation costs and the reasons for under-adaptation (Bower and Weerasinghe, 2021; Berrang-Ford et al., 2021), but the current extent of empirical evidence quantifying sub-optimal adaptation is limited. If and when such evidence is available, the modularity of pyCIAM enables future integration of these estimates to improve its adaptation cost-benefit implementation.

Better global data describing existing coastal protection infrastructure would improve the accuracy of pyCIAM. Currently, the model incorporates coastal barriers that are well documented, such as seawall and levee systems in The Netherlands and the U.S. However, spatially Spatially resolved data on constructed protection around the globe is sparse. To overcome this, some studies assume a certain level of protection as being present in all coastal regions, making stylized assumptions based on population densities and national GDP (Sadoff et al., 2015). Other studies develop statistical models to empirically ground such relationships (Scussolini et al., 2016), and these have been incorporated in other global coastal adaptation models (Tiggeloven et al., 2020) and could be evaluated for use in future versions of pyCIAM. Further improvements to certain regions could also be made using protection data collected by Hallegatte et al. (2013) for 136 coastal cities.

Our reflection of local mean and extreme sea levels is limited by the resolution of our local MSL projections (1 degree in FACTS, 2 degrees in LocalizeSL) and our ESL distributions from CoDEC (50km coastline spacing). Because of the desire to build a globally consistent model using these inputs, we employ a "local bathtub" model in which all points nearest to a given pair of ESL and MSL prediction points receive the same mean and extreme sea level projections. While this local model preserves the substantial large-scale spatial heterogeneity in SLR and ESL, sub-grid-scale variation is ignored. In particular, bathtub models are known to overestimate storm surge in inland areas largely due to the deceleration of flows caused by surface roughness (Bootsma, 2022; Vousdoukas et al., 2016). A more sophisticated, dynamic representation of ESL based on local hydrodynamic simulations for each MSL/ESL combination is beyond the computational scope of this analysis but may yield improved future results and could be incorporated either "on-the-fly" within the pyCIAM model or in a pre-processing step that updates the ESL distributions in SLIIDERS.

Because pyCIAM linearly combines present-day ESL estimates and SLR predictions, our current approach also ignores changing ESL distributions due to (a) climate-driven changes to storm surge distributions from, for example, altered tropical cyclone frequency and intensity; and (b) the dynamic interaction between storm surge and MSL, moderated by local topography.

Despite these limitations in estimating sea levels, it is important to note that when isolating climate change-induced coastal costs, we difference the costs of a no-climate change baseline scenario that uses the same local bathtub flood model. This differencing also serves as a bias correction step, partially mitigating any over-estimates of flooding damages potentially introduced by the bathtub approach, though some high or low bias may still be present in the final results. Total (un-differenced) cost estimates (Fig. B1), however, will reflect any bias associated with the bathtub flood model. Accounting for these future changes is important for planning purposes, but represents a major computational challenge.

Additional geophysical dynamics associated with SLR inundation and related flooding, such as erosion, salinization of aquifers and estuaries, are also not currently addressed in our approach. Finer-scale wave setup and ESL behavior within complex coastlines at the sub-segment scale could also be useful to capture in future modeling. This would require estimates of ESLs at a much higher spatial resolution than is provided in the CoDEC dataset and is therefore currently infeasible given available input data.

Finally, our hydraulic connectivity model masks only those regions that are not connected at 20 meters of SLR relative to 2005 levels. Some areas may not meet this criteria but still may be non-connected at lower sea levels. For example, a location that is at 1 meter above sea level but is behind a hill at 2 meters above sea level would be flooded by our model for sea levels of 1.5 meters. Future work could address this by assigning each pixel not only an elevation but a barrier height that would be treated similar to how manmade protection heights are treated in pyCIAM. This would increase the dimensionality of several calculations in pyCIAM and is thus outside of the scope of the current implementation.

4 Conclusion

Modeling the social and economic impact of future sea level rise can inform our understanding of costs in different climate change mitigation scenarios and support the analysis of adaptation policies. To construct global estimates, modelers face the dual challenge of developing a ~~global approach~~ globally generalizable approach that is also capable of representing the detailed local information relevant to accurately estimating SLR impacts and adaptation. Prior modeling studies have developed ~~valuable~~ frameworks for conducting such analyses; however, continued iteration of these data and models is necessary in order to improve the accuracy and precision of projections and to keep pace with relevant advancements in data, modeling, and computing. Achieving this through community-wide collaboration requires a collection of open-source and transparent datasets as well as modeling tools.

This paper has summarized improvements to the quality and accessibility of both coastal impact data products and related modeling platforms. The Sea Level Impacts Input Dataset by Elevation, Region and Scenarios (**SLIIDERS**) ~~dataset~~ represents a globally comprehensive and consistent collection of physical, ecological and socioeconomic variables for roughly ~~ten thousand~~ 10,000 coastal localities. SLIIDERS is a segment-wise data product for coastal impacts, similar to previous products like DIVA (Vafeidis et al., 2008), but with significant improvements to the quality of represented variables~~and~~. It is available as an open-source resource following FAIR guidelines (Wilkinson et al., 2016). Any researcher can download, inspect and alter SLIIDERS to utilize in their own coastal modeling studies.

The Python-Coastal Impacts and Adaptation Model (~~pyCIAM~~**pyCIAM**), a companion model that utilizes ~~SLIIDERS~~ **SLIIDERS** as an input, was developed as an open-source update to the original Coastal Impacts and Adaptation Model Diaz (2016) ~~which~~ and incorporates numerous improvements to model functionality and efficiency. pyCIAM is also made available as a modular, open-source tool meant to be modified by users seeking to add functionality or improve input sources, with users able to combine the model with their own input datasets, provided they are formatted similarly to SLIIDERS. An additional key advance of pyCIAM is that it is designed to simulate impacts from tens to hundreds of thousands of future SLR scenarios in parallel, facilitating scalable probabilisitic impact modeling research.

Results from pyCIAM v1~~.0~~.1, paired with SLIIDERS v1~~.0~~.1, show the model produces roughly similar estimates of the global net present cost of ~~SLR-driven costs~~ SLR to those of CIAM (Diaz, 2016) under the SSP5 socioeconomic scenario, with all other ~~SSP-IAM configurations producing~~ SSP-economic growth model configurations producing slightly smaller values (Fig. 4). Median annual, end of century costs under optimal adaptation in pyCIAM are also very similar to CIAM when averaging across all SSPs and growth models. When prohibiting proactive adaptation, costs are higher in pyCIAM for almost all scenarios as compared to CIAM. However, when comparing total yearly coastal damages, rather than just the climate-driven component, pyCIAM projects global NPV of all coastal damages between ~~2000-2100~~ 2005-2100 to be roughly 3-4× those of CIAM (Fig. B1), likely due to greater population and capital stock estimates in these SSPs as compared to the trajectories used in Diaz (2016). The median annual, end of century total costs under optimal adaptation in pyCIAM are also higher than CIAM for all scenarios, with only the SSP4-IIASA scenario producing similar values.

Despite the improvements represented by the SLIIDERS data product and pyCIAM platform, there are aspects of them that should be improved in the future. We believe that a priority for future work should be to incorporate empirical evidence on coastal damages and adaptation behavior due to rising and extreme sea levels in order to better inform model assumptions. We hope that improvements to SLIIDERS can be made regularly as new, higher quality data sources for each of its constituent variables are ~~mode~~ made available. Additionally, the segmentation of coastlines in SLIIDERS v1~~.0 can likely~~ .1 can be improved beyond a uniform (50km) spacing nested at the country level to better ~~delineate between~~ approximate coastal regions that ~~are more likely to represent autonomous,~~ behave as distinct decision making units, ~~such as extents~~ for example by capturing the extent of coastal urban centers. We intend to make many of these improvements moving forward, and will make updated versions available as such efforts are carried out. However, our hope is that the open-source nature of both SLIIDERS and pyCIAM will enable community-driven development to spur more rapid and substantial improvements to both tools.

5 Code and data availability

Version 1.1 of both the SLIIDERS dataset and pyCIAM model, is associated with the results presented in this manuscript. The SLIIDERS dataset, along with the code to create it, is available at https://doi.org/10.5281/zenodo.7693868. Source code for SLIIDERS is also available at https://github.com/ClimateImpactLab/sliiders, where the 1.1 release corresponds to the version used in this manuscript and included in the Zenodo deposit. The model outputs used in this manuscript, along with the pyCIAM source code, are available at https://doi.org/10.5281/zenodo.7693869. Similarly, the pyCIAM source code is available at https://github.com/ClimateImpactLab/pyCIAM, with release 1.1 again corresponding to the model used for this manuscript. pyCIAM is also available on PyPI as the *python-CIAM* package. Scripts and notebooks associated with running pyCIAM and creating the results contained in this manuscript are also included in the pyCIAM GitHub repository and the Zenodo repository.

Appendix A: Supplemental Information

A1 Coastlines Creation and Length Calculation

To create each segment represented in SLIIDERS and used in pyCIAM, we assembled a set of polylines according to the following steps[7]:

1. Downloaded highly-resolved 1:~~50m and 1:~~10m Natural Earth Coastlines (~~). For the majority of segments, the moderately resolved 1:50m coastlines were used, with the fine scale of the 1:10m layer required for small island polygons not represented in the 1:50m layer.~~ www.naturalearthdata.com/downloads/10m-physical-vectors).
2. Removed Caspian Sea borders from both coastline layers to avoid modeling along this inland sea.
3. Removed all line segments south of 60S (Antarctica) from both coastline layers to avoid inclusion of these coastlines in any final coastal segments, due to the lack of population and capital exposure any latitudes below 60S.

[7] ~~Steps 2-6 and 8 used the Quantum Geographical Information Systems (QGIS) v3.16 software.~~

4. Converted ~~both coastline~~ coastlines layers to polygons in order to get land areas that correspond to the ~~fine (~~1:10m ~~) and medium (1:50m)~~ scale coastline resolutions.
5. ~~identified all land area polygons derived from the 1:10m coastline layer that are not represented by 1:50m coastlines, which preserves many smaller island areas.~~
6. ~~Merged these 1:10m polygons with the 1:50m polygons into a single layer~~
7. Intersected resulting polygon layer of land masses with exposure grid of population and capital assets, and removed land masses that contained no capital or population exposure. In these completely ~~un-populated~~ unpopulated areas, we cannot accurately represent value of lost land within the pyCIAM framework, nor is this value likely to be large.
8. Converted this ~~hybrid~~ 1:10m ~~and 1:50m~~ land area polygon layer back to polylines for use as our final vector layer of global coastlines.
9. Constructed a set of Voronoi polygons from the CoDEC-derived coastal segment centroids and intersected these with the coastlines layer constructed in Steps 1-8. This partitioned coastlines according to segment, allowing for the calculation of the total length (in kilometers) of coastline by coastal segment.

A2 Aligning geographic and socioeconomic datasets to build ~~SLIIDERS-ECON~~SLIIDERS

Socioeconomic variables expressed in ~~SLIIDERS-ECON~~ SLIIDERS and used in pyCIAM are defined at various geographic aggregation levels, from the fine "elevation bin by admin-1 region" scale to the coarse country scale. Input data sources also come in various formats, from gridded estimates of coastal elevation, population and capital distribution, and wetland area, to country-level SSP-based projections of income, population, and capital growth trajectories, to vector representations of country boundaries and coastlines. To create ~~SLIIDERS-ECON~~SLIIDERS, we must harmonize these various input sources. We start by assigning admin-1 and country labels to each grid cell in the gridded elevation and exposure input sources, using boundaries from GADM ~~v3.6~~4.1 (GAD). Notably, GADM ~~considers as a~~ uses the "country" ~~any region with an ISO country code,~~ label broadly, including many inhabited and uninhabited islands, regardless of sovereignty.

There are ~~199 such countries~~ 211 countries in GADM 4.1 that are coastal and contain non-zero land under 20 m elevation. The boundaries of the admin-1 regions within these 199 countries are overlaid on gridded elevation and exposure datasets, including those defining spatial distributions of population (~~LANDSCAN 2019~~LandScan 2021) and physical capital (LitPop and GEG-15), to assign elevations and admin-1 labels to each grid cell. The gridded dryland and wetland area, population, and physical capital estimates are then binned by 10 cm elevation increments and grouped within admin-1 regions and coastal segments. Each admin-1 region is then assigned its corresponding country label, which is matched to the SSP-based country-level growth trajectories.

A3 ~~Imputing initial-year (2010)~~ Estimating 2005-2020 capital stock values

Out of the ~~199~~ 204 inhabited countries included in ~~SLIIDERS-ECON, 146~~ SLIIDERS, 143 have capital stock values ~~in 2010 in~~ from 2005 to 2019 in PWT 10.0 that we use as initial conditions for projecting capital stock consistent with the SSPs. We ~~must impute the 53 remaining values ; while only 2010 values are needed to seed the capital growth model, we take an approach~~

that allows for simultaneous estimation of a time series of capital stock beginning in 1950. This approach generates estimates of historical capital consistent with those of other ongoing work. Our estimation process consists of the following stepsextend these one year using the Perpetual Inventory Method (PIM) and fill and/or impute the 61 remaining values using the following approach:

1. We impute any missing historical GDP estimates from 1950-2020 (Section **??**) within our aggregation of GDP data sources (Sect. 2.6.2) .
2. We estimate the relationship between historical investment-to-GDP ratio, income, and population share values, and impute historical investment, following Higgins (1998) (Section **??**).
3. For the countries with 2005 capital stock estimates in GEG-15 (Bono and Chatenoux, 2014) and 2014 estimates in LitPop (Eberenz et al., 2020), but with no estimates in PWT 10.0, we exponentially interpolate to 2010.
4. For the remaining countries with 2005 estimates in GEG-15 but no 2014 estimates in LitPop, we use the perpetual inventory method with historical investment estimates from Step 2 to estimate 2010 capital stock.
5. For the remaining countries with 2014 estimates in LitPop but no 2005 estimates in GEG-15 or For 10 countries with ratios of non-financial wealth (NFW) to nominal GDP recorded in the 2022 Credit Suisse Global Wealth Databook (GWDB, Credit Suisse Research Institute (2022)) we use these ratios applied to previously gathered GDP estimates from PWT 10.0 , we first estimate the 1950 capital stock values following Inklaar et al. (2019) using the actual and estimated GDP and investment-to-GDP ratio. Then, we exponentially interpolate to 2010.
6. For the final set of countries with no capital stock estimates in any of these three sources , we follow Eberenz et al. (2020) and estimate the 2014 capital stock values by multiplying GDP estimates by a capital-to-GDP ratio of 1.24724 from Credit Suisse Research Institute (2017). Then, we follow Step 5 to obtain 2010 estimates. In the parts below, we describe the processes for imputing missing historical GDP and income values, historical investment-to-GDP ratios, and missing capital depreciation rates, and for estimating the missing 1950 capital stockvalues.

A3.1 Imputing missing historical (1950-2020) GDP

The capital stock imputation described above relies, in some cases, on a complete time series of GDP. While this exists for many countries after aggregating across the multiple data sources described in Sect. 2.6.2, some countries and territories are missing observations for some of this time series. For territories, whose growth often converges to that of the corresponding sovereign state (Bertram, 2004), we impute GDP in missing years using the average ratio of the territory's GDP to that of the sovereign state during non-missing years. For other cases, we find five "nearest" countries, such that the sum of squared differences of yearly GDP growth rates to that of the target country are minimized across all non-missing years. We then impute the growth rates for missing years using a weighted average of these five end members, weighted by the inverse of the SSEs, and interpolate/extrapolate around non-missing observation using these growth rates.

A3.1 ~~Imputing missing historical (1950-2020) investment-to-GDP ratios~~

~~Investment-to-GDP ratios are imputed via a regression across non-missing years of this ratio on per capita GDP levels and growth rates as well as population age distributions. The regression used is borrowed from Foure et al. (2012) and adjusted R^2, AIC, and BIC are compared across models with and without the age distribution variables. The model that includes those variables performs better and thus we use that model for the necessary imputations. See the code repository that accompanies this manuscript for further details on method and for a summary of regression results.~~

A3.1 ~~Imputing missing capital depreciation rates~~

~~We use PWT 10.0 as our main source for historical capital depreciation rates. However, many of the countries considered in our workflow are either not included in PWT 10.0, or they are included but are missing values for certain years. In these cases, we impute the depreciation rate of country j in year t by taking an unweighted average of the available depreciation rates across all countries in year t. To project future capital depreciation for each country, necessary to project future capital stock levels, we simply extend our estimatesof 2010 capital depreciation rates to all future years. The projection method described in Dellink et al. (2017) also requires a global capital depreciation rate used when deriving long-run investment-to-GDP ratios, for which we use the 2010 global average depreciation rate in PWT 10.0, which is approximately 4.416%, comparable to the 5% global depreciation rate used in Dellink et al. (2017).~~

A3.1 ~~Imputing 1950 capital stock~~

~~We follow the method used in PWT 10.0 (Inklaar et al., 2019) to estimate capitalstock in 1950 where needed for imputation, using GDP~~ and ~~investment-to-GDP ratios estimated from the data sources compiled in Sect. 2.6.2 and imputed via the previously described approaches. We update the bounds and annual increment of capital intensity (a .k.a. capital-to-GDP ratio) used in the algorithm based on the compiled data. Inklaar et al. (2019) sets bounds of 0.5, 4.0and an annual increment of 0.02; however, capital intensities and their increments vary greatly across countries. Thus, we apply a k-means clustering analysis of the 2014-2020 capital intensity values to classify countries into three groups based on their capital intensity values and growth rates.As a result, we use the following triples of lower bound, upper bound, and annual increment of capital intensity for each cluster: (0.861~~other sources and assume that the resulting NFW values are equivalent to physical capital stock, ~~3.902~~following the assumptions in Eberenz et al. (2020).

7. For 5 island departments of France, we use the NFW:GDP ratio from mainland France.
8. for 44 additional countries without individual estimates in the GWDB, we use regional averages, with regions defined by UNSTATS subregions (UNSD, 2021).
9. For North Korean estimates, ~~0.014), (1.810, 6.298, 0.037), and (2.616, 13.853, 0.166). Note that as opposed to using minimum and maximum values as the lower and upper capital intensity bounds as in Inklaar et al. (2019), we use bottom and top decile within each cluster due to heavy tailed distributions of capital intensity in PWT 10.0.~~ we use

capital:GDP ratios estimated in Pyo and Kim (2020) along with a Perpetual Inventory Method (PIM) parameterized by other parameters from Pyo and Kim (2020).

10. For Cuba, we take ratios of Cuban to U.S. captial stock from Berlemann and Wesselhöft (2017).

A4 Projecting SSP-consistent (~~2010-2100~~2020-2100) capital stock values

Using actual and imputed historical ~~2010~~ 2020 country-level capital stocks as initial conditions, we extract the capital portion of the OECD Env-Growth model (Dellink et al., 2017) and apply it to the SSP trajectories of GDP and population. The model requires global GDP elasticity of capital and ~~2010~~ 2020 country-level marginal products of capital (MPK), which are not described in Dellink et al. (2017). We use a global GDP elasticity of capital of 0.326 from Crespo Cuaresma (2017) and estimate 2010 MPKs using a modified Cobb-Douglas production function that contains only capital inputs. Coefficients of the function are derived by fitting to the compiled dataset of historical GDP and capital. Alternative approaches for obtaining these necessary inputs, including the use of a production function with labor and capital inputs and deriving the global elasticity directly from the production function, were also evaluated; however, these approaches yielded greater discrepancies in projected capital stocks when compared with the limited set of results presented in Dellink et al. (2017). To align most closely with citeEnvGrowth the aforementioned specification was chosen. The comparison of these alternative specifications is available in the SLIIDERS code repository accompanying this manuscript.

Appendix B: Supplemental Figures

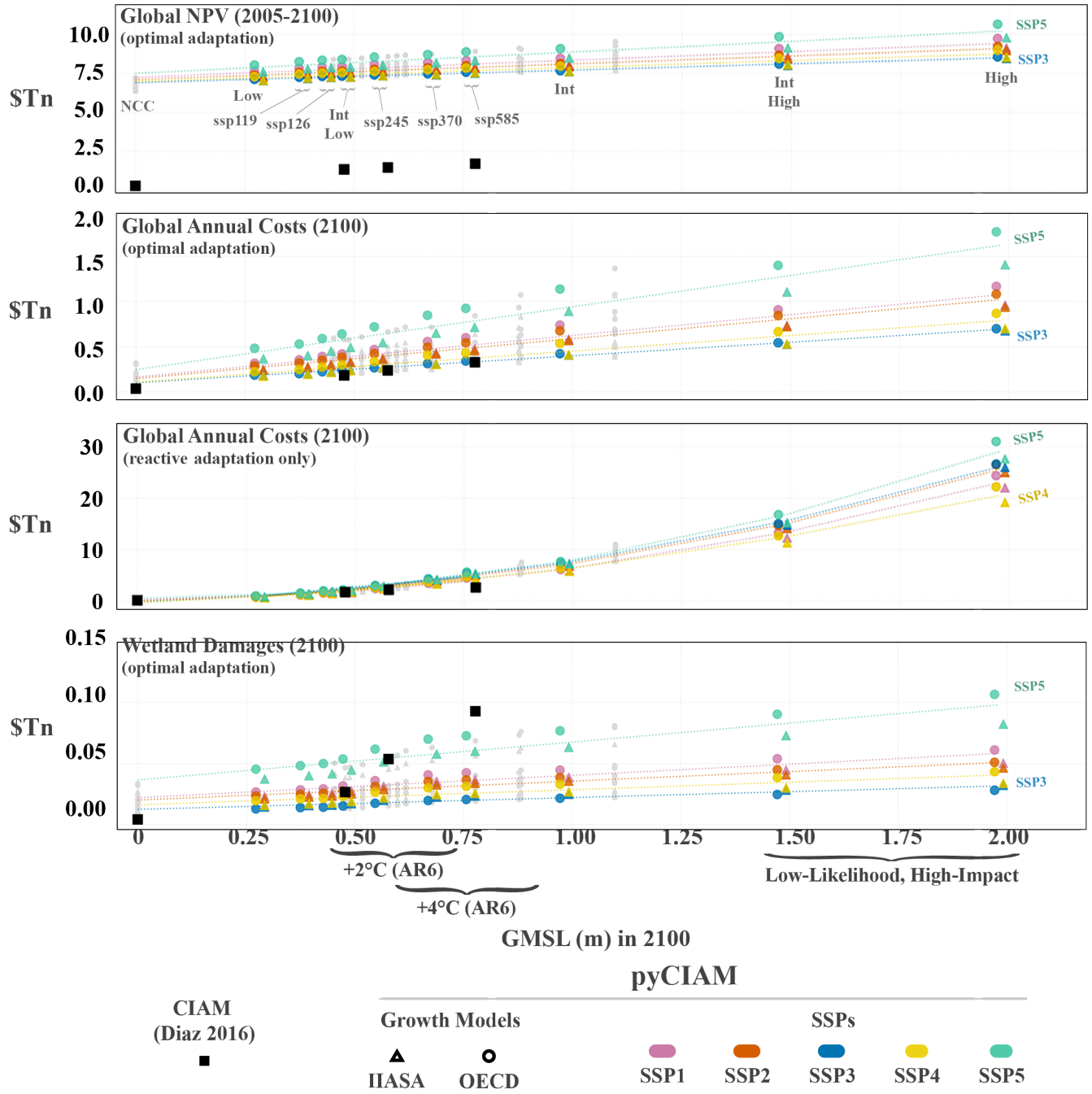

Figure B1. Comparison of ~~four~~ global cost metrics for median model results under each SLR scenario~~, for CIAM (black) and pyCIAM (colored)~~. Values represent total coastal losses (inclusive of hazards not attributable to climate change)~~. All costs are~~ , expressed in constant 2019 PPP USD. Each vertical group of points ~~represents~~ is a single SLR scenario~~(Table 2)~~, with each point in the group representing a unique combination of ~~SSP and~~ SSP-economic growth model. Differencing ~~the~~ values associated with 0 GMSL rise from the other values yields Fig. 4. ~~n.b. The D21-RCP8.5~~ For visual clarity, only *medium confidence* AR6 and ~~B19-High SLR~~ Sweet et al. (2022) scenarios ~~share~~ are indicated with colored markers and jittered slightly along the ~~same projected GMSL in 2100~~ x-axis based on runs using the OECD

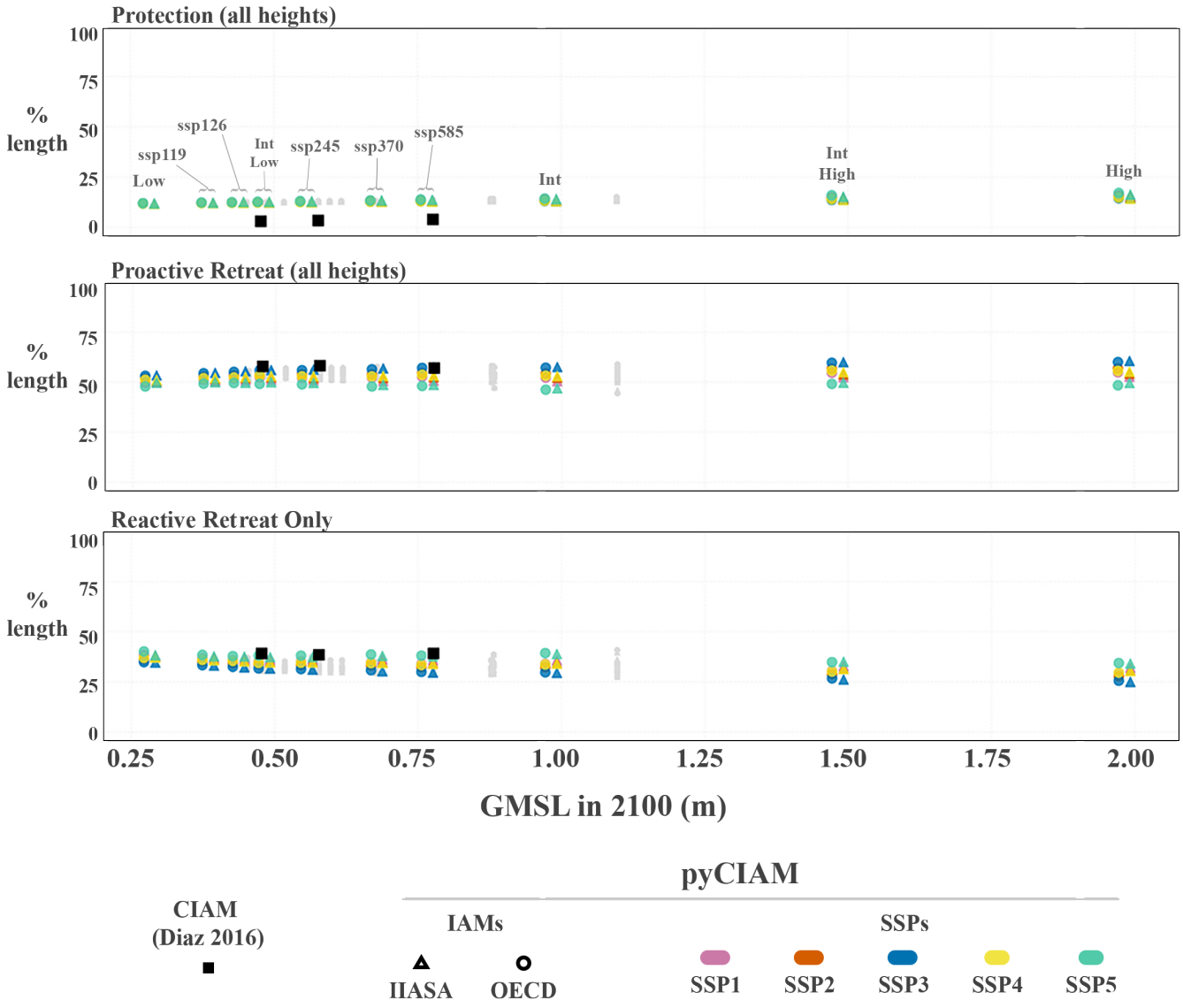

Figure B2. Comparison of optimal adaptation strategies adopted across all segments. Values represent percentages of global coastline associated with segments adopting each respective adaptation strategy. Proactive retreat and protection values are aggregates of all possible heights for each. Solid black squares represent the results from Diaz (2016). For visual clarity, only *medium confidence* AR6 and ~~the~~ Sweet et al. (2022) scenarios are indicated with colored ~~circle and triangle~~ markers ~~represent pyCIAM/SLIIDERS results for all SLR~~ and jittered slightly along the x-axis based on runs using the OECD (~~differentiated by GMSL values~~-1cm) ~~, SSP and~~ or IIASA (+1cm) economic growth model~~scenarios~~. ~~n.b.~~ The ~~D21-RCP8.5 and B19-High~~ remaining SLR scenarios ~~share the same projected GMSL~~ are shown in ~~2100 (1.11m) and were jittered by +/- 0.007m for plotting clarity~~grey without jitter.

Appendix C: Supplemental Tables

~~Input Dataset~~ ID	~~Source & Description~~ SLR Scenario	~~DOI~~ Model Used	GMSL in 2100 [m] (17th-percentile)	GMSL in 2100 [m] (83rd-percentile)
~~Coastal Segments~~ NCC	~~CoDEC, Natural Earth (Muis et al., 2020) 0.3cm Thinned European coastal points in CoDEC from 10km spacing to 50km and made 15 manual additions to ensure all countries contain at least one segment . Coastline shapes were taken from Natural Earth (1:50m and 1:10m) . No~~ Climate Change*	~~10.5281~~ CIAM pyCIAM	0.00	0.00
AR6-Med	IPCC AR6 *Medium Confidence* (2021) (SSP1-1.9, SSP1-2.6, SSP2-4.5, SSP3-7.0, SSP5-8.5)	pyCIAM	0.28, 0.32, 0.44, 0.55, 0.63	0.55, 0.61, 0.76, 0.90, 1.02
AR6-Low	IPCC AR6 *Low Confidence* (2021) (SSP1-2.6, SSP5-8.5)	pyCIAM	0.32, 0.63	0.79, 1.61
Sweet	US Interagency SLR Technical Report (2022) (Low, Int-Low, Int, Int-High, High)	pyCIAM	0.28, 0.48, 0.98, 1.47, 1.95	0.29, 0.49, 0.99, 1.50, 2.02
K14	Kopp et al. (2014) (RCP 2.6, RCP 4.5, RCP 8.5)	CIAM, pyCIAM	0.35, 0.43, 0.61	0.65, 0.76, 1.00
SR	IPCC-SROCC (2019) (RCP 2.6, RCP 4.5, RCP 8.5)	pyCIAM	0.39, 0.48, 0.71	0.60, 0.76, 1.11
B19	Bamber et al. (2019) (Low, High)	pyCIAM	0.48, 0.79	0.5ex 0.96, 1.71 0.5ex>
D21	DeConto et al. (2021) (RCP 2.6, RCP 4.5, RCP 8.5)	pyCIAM	0.43, 0.52, 0.90	0.61, 0.74, 1.32

2ex

*Includes local background rates of relative sea level rise at each segment due to non-climatic background processes

SLR Scenario	Model	Socioecon. Scenario	GMSL [m] (2100)	NPV $Tn (bp) *Optimal*	NPV $Tn (bp) *Reactive*	Costs (2100) $Tn (bp) *Optimal*	Costs (2100) $Tn (bp) *Reactive*
RCP 2.6	pyCIAM	SSP2/~~zenodo.3660927 0.3cm (Unaltered CoDEC)~~ IIASA	0.48	1.00 (2)	2.94 (6)	0.14 (3)	1.67 (32)
RCP 2.6	*CIAM*	*IMF WEO*	*0.48*	*1.05*	*6.84*	*0.15 (8)*	*1.58 (92)*
RCP 4.5	pyCIAM	SSP2/IIASA	0.58	1.11 (2)	3.80 (8)	0.18 (3)	2.53 (48)
RCP 4.5	*CIAM*	*IMF WEO*	*0.58*	*1.17*	*7.93*	*0.20 (12)*	*2.04 (118)*
RCP 8.5	pyCIAM	SSP2/IIASA	0.78	1.31 (3)	5.83 (13)	0.27 (5)	4.68 (89)
RCP 8.5	*CIAM*	*IMF WEO*	*0.78*	*1.42*	*9.70*	*0.29 (17)*	*2.50 (145)*

Table C2. Comparison of global estimated NPV (2005-2100) and annual costs of climate-driven SLR in 2100, expressed in constant 2019 PPP USD, between pyCIAM and Diaz (2016). Each metric is presented for both the optimal adaptation and reactive retreat modeling configurations. pyCIAM results are shown for the SSP2/IIASA socioeconomic growth scenario, while Diaz (2016) results are shown for the IMF World Economic Outlook (2011) projections used in that analysis. NPV for Diaz (2016) have been recalculated to be consistent with the 2005-2100 period used in pyCIAM. Numbers in parentheses show the fraction of global GDP associated with these costs in units of basis points (1/100ths of a percent). For columns 3 and 4, the NPV of GDP 2005-2100 is used for this calculation; for columns 5 and 6, GDP in 2100 is used. For Diaz (2016) scenarios, the 2100 global GDP used associated with the socioeconomic projections used in that analysis ($147.6 trillion 2010 USD) is reported in the paper. We use that value, adjusted to 2019 USD, to normalize the GDP impacts from Diaz (2016) scenarios. The NPV of GDP from 2005-2010 is not reported in Diaz (2016); thus we do not normalize Diaz (2016) NPV impacts.

Input Dataset	Source & Description	DOI/URL
Coastal Segments	**CoDEC** (Muis et al., 2020): Defines segment centroids **Natural Earth 10m Physical Layers**: Defines global coastlines	10.5281/zenodo.3660927 https://www.naturalearthdata.com/downloads/10m-physical-vectors/
Extreme sea levels (ESLs) ~~0.5ex~~	**CoDEC** (Muis et al., 2020) ~~0.2cm ESL values in CoDEC are calculated from the Global Tide and Surge Model (GTSMv3.0)~~	10.5281/zenodo.3660927 ~~0.2cm (Unaltered CoDEC)~~
Elevation	**CoastalDEM** ~~v1~~**v2.1** ~~(Kulp and Strauss, 2019) 0.2cm Corrects significant high bias of coastal elevations found in previous DEMs~~ (Kulp and Strauss, 2021): Primary elevation data source **SRTM15+ v2.5** (Tozer et al., 2019): Used to fill elevation data where CoastalDEM is undefined (e.g. ~~SRTM) 0.1cm~~ ~~**SRTM15+ v2.3** (Tozer et al., 2019) 0.2cm Global topography and bathymetry at 15 arc-second resolution. Used wherever CoastalDEM is undefined 0.1cm~~ ~~**MDT Global CNES-CLS18** (Mulet et al., 2021) 0.2cm Mean dynamic topography at 1/8° resolution 0.1cm~~ ~~**XGM2019e** (Zingerle et al., 2020) 0.2cm Experimental gravity field model at 2 arc-minute resolution~~ polar latitudes)	https://assets.ctfassets.net/cxgxgstp8r5d/3f1LzJSnp7ZjFD4loDYnrA/71eaba2b8f8d642dd9a7e6581dce0c66/CoastalDEM_2.1_Scientific_Report_.pdf ~~10.1038/s41467-019-12808-z 1.4cm~~ 10.1029/2019EA000658 ~~1.35cm~~

0.5ex	**MDT Global CNES-CLS18** (Mulet et al., 2021): Estimates of present-day mean sea level height relative to geoid	10.5194/os-17-789-2021 0.9cm 10.1007/s00190-020-01398-0
Wetland and Mangrove Extent 0.5ex	**GLOBCOVER v2.3** (European Space Agency and UCLouvain, 2010)(wetlands) 0.1cm : Defines wetland extent	10.1594/PANGAEA.787668
	Global Mangrove Watch 2016 (Bunting et al., 2018)(mangroves) : Defines mangroves extent	N/A 0.6cm 10.3390/rs1010669
Sea Local and global sea level rise projections 0.5ex	**LocalizeSL** (projections corresponding to Kopp et al., 2014; Bamber et al., 2019; Oppenheimer et al., 2019; DeConto et al., 2021)0.2cm Localized probabilistic estimates of global SLR at each coastal segment conditional on a certain level of global SLR in a certain year and under a variety of physical assumptions : Local sea level rise projection outputs from the LocalizeSL model (used with AR5 emissions scenarios and other custom global temperature trajectories)	10.5281/zenodo.6029807
	Framework for Assessing Changes to Sea Level (FACTS) (Fox-Kemper et al., 2021; Kopp et al., 2023; Garner et al., 2022; Sweet et al., 2022) : Local sea level rise projection outputs from the FACTS model (used with AR6 and Sweet projections.	10.5281/zenodo.6382554, 10.5281/zenodo.6382554

2ex	

Table C3: Summary of SLIIDERS datasets and pyCIAM inputs for Input data sources used to construct physical variables in SLIIDERS.

Input Dataset	Source & Description	DOI/URL
Current Historical Population	**LandScan 20192021** (Rose et al., 2020) 0.2cm (Sims et al., 2022): Spatial distribution of global population in 2019 at a 30 arc-second resolution (∼1km at equator) 0.1cm	10.48690/1527702
	PWT 10.0 (Feenstra et al., 2015),—: Country-level time series of population	10.34894/QT5BCC
	UN World Population Prospects (UN DESA, 2019)0.2cm Country-level population estimates : Used to fill population data for countries missing in PWT	https://population.un.org/wpp/Download
0.5ex	**CIA World Factbook** (Agency, 2021): Used to fill population data for countries missing in PWT	https://www.cia.gov/the-world-factbook/
	World Bank World Development Indicators (Bank, 2021): Used to fill population data for countries missing in PWT	10.57966/6rwy-0b07
	Statistics and Research Åland (Ala): Used to estimate population in Åland Islands	https://www.asub.ax/en
	StatBank Norway (Sta): Used to estimate population in Svalbard and Jan Mayen	https://www.ssb.no/en/statbank/table/07429

~~Current Income~~ Historical GDP	**PWT 10.0** (Feenstra et al., 2015)~~0.1cm~~ : Country-level estimates of GDP per capita	10.34894/QT5BCC
	Fariss et al. (2022): Used to fill GDP data for countries missing in PWT	10.1177/0022002721105443
	World Bank World Development Indicators (Bank, 2021)~~0.1cm~~ : Used to fill GDP data for countries missing in PWT	10.57966/6rwy-0b07
	IMF World Economic Outlook (IMF, 2021)~~0.1cm~~ ~~**Maddison Project Database** (Bolt and van Zanden, 2020)~~ ~~0.1cm~~ : Used to fill GDP data for countries missing in PWT	https://www.imf.org/en/Publications/WEO/weo-database/2022/April
	OECD regional statistics (for Economic Cooperation and Development, 2020)~~0.1cm~~ ~~**CIA World Factbook** (Agency, 2021)~~ ~~0.2cm Collection of contemporary datasets to estimate national income levels~~ : Used to disaggregate French population into overseas departments	10.1787/region-data-en
~~0.5ex~~	**United Nations System of National Accounts** (UNSD, 2021): Used to fill GDP data for countries missing in PWT	https://unstats.un.org/unsd/snaama
Physical capital	**LitPop** (Eberenz et al., 2020)~~,~~ : Gridded estimates of physical capital stock	10.3929/ethz-b-000331316

0.5ex	**2015 Global Assessment Report (GEG-15)** (Bono and Chatenoux, 2014)0.2cm Spatially downscaled (30 arc-second and 1/24°, respectively) estimates : Gridded of physical capital stock 0.1cm used to fill missing regions in LitPop	https://www.undrr.org/quick/11514
	PWT 10.0 (Feenstra et al., 2015)0.2cm : Country-level physical capital stock levels time series of capital stock estimates	10.34894/QT5BCC
	Credit Suisse Global Wealth Databook (Credit Suisse Research Institute, 2022): Country-level time series of non-financial wealth used to fill capital stock estimates for countries missing in PWT	https://www.credit-suisse.com/about-us/en/reports-research/global-wealth-report.html
	Berlemann and Wesselhöft (2017); Pyo and Kim (2020) : Estimates of capital stock:GDP ratios for select countries not contained in other sources	10.15370/ree.2017-0004 10.1088/1748-9326/aaac87
Mobile capital fraction 0.5ex	**PWT 10.0** (Feenstra et al., 2015)0.2cm : Capital is reported in PWT by category; structures are assumed to be immobile, with all other categories assumed as mobile	10.34894/QT5BCC

~~Economic~~ Socioeconomic growth trajectories ~~0.5ex~~	**Shared Socioeconomic Pathways** (Riahi et al., 2017)~~and capital growth modeled by **Dellink et al. 2017** (Dellink et al., 2017)~~ ~~0.2cm Updated growth trajectories to match those used by the IPCC~~ : Contains population projections from Kc and Lutz (2017) and GDP projections from Crespo Cuaresma (2017) and Dellink et al. (2017). We augment these with capital stock projections derived from the model defined in Dellink et al. (2017)	110.1016/j.gloenvcha.2016.05.009 10.1016/j.gloenvcha.2014.06.004 10.1016/j.gloenvcha.2015.02.012 10.1016/j.gloenvcha.2015.06.004
Construction cost indices ~~0.5ex~~ ~~2ex~~	**World Bank ICP** ~~(World Bank, 2020; Lincke and Hinkel, 2021)~~ (World Bank, 2020) **Lincke and Hinkel (2021)**	10.57966/vm5h-a627 10.1029/2020EF001965

Table C4: ~~Summary of SLIIDERS datasets and pyCIAM inputs for~~ Input data sources used to construct socioeconomic variables in SLIIDERS.

Author contributions. Project conceptualized by IB, SH, REK. Data curation by DA, IB, JC, ND, AH. Methodology development, investigation, and formal analysis conducted by DA, IB, JC, ND. Map and figure visualizations were done by ND. Code base developed by DA, IB, JC, ND. Software developed by DA, IB, JC and ND. Model validation performed by IB and ND. Project administered by IB, ND, SH. Original draft written by IB, JC, DA, ND. Manuscript review and editing by DA, IB, JC, ND, SH, REK, MG. Funding acquisition by MG, SH, TH, REK. Supervision by MD, MG, SH, REK.

Competing interests. The authors declare that they have no conflict of interest

Acknowledgements. We thank Maya Norman for conducting her review and evaluation of relevant exposure datasets. Thank you also to Delavane Diaz, who contributed invaluable assistance in the access and interpretation of the CIAM model. We also thank members of the Climate Impact Lab who provided important feedback and guidance during frequent discussions about model objectives and developments. This project is an output of the Climate Impact Lab that gratefully acknowledges funding from the Energy Policy Institute of Chicago (EPIC), International Growth Centre, National Science Foundation (ICER-1663807), Sloan Foundation, Carnegie Corporation, and Tata Center for Development.

References

Statistics | Ålands, https://www.asub.ax/en/statistics.

GADM, https://gadm.org/index.html.

StatBank Norway, https://www.ssb.no/en/statbank.

Global Land One-kilometer Base Elevation (GLOBE), Documentation, National Oceanic and Atmospheric Administration, Boulder, CO, https://www.ngdc.noaa.gov/mgg/topo/report/globedocumentationmanual.pdf, 1999.

Agency, C. I.: The World Factbook, https://www.cia.gov/the-world-factbook/, 2021.

Armstrong, S. B., Lazarus, E. D., Limber, P. W., Goldstein, E. B., Thorpe, C., and Ballinger, R. C.: Indications of a positive feedback between coastal development and beach nourishment, Earth's Future, 4, 626–635, https://doi.org/10.1002/2016EF000425, 2016.

Bakkensen, L. A. and Mendelsohn, R. O.: Risk and Adaptation: Evidence from Global Hurricane Damages and Fatalities, Journal of the Association of Environmental and Resource Economists, 3, 555–587, https://doi.org/10.1086/685908, 2016.

Bakkensen, L. A., Park, D.-S. R., and Sarkar, R. S. R.: Climate costs of tropical cyclone losses also depend on rain, Environmental Research Letters, 13, 074 034, https://doi.org/10.1088/1748-9326/aad056, 2018.

Bamber, J. L., Oppenheimer, M., Kopp, R. E., Aspinall, W. P., and Cooke, R. M.: Ice sheet contributions to future sea-level rise from structured expert judgment, Proceedings of the National Academy of Sciences, 116, 11 195–11 200, https://doi.org/10.1073/pnas.1817205116, 2019.

Bank, T. W.: World Development Indicators, https://datacatalog.worldbank.org/dataset/world-development-indicators, 2021.

Berlemann, M. and Wesselhöft, J.-E.: Aggregate Capital Stock Estimations for 122 Countries: An Update, Review of Economics, 68, 75–92, https://doi.org/10.1515/roe-2017-0004, 2017.

Berrang-Ford, L., Siders, A. R., Lesnikowski, A., Fischer, A. P., Callaghan, M. W., Haddaway, N. R., Mach, K. J., Araos, M., Shah, M. A. R., Wannewitz, M., Doshi, D., Leiter, T., Matavel, C., Musah-Surugu, J. I., Wong-Parodi, G., Antwi-Agyei, P., Ajibade, I., Chauhan, N., Kakenmaster, W., Grady, C., Chalastani, V. I., Jagannathan, K., Galappaththi, E. K., Sitati, A., Scarpa, G., Totin, E., Davis, K., Hamilton, N. C., Kirchhoff, C. J., Kumar, P., Pentz, B., Simpson, N. P., Theokritoff, E., Deryng, D., Reckien, D., Zavaleta-Cortijo, C., Ulibarri, N., Segnon, A. C., Khavhagali, V., Shang, Y., Zvobgo, L., Zommers, Z., Xu, J., Williams, P. A., Canosa, I. V., van Maanen, N., van Bavel, B., van Aalst, M., Turek-Hankins, L. L., Trivedi, H., Trisos, C. H., Thomas, A., Thakur, S., Templeman, S., Stringer, L. C., Sotnik, G., Sjostrom, K. D., Singh, C., Siña, M. Z., Shukla, R., Sardans, J., Salubi, E. A., Safaee Chalkasra, L. S., Ruiz-Díaz, R., Richards, C., Pokharel, P., Petzold, J., Penuelas, J., Pelaez Avila, J., Murillo, J. B. P., Ouni, S., Niemann, J., Nielsen, M., New, M., Nayna Schwerdtle, P., Nagle Alverio, G., Mullin, C. A., Mullenite, J., Mosurska, A., Morecroft, M. D., Minx, J. C., Maskell, G., Nunbogu, A. M., Magnan, A. K., Lwasa, S., Lukas-Sithole, M., Lissner, T., Lilford, O., Koller, S. F., Jurjonas, M., Joe, E. T., Huynh, L. T. M., Hill, A., Hernandez, R. R., Hegde, G., Hawxwell, T., Harper, S., Harden, A., Haasnoot, M., Gilmore, E. A., Gichuki, L., Gatt, A., Garschagen, M., Ford, J. D., Forbes, A., Farrell, A. D., Enquist, C. A. F., Elliott, S., Duncan, E., Coughlan de Perez, E., Coggins, S., Chen, T., Campbell, D., Browne, K. E., Bowen, K. J., Biesbroek, R., Bhatt, I. D., Bezner Kerr, R., Barr, S. L., Baker, E., Austin, S. E., Arotoma-Rojas, I., Anderson, C., Ajaz, W., Agrawal, T., and Abu, T. Z.: A systematic global stocktake of evidence on human adaptation to climate change, Nature Climate Change, 11, 989–1000, https://doi.org/10.1038/s41558-021-01170-y, 2021.

Bertram, G.: On the Convergence of Small Island Economies with Their Metropolitan Patrons, World Development, 32, 343–364, https://doi.org/10.1016/j.worlddev.2003.08.004, 2004.

Bolt, J. and van Zanden, J. L.: Maddison style estimates of the evolution of the world economy. A new 2020 update, Maddison-Project Working Paper, pp. 1–43, https://www.rug.nl/ggdc/historicaldevelopment/maddison/publications/wp15.pdf, 2020.

Bono, A. D. and Chatenoux, B.: A Global Exposure Model for GAR 2015, Input Paper prepared for the Global Assessment Report on Disaster Risk Reduction, The United Nations Office for Disaster Risk Reduction, Geneva, Switzerland, https://www.preventionweb.net/english/hyogo/gar/2015/en/bgdocs/risk-section/De%20Bono,%20Andrea,%20Bruno%20Chatenoux.%202015.%20A%20Global%20Exposure%20Model%20for%20GAR%202015,%20%20UNEP-GRID.pdf, 2014.

Bootsma, J.: Evaluating methods to assess the coastal flood hazard on a global scale : a comparative analysis between the Bathtub approach and the LISFLOOD-AC model, http://essay.utwente.nl/90697/, 2022.

Bower, E. and Weerasinghe, S.: Enhancing the Evidence Base on Planned Relocation Cases in the Context of Hazards, Disasters, and Climate Change, 2021.

Bunting, P., Rosenqvist, A., Lucas, R. M., Rebelo, L.-M., Hilarides, L., Thomas, N., Hardy, A., Itoh, T., Shimada, M., and Finlayson, C. M.: The Global Mangrove Watch—A New 2010 Global Baseline of Mangrove Extent, Remote Sensing, 10, 1669, https://doi.org/10.3390/rs10101669, 2018.

Carleton, T., Jina, A., Delgado, M., Greenstone, M., Houser, T., Hsiang, S., Hultgren, A., Kopp, R. E., McCusker, K. E., Nath, I., Rising, J., Rode, A., Seo, H. K., Viaene, A., Yuan, J., and Zhang, A. T.: Valuing the Global Mortality Consequences of Climate Change Accounting for Adaptation Costs and Benefits*, The Quarterly Journal of Economics, 137, 2037–2105, https://doi.org/10.1093/qje/qjac020, 2022.

Carleton, T. A., Jina, A., Delgado, M. T., and Others: VALUING THE GLOBAL MORTALITY CONSEQUENCES OF CLIMATE CHANGE ACCOUNTING FOR ADAPTATION COSTS AND BENEFITS, NBER WORKING PAPER SERIES, 2020.

Church, J., P.U. Clark, A. Cazenave, J.M. Gregory, S. Jevrejeva, A. Levermann, M.A. Merrifield, G.A. Milne, R.S. Nerem, P.D. Dunn, A.J. Payne, W.T. Pfeffer, D. Stammer, and A.S. Unnikrishnan: 2013: Sea Level Change, in: Climate Change 2013: The Physical Science Basis. Contribution of Working Group I to the Fifth Assessment Report of the Intergovernmental Panel on Climate Change, edited by Stocker, T., D. Qin, G.-K. Plattner, M. Tignor, S.K. Allen, J. Boschung, A. Nauels, Xia, Y., V. Bex, and P.M. Midgley, Cambridge University Press, Cambridge, United Kingdom and New York, NY, USA, https://www.ipcc.ch/site/assets/uploads/2018/02/WG1AR5_Chapter13_FINAL.pdf, 2013.

Climate Impact Lab (CIL): Data-driven Spatial Climate Impact Model User Manual, Version 092022-EPA, https://impactlab.org/research/dscim-user-manual-version-092022-epa/, 2022.

Council, M. M.: Natural Hazard Mitigation Saves: 2017 Interim Report, p. 22, 2017.

Craig, R. K.: Coastal adaptation, government-subsidized insurance, and perverse incentives to stay, Climatic Change, 152, 215–226, https://doi.org/10.1007/s10584-018-2203-5, 2019.

Credit Suisse Research Institute: Global Wealth Report 2017: Where Are We Ten Years after the Crisis?, Tech. rep., https://www.credit-suisse.com/about-us-news/en/articles/news-and-expertise/global-wealth-report-2017-201711.html, 2017.

Credit Suisse Research Institute: Global Wealth Databook 2022, Tech. rep., Zurich, Switzerland, https://www.credit-suisse.com/media/assets/corporate/docs/about-us/research/publications/global-wealth-databook-2022.pdf, 2022.

Crespo Cuaresma, J.: Income projections for climate change research: A framework based on human capital dynamics, Global Environmental Change, 42, 226–236, https://doi.org/10.1016/j.gloenvcha.2015.02.012, 2017.

DeConto, R. M., Pollard, D., Alley, R. B., Velicogna, I., Gasson, E., Gomez, N., Sadai, S., Condron, A., Gilford, D. M., Ashe, E. L., Kopp, R. E., Li, D., and Dutton, A.: The Paris Climate Agreement and future sea-level rise from Antarctica, Nature, 593, 83–89, https://doi.org/10.1038/s41586-021-03427-0, 2021.

Dellink, R., Chateau, J., Lanzi, E., and Magné, B.: Long-term economic growth projections in the Shared Socioeconomic Pathways, Global Environmental Change, 42, 200–214, https://doi.org/10.1016/j.gloenvcha.2015.06.004, 2017.

Diaz, D. B.: Estimating global damages from sea level rise with the Coastal Impact and Adaptation Model (CIAM), Climatic Change, 137, 143–156, https://doi.org/10.1007/s10584-016-1675-4, 2016.

Dronkers, J., Gilbert, J. T. E., Butler, L. W., Carey, J. J., Campbell, J., James, E., Mckenzie, C., Misdorp, R., Quin, N., Vallianos, L., and Dadelszen, J. V.: Strategies for Adaptation to Sea Level Rise, 1990.

Eberenz, S., Stocker, D., Röösli, T., and Bresch, D. N.: Asset exposure data for global physical risk assessment, Earth System Science Data, 12, 817–833, https://doi.org/10.5194/essd-12-817-2020, 2020.

European Space Agency and UCLouvain: Globcover 2009, http://due.esrin.esa.int/page_globcover.php, 2010.

Fariss, C. J., Anders, T., Markowitz, J. N., and Barnum, M.: New Estimates of Over 500 Years of Historic GDP and Population Data, Journal of Conflict Resolution, 66, 553–591, https://doi.org/10.1177/00220027211054432, publisher: SAGE Publications Inc, 2022.

Feenstra, R. C., Inklaar, R., and Timmer, M. P.: The Next Generation of the Penn World Table, American Economic Review, 105, 3150–3182, https://doi.org/10.1257/aer.20130954, 2015.

for Economic Cooperation and Development, O.: Regions and Cities: OECD Statistics, https://stats.oecd.org/, 2020.

Foure, J., Bénassy-Quéré, A., and Fontagne, L.: The Great Shift: Macroeconomic Projections for the World Economy at the 2050 Horizon, SSRN Scholarly Paper ID 2004332, Social Science Research Network, Rochester, NY, https://doi.org/10.2139/ssrn.2004332, 2012.

Fox-Kemper, B., Hewitt, H. T., Xiao, C., Aðalgeirsdóttir, G., Drijfhout, S. S., Edwards, T. L., Golledge, N. R., Hemer, M., Kopp, R. E., and Krinner, G.: Ocean, cryosphere and sea level change, Climate Change 2021: The Physical Science Basis. Contribution of Working Group I to the Sixth Assessment Report of the Intergovernmental Panel on Climate Change [Masson-Delmotte, V., P. Zhai, A. Pirani, S.L. Connors, C. Péan, S. Berger, N. Caud, Y. Chen, L. Goldfarb, M.I. Gomis, M. Huang, K. Leitzell, E. Lonnoy, J.B.R. Matthews, T.K. Maycock, T. Waterfield, O. Yelekçi, R. Yu, and B. Zhou (eds.)], pp. 1211–1362, https://doi.org/10.1017/9781009157896.011, 2021.

Garner, G. G., Hermans, T., Kopp, R. E., Slangen, A. B. A., Edwards, T. L., Levermann, A., Nowicki, S., Palmer, M. D., Smith, C., Fox-Kemper, B., Hewitt, H. T., Xiao, C., Aðalgeirsdóttir, G., Drijfhout, S. S., Golledge, N. R., Hemer, M., Krinner, G., Mix, A., Notz, D., Nurhati, I. S., Ruiz, L., Sallée, J.-B., Yu, Y., Hua, L., Palmer, T., and Pearson, B.: IPCC AR6 WGI Sea Level Projections, https://cera-www.dkrz.de/WDCC/ui/Compact.jsp?acronym=IPCC-DDC_AR6_Sup_SLPr, publisher: World Data Center for Climate (WDCC) at DKRZ Type: dataset, 2022.

Gregory, J. M., Griffies, S. M., Hughes, C. W., Lowe, J. A., Church, J. A., Fukimori, I., Gomez, N., Kopp, R. E., Landerer, F., Cozannet, G. L., Ponte, R. M., Stammer, D., Tamisiea, M. E., and van de Wal, R. S. W.: Concepts and Terminology for Sea Level: Mean, Variability and Change, Both Local and Global, Surveys in Geophysics, 40, 1251–1289, https://doi.org/10.1007/s10712-019-09525-z, 2019.

Haasnoot, M., Brown, S., Scussolini, P., Jimenez, J. A., Vafeidis, A. T., and Nicholls, R. J.: Generic adaptation pathways for coastal archetypes under uncertain sea-level rise, Environmental Research Communications, 1, https://doi.org/10.1088/2515-7620/ab1871, 2019.

Haer, T., Botzen, W. J., de Moel, H., and Aerts, J. C.: Integrating Household Risk Mitigation Behavior in Flood Risk Analysis: An Agent-Based Model Approach, Risk Analysis, 37, 1977–1992, https://doi.org/10.1111/risa.12740, 2017.

Hallegatte, S., Green, C., Nicholls, R. J., and Corfee-Morlot, J.: Future flood losses in major coastal cities, Nature Climate Change, 3, 802–806, https://doi.org/10.1038/nclimate1979, 2013.

Heston, A., Summers, R., and Aten, B.: Penn World Table Version 7.0, Tech. rep., Center for International Comparisons of Production, Income and Prices at the University of Pennsylvania, https://www.rug.nl/ggdc/productivity/pwt/pwt-releases/pwt-7.0, 2011.

Higgins, M.: Demography, National Savings, and International Capital Flows, International Economic Review, 39, 343–369, https://doi.org/10.2307/2527297, 1998.

Hinkel, J. and Klein, R. J. T.: Integrating knowledge to assess coastal vulnerability to sea-level rise: The development of the DIVA tool, Global Environmental Change, 19, 384–395, https://doi.org/10.1016/j.gloenvcha.2009.03.002, 2009.

Hinkel, J., van Vuuren, D. P., Nicholls, R. J., and Klein, R. J. T.: The effects of adaptation and mitigation on coastal flood impacts during the 21st century. An application of the DIVA and IMAGE models, Climatic Change, 117, 783–794, https://doi.org/10.1007/s10584-012-0564-8, 2013.

Hinkel, J., Lincke, D., Vafeidis, A. T., Perrette, M., Nicholls, R. J., Tol, R. S., Marzeion, B., Fettweis, X., Ionescu, C., and Levermann, A.: Coastal flood damage and adaptation costs under 21st century sea-level rise, Proceedings of the National Academy of Sciences of the United States of America, 111, 3292–3297, https://doi.org/10.1073/pnas.1222469111, 2014.

Hinkel, J., Aerts, J. C. J. H., Brown, S., Jiménez, J. A., Lincke, D., Nicholls, R. J., Scussolini, P., Sanchez-Arcilla, A., Vafeidis, A., and Addo, K. A.: The ability of societies to adapt to twenty-first-century sea-level rise, Nature Climate Change, 8, 570–578, https://doi.org/10.1038/s41558-018-0176-z, 2018.

Hoozemans, F. M., Marchand, M., and Pennekamp, H.: A global vulnerability analysis: vulnerability assessment for population, coastal wetlands and rice production on a global scale, Technical Report 2nd Edition, Delft Hydraulics, The Netherlands, https://www.researchgate.net/publication/282669649_A_global_vulnerability_analysis_vulnerability_assessment_for_population_coastal_wetlands_and_rice_production_on_a_global_scale, 1993.

Houser, T., Hsiang, S., Kopp, R., Larsen, K., Delgado, M., Jina, A., Mastrandrea, M., Mohan, S., Muir-Wood, R., Rasmussen, D. J., Rising, J., and Wilson, P.: Economic Risks of Climate Change: An American Prospectus, Columbia University Press, 2015.

Hu, S., Niu, Z., and Chen, Y.: Global Wetland Datasets: a Review, Wetlands, 37, 807–817, https://doi.org/10.1007/s13157-017-0927-z, 2017.

IMF, I. M.: World Economic Outlook Database 2011, Tech. rep., https://www.imf.org/en/Publications/WEO/weo-database/2011/September, 2011.

IMF, I. M.: World Economic Outlook Database, April 2021, https://www.imf.org/en/Publications/WEO/weo-database/2021/April, 2021.

Inklaar, R., Woltjer, P., and Albarrán, D. G.: The Composition of Capital and Cross-Country Productivity Comparisons, International Productivity Monitor, 36, 34–52, https://ideas.repec.org/a/sls/ipmsls/v36y20192.html, 2019.

Jones, B. and O'Neill, B. C.: Spatially explicit global population scenarios consistent with the Shared Socioeconomic Pathways, Environmental Research Letters, 11, 084 003, https://doi.org/10.1088/1748-9326/11/8/084003, 2016.

Jonkman, S. and Vrijling, J.: Loss of life due to floods, Journal of Flood Risk Management, 1, 43–56, https://doi.org/10.1111/j.1753-318X.2008.00006.x, 2008.

Kc, S. and Lutz, W.: The human core of the shared socioeconomic pathways: Population scenarios by age, sex and level of education for all countries to 2100, Global Environmental Change, 42, 181–192, https://doi.org/10.1016/j.gloenvcha.2014.06.004, 2017.

Kopp, R. E., Horton, R. M., Little, C. M., Mitrovica, J. X., Oppenheimer, M., Rasmussen, D. J., Strauss, B. H., and Tebaldi, C.: Probabilistic 21st and 22nd century sea-level projections at a global network of tide-gauge sites, Earth's Future, 2, 383–406, https://doi.org/10.1002/2014ef000239, 2014.

Kopp, R. E., DeConto, R. M., Bader, D. A., Hay, C. C., Horton, R. M., Kulp, S., Oppenheimer, M., Pollard, D., and Strauss, B. H.: Evolving Understanding of Antarctic Ice-Sheet Physics and Ambiguity in Probabilistic Sea-Level Projections, Earth's Future, 5, 1217–1233, https://doi.org/10.1002/2017EF000663, 2017.

Kopp, R. E., Gilmore, E. A., Little, C. M., Lorenzo-Trueba, J., Ramenzoni, V. C., and Sweet, W. V.: Usable Science for Managing the Risks of Sea-Level Rise, Earth's Future, 7, 1235–1269, https://doi.org/10.1029/2018EF001145, 2019.

Kopp, R. E., Garner, G. G., Hermans, T. H. J., Jha, S., Kumar, P., Slangen, A. B. A., Turilli, M., Edwards, T. L., Gregory, J. M., Koubbe, G., Levermann, A., Merzky, A., Nowicki, S., Palmer, M. D., and Smith, C.: The Framework for Assessing Changes To Sea-level (FACTS) v1.0-rc: A platform for characterizing parametric and structural uncertainty in future global, relative, and extreme sea-level change, EGUsphere, pp. 1–34, https://doi.org/10.5194/egusphere-2023-14, publisher: Copernicus GmbH, 2023.

Kulp, S. A. and Strauss, B. H.: CoastalDEM: A global coastal digital elevation model improved from SRTM using a neural network, Remote Sensing of Environment, 206, 231–239, https://doi.org/10.1016/j.rse.2017.12.026, 2018.

Kulp, S. A. and Strauss, B. H.: New elevation data triple estimates of global vulnerability to sea-level rise and coastal flooding, Nature Communications, 10, https://doi.org/10.1038/s41467-019-12808-z, 2019.

Kulp, S. A. and Strauss, B. H.: CoastalDEM v2.1: A high-accuracy and high-resolution global coastal elevation model trained on ICESat-2 satellite lidar, p. 17, 2021.

Lagerlöf, N.-P. and Basher, S. A.: Geography, population density, and per-capita income gaps across US states and Canadian provinces, 2005.

Lickley, M. J., Lin, N., and Jacoby, H. D.: Analysis of coastal protection under rising flood risk, Climate Risk Management, 6, 18–26, https://doi.org/10.1016/j.crm.2015.01.001, 2014.

Lincke, D. and Hinkel, J.: Economically robust protection against 21st century sea-level rise, Global Environmental Change, 51, 67–73, https://doi.org/10.1016/j.gloenvcha.2018.05.003, 2018.

Lincke, D. and Hinkel, J.: Coastal Migration due to 21st Century Sea-Level Rise, Earth's Future, 9, e2020EF001 965, https://doi.org/10.1029/2020EF001965, 2021.

Lorie, M., Neumann, J. E., Sarofim, M. C., Jones, R., Horton, R. M., Kopp, R. E., Fant, C., Wobus, C., Martinich, J., O'Grady, M., and Gentile, L. E.: Modeling coastal flood risk and adaptation response under future climate conditions, Climate Risk Management, 29, 100 233, https://doi.org/10.1016/j.crm.2020.100233, 2020.

McNamara, D. E. and Keeler, A.: A coupled physical and economic model of the response of coastal real estate to climate risk, Nature Climate Change, 3, 559–562, https://doi.org/10.1038/nclimate1826, 2013.

McNamara, D. E., Gopalakrishnan, S., Smith, M. D., and Murray, A. B.: Climate adaptation and policy-induced inflation of coastal property value, PLoS ONE, 10, 1–12, https://doi.org/10.1371/journal.pone.0121278, 2015.

Mendelsohn, R. O., Schiavo, J. G., and Felson, A.: Are American Coasts Under-Protected?, Coastal Management, 48, 23–37, https://doi.org/10.1080/08920753.2020.1691482, 2020.

Merkens, J.-L., Reimann, L., Hinkel, J., and Vafeidis, A. T.: Gridded population projections for the coastal zone under the Shared Socioeconomic Pathways, Global and Planetary Change, 145, 57–66, https://doi.org/10.1016/j.gloplacha.2016.08.009, 2016.

Muis, S., Verlaan, M., Winsemius, H. C., Aerts, J. C. J. H., and Ward, P. J.: A global reanalysis of storm surges and extreme sea levels, Nature Communications, 7, 11 969, https://doi.org/10.1038/ncomms11969, 2016.

Muis, S., Apecechea, M. I., Dullaart, J., de Lima Rego, J., Madsen, K. S., Su, J., Yan, K., and Verlaan, M.: A High-Resolution Global Dataset of Extreme Sea Levels, Tides, and Storm Surges, Including Future Projections, Frontiers in Marine Science, 7, 263, https://doi.org/10.3389/fmars.2020.00263, 2020.

Mulet, S., Rio, M.-H., Etienne, H., Artana, C., Cancet, M., Dibarboure, G., Feng, H., Husson, R., Picot, N., Provost, C., and Strub, P. T.: The new CNES-CLS18 global mean dynamic topography, Ocean Science, 17, 789–808, https://doi.org/10.5194/os-17-789-2021, 2021.

Neumann, B., Vafeidis, A. T., Zimmermann, J., and Nicholls, R. J.: Future coastal population growth and exposure to sea-level rise and coastal flooding - A global assessment, PLoS ONE, 10, https://doi.org/10.1371/journal.pone.0118571, 2015.

Nicholls, R., Klein, R., and Tol, R.: Managing coastal vulnerability and climate change: a national to global perspective, 2006.

Nicholls, R. J.: Analysis of global impacts of sea-level rise: a case study of flooding, Physics and Chemistry of the Earth, Parts A/B/C, 27, 1455–1466, https://doi.org/10.1016/S1474-7065(02)00090-6, 2002.

Nicholls, R. J.: Coastal flooding and wetland loss in the 21st century: changes under the SRES climate and socio-economic scenarios, Global Environmental Change, 14, 69–86, https://doi.org/10.1016/j.gloenvcha.2003.10.007, 2004.

O'Neill, B. C., Kriegler, E., Ebi, K. L., Kemp-Benedict, E., Riahi, K., Rothman, D. S., van Ruijven, B. J., van Vuuren, D. P., Birkmann, J., Kok, K., Levy, M., and Solecki, W.: The roads ahead: Narratives for shared socioeconomic pathways describing world futures in the 21st century, Global Environmental Change, 42, 169–180, https://doi.org/10.1016/j.gloenvcha.2015.01.004, 2017.

Oppenheimer, M., Glavovic, B., Hinkel, J., van de Wal, R., Magnan, A. K., Abd-Elgawad, A., Cai, R., Cifuentes-Jara, M., Deconto, R. M., Ghosh, T., Hay, J., Isla, F., Marzeion, B., Meyssignac, B., and Sebesvari, Z.: Chapter 4: Sea Level Rise and Implications for Low Lying Islands, Coasts and Communities, in: IPCC Special Report on the Ocean and Cryosphere in a Changing Climate, edited by P\"ortner, H.-O., Roberts, D. C., Masson-Delmotte, V., Zhai, P., Tignor, M., Poloczanska, E., Mintenbeck, K., Alegr\'eia, A., Nicolai, M., Okem, A., Petzold, J., Rama, B., and Weyer, N. M., 2019.

Pardaens, A. K., Lowe, J. A., Brown, S., Nicholls, R. J., and de Gusmão, D.: Sea-level rise and impacts projections under a future scenario with large greenhouse gas emission reductions, Geophysical Research Letters, 38, https://doi.org/10.1029/2011GL047678, 2011.

Pyo, H. K. and Kim, M.: Estimating Capital Stock in North Korea and Its Implications, https://doi.org/10.2139/ssrn.3727104, 2020.

Rasmussen, D. J., Bittermann, K., Buchanan, M. K., Kulp, S., Strauss, B. H., Kopp, R. E., and Oppenheimer, M.: Extreme sea level implications of 1.5 °C, 2.0 °C, and 2.5 °C temperature stabilization targets in the 21st and 22nd centuries, Environmental Research Letters, 13, 034 040, https://doi.org/10.1088/1748-9326/aaac87, 2018.

Rasmussen, D. J., Buchanan, M. K., Kopp, R. E., and Oppenheimer, M.: A Flood Damage Allowance Framework for Coastal Protection With Deep Uncertainty in Sea Level Rise, Earth's Future, 8, e2019EF001 340, https://doi.org/10.1029/2019EF001340, 2020.

Rennert, K., Errickson, F., Prest, B. C., Rennels, L., Newell, R. G., Pizer, W., Kingdon, C., Wingenroth, J., Cooke, R., Parthum, B., Smith, D., Cromar, K., Diaz, D., Moore, F. C., Müller, U. K., Plevin, R. J., Raftery, A. E., Ševčíková, H., Sheets, H., Stock, J. H., Tan, T., Watson, M., Wong, T. E., and Anthoff, D.: Comprehensive evidence implies a higher social cost of CO2, Nature, 610, 687–692, https://doi.org/10.1038/s41586-022-05224-9, number: 7933 Publisher: Nature Publishing Group, 2022.

Riahi, K., van Vuuren, D. P., Kriegler, E., Edmonds, J., O'Neill, B. C., Fujimori, S., Bauer, N., Calvin, K., Dellink, R., Fricko, O., Lutz, W., Popp, A., Cuaresma, J. C., Kc, S., Leimbach, M., Jiang, L., Kram, T., Rao, S., Emmerling, J., Ebi, K., Hasegawa, T., Havlik, P., Humpenöder, F., Da Silva, L. A., Smith, S., Stehfest, E., Bosetti, V., Eom, J., Gernaat, D., Masui, T., Rogelj, J., Strefler, J., Drouet, L., Krey, V., Luderer, G., Harmsen, M., Takahashi, K., Baumstark, L., Doelman, J. C., Kainuma, M., Klimont, Z., Marangoni, G., Lotze-Campen, H., Obersteiner, M., Tabeau, A., and Tavoni, M.: The Shared Socioeconomic Pathways and their energy, land use, and greenhouse gas emissions implications: An overview, Global Environmental Change, 42, 153–168, https://doi.org/10.1016/j.gloenvcha.2016.05.009, 2017.

Rode, A., Carleton, T., Delgado, M., Greenstone, M., Houser, T., Hsiang, S., Hultgren, A., Jina, A., Kopp, R. E., McCusker, K. E., Nath, I., Rising, J., and Yuan, J.: Estimating a social cost of carbon for global energy consumption, Nature, 598, 308–314, https://doi.org/10.1038/s41586-021-03883-8, 2021.

Rodriguez, E., Morris, C. S., Belz, J. E., Chapin, E. C., Martin, J. M., Daffer, W., and Hensley, S.: An assessment of the SRTM topographic products, 2005.

Román, M. O., Wang, Z., Sun, Q., Kalb, V., Miller, S. D., Molthan, A., Schultz, L., Bell, J., Stokes, E. C., Pandey, B., Seto, K. C., Hall, D., Oda, T., Wolfe, R. E., Lin, G., Golpayegani, N., Devadiga, S., Davidson, C., Sarkar, S., Praderas, C., Schmaltz, J., Boller, R., Stevens,

J., Ramos González, O. M., Padilla, E., Alonso, J., Detrés, Y., Armstrong, R., Miranda, I., Conte, Y., Marrero, N., MacManus, K., Esch, T., and Masuoka, E. J.: NASA's Black Marble nighttime lights product suite, Remote Sensing of Environment, 210, 113–143, https://doi.org/10.1016/j.rse.2018.03.017, 2018.

Rose, A. N., McKee, J. J., Sims, K. M., Bright, E. A., Reith, A. E., and Urban, M. L.: LandScan 2019, https://landscan.ornl.gov/, 2020.

Sadoff, C. W., Hall, J. W., Grey, D., Aerts, J. C. J. H., Ait-Kadi, M., Brown, C., Cox, A., Dadson, S., Garrick, D., Kelman, J., McCornick, P., Ringler, C., Rosegrant, M., Whittington, D., and Wiberg, D.: Securing water, sustaining growth. Report of the GWP/OECD Task Force on Water Security and Sustainable Growth, Tech. rep., University of Oxford, http://www.water.ox.ac.uk/wp-content/uploads/2015/04/SCHOOL-OF-GEOGRAPHY-SECURING-WATER-SUSTAINING-GROWTH-DOWNLOADABLE.pdf, 2015.

Scussolini, P., Aerts, J. C. J. H., Jongman, B., Bouwer, L. M., Winsemius, H. C., de Moel, H., and Ward, P. J.: FLOPROS: an evolving global database of flood protection standards, Natural Hazards and Earth System Sciences, 16, 1049–1061, https://doi.org/10.5194/nhess-16-1049-2016, 2016.

Sims, K., Reith, A., Bright, E., McKee, J., and Rose, A.: LandScan Global 2021, https://doi.org/10.48690/1527702, edition: 2021 Place: Oak Ridge, TN Section: July 01, 2022, 2022.

Suckall, N., Tompkins, E. L., Nicholls, R. J., Kebede, A. S., Lázár, A. N., Hutton, C., Vincent, K., Allan, A., Chapman, A., Rahman, R., Ghosh, T., and Mensah, A.: A framework for identifying and selecting long term adaptation policy directions for deltas, Science of the Total Environment, 633, 946–957, https://doi.org/10.1016/j.scitotenv.2018.03.234, 2018.

Sweet, W., Horton, R., Kopp, R., LeGrande, A., and Romanou, A.: Ch. 12: Sea Level Rise. Climate Science Special Report: Fourth National Climate Assessment, Volume I, Tech. rep., U.S. Global Change Research Program, https://doi.org/10.7930/J0VM49F2, 2017.

Sweet, W., Hamlington, B., Kopp, R., Weaver, C., Barnard, P., Bekaert, D., Brooks, W., Craghan, M., Dusek, G., Frederikse, T., and others: Global and regional sea level rise scenarios for the United States: Updated mean projections and extreme water level probabilities along US coastlines, Tech. rep., NOAA Technical Report, 2022.

Taylor, K. E., Stouffer, R. J., and Meehl, G. A.: An Overview of CMIP5 and the Experiment Design, Bulletin of the American Meteorological Society, 93, 485–498, https://doi.org/10.1175/BAMS-D-11-00094.1, 2012.

Tebaldi, C., Ranasinghe, R., Vousdoukas, M., Rasmussen, D. J., Vega-Westhoff, B., Kirezci, E., Kopp, R. E., Sriver, R., and Mentaschi, L.: Extreme sea levels at different global warming levels, Nature Climate Change, 11, 746–751, https://doi.org/10.1038/s41558-021-01127-1, number: 9 Publisher: Nature Publishing Group, 2021.

Tiggeloven, T., Moel, H. d., Winsemius, H. C., Eilander, D., Erkens, G., Gebremedhin, E., Loaiza, A. D., Kuzma, S., Luo, T., Iceland, C., Bouwman, A., Huijstee, J. v., Ligtvoet, W., and Ward, P. J.: Global-scale benefit-cost analysis of coastal flood adaptation to different flood risk drivers using structural measures., Natural Hazards and Earth System Sciences, 20, 1025–1025, https://go.gale.com/ps/i.do?p=AONE&sw=w&issn=15618633&v=2.1&it=r&id=GALE%7CA621126931&sid=googleScholar&linkaccess=fulltext, 2020.

Tol, R. S. J.: The damage costs of climate change towards a dynamic representation, Ecological Economics, 19, 67–90, https://doi.org/10.1016/0921-8009(96)00041-9, 1996.

Tozer, B., Sandwell, D. T., Smith, W. H. F., Olson, C., Beale, J. R., and Wessel, P.: Global Bathymetry and Topography at 15 Arc Sec: SRTM15+, Earth and Space Science, 6, 1–18, https://doi.org/10.1029/2019EA000658, 2019.

UN DESA, Department of Economic and Social Affairs, P. U. N.: World Population Prospects 2012: Volume I: Comprehensive Tables, Tech. rep., https://population.un.org/wpp/Publications/Files/WPP2019_Volume-I_Comprehensive-Tables.pdf, 2012.

UN DESA, Department of Economic and Social Affairs, P. U. N.: World Population Prospects 2019: Volume I: Comprehensive Tables, Tech. rep., https://population.un.org/wpp/Publications/Files/WPP2019_Volume-I_Comprehensive-Tables.pdf, 2019.

United Nations, Department of Economic and Social Affairs, Population Division: World Population Prospects 2022, Online Edition, https://population.un.org/wpp/Download/Standard/MostUsed/, 2022.

University, C. F. I. E. S. I. N.-C.-C.: Gridded Population of the World, Version 4 (GPWv4): Population Density, http://beta.sedac.ciesin.columbia.edu/data/set/gpw-v4-population-density, 2016.

UNSD: National accounts—analysis of main aggregates (AMA), United Nations Statistics Division (UNSD), 2021.

US Army Corps of Engineers: National Levee Database, https://levees.sec.usace.army.mil/#/.

Vafeidis, A. T., Nicholls, R. J., McFadden, L., Tol, R. S. J., Hinkel, J., Spencer, T., Grashoff, P. S., Boot, G., and Klein, R. J. T.: A New Global Coastal Database for Impact and Vulnerability Analysis to Sea-Level Rise, Journal of Coastal Research, 24, 917–924, https://www.jstor.org/stable/40065185, 2008.

von Krogh, G. and von Hippel, E.: The Promise of Research on Open Source Software, Management Science, 52, 975–983, https://doi.org/10.1287/mnsc.1060.0560, 2006.

Vousdoukas, M. I., Voukouvalas, E., Mentaschi, L., Dottori, F., Giardino, A., Bouziotas, D., Bianchi, A., Salamon, P., and Feyen, L.: Developments in large-scale coastal flood hazard mapping, Natural Hazards and Earth System Sciences, 16, 1841–1853, https://doi.org/10.5194/nhess-16-1841-2016, 2016.

Wilkinson, M. D., Dumontier, M., Aalbersberg, I. J., Appleton, G., Axton, M., Baak, A., Blomberg, N., Boiten, J.-W., da Silva Santos, L. B., Bourne, P. E., Bouwman, J., Brookes, A. J., Clark, T., Crosas, M., Dillo, I., Dumon, O., Edmunds, S., Evelo, C. T., Finkers, R., Gonzalez-Beltran, A., Gray, A. J. G., Groth, P., Goble, C., Grethe, J. S., Heringa, J., 't Hoen, P. A. C., Hooft, R., Kuhn, T., Kok, R., Kok, J., Lusher, S. J., Martone, M. E., Mons, A., Packer, A. L., Persson, B., Rocca-Serra, P., Roos, M., van Schaik, R., Sansone, S.-A., Schultes, E., Sengstag, T., Slater, T., Strawn, G., Swertz, M. A., Thompson, M., van der Lei, J., van Mulligen, E., Velterop, J., Waagmeester, A., Wittenburg, P., Wolstencroft, K., Zhao, J., and Mons, B.: The FAIR Guiding Principles for scientific data management and stewardship, Scientific Data, 3, 160 018, https://doi.org/10.1038/sdata.2016.18, 2016.

World Bank: International Comparison Program 2017, Database, https://www.worldbank.org/en/programs/icp#1, 2020.

Yohe, G. and Tol, R. S.: Indicators for social and economic coping capacity - Moving toward a working definition of adaptive capacity, Global Environmental Change, 12, 25–40, https://doi.org/10.1016/S0959-3780(01)00026-7, 2002.

Yohe, G., Neumann, J., and Ameden, H.: Assessing the economic cost of greenhouse-induced sea level rise: methods and application in support of a national survey, Journal of Environmental Economics and Management, 29, S78–S97, 1995.

Zingerle, P., Pail, R., Gruber, T., and Oikonomidou, X.: The combined global gravity field model XGM2019e, Journal of Geodesy, 94, 1–12, https://doi.org/10.1007/s00190-020-01398-0, 2020.